

June 2011 - Update



Thermohydrodynamic Analysis of Bump Type Gas Foil Bearings: A Model Anchored to Test Data

Luis San Andrés

Mast-Childs Professor

Tae Ho Kim

Post-Doc Research Associate

Keun Ryu

PhD Research Assistant

**This material is based upon work supported by NASA NNH06ZEA001N-SSRW2,
Fundamental Aeronautics: Subsonic Rotary Wing Project and the Texas A&M
Turbomachinery Research Consortium**

Outline

- **Statement of Work & Sources for Presentation**
- **Objectives and accomplished work in 2007-08**
 - Computational model. Validation with published data.**
 - Rotordynamic measurements at TAMU**
- **Objectives and accomplished work in 2008-09**
 - Description of test rig and foil bearings at TAMU**
 - Effect of temperature on bearing temperatures, coastdown speed and rotor motions**
 - Effect of cooling flow on shaft and bearing temperatures. Validation of computational model**
- * **The computational code**
 - Graphical User Interface. Further predictions**
- **GFB thermal management tests and preds.**
- **Added Value and Closure**

Topic

- **Statement of Work & Sources for Presentation**

- **Objectives and accomplished work in 2007-08**

 - Computational model. Validation with published data.

 - Rotordynamic measurements at TAMU

- **Objectives and accomplished work in 2008-09**

 - Description of test rig and foil bearings at TAMU

 - Effect of temperature on bearing temperatures,
coastdown speed and rotor motions

 - Effect of cooling flow on bearing and shaft
temperatures. Validation of computational model

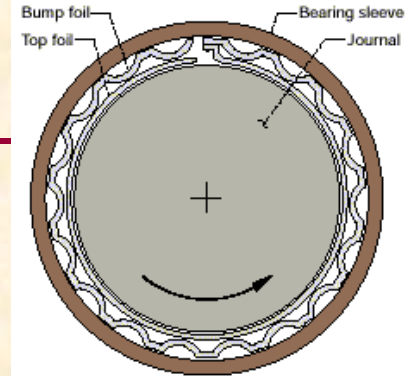
- * **The computational code**

 - Graphical User Interface. Further predictions

- **GFB thermal management tests and preds.**

- **Closure & added value**

Gas Foil Bearings (+/-)



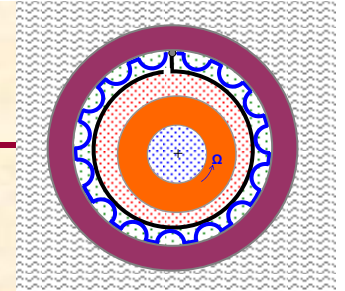
- Increased reliability: large load capacity (< 100 psi)
- No lubricant supply system, i.e. reduce weight
- High and low temperature capability (up to 2,500 K)
- No scheduled maintenance
- Ability to sustain high vibration and shock load. Quiet operation



- Less load capacity than rolling or oil bearings
- Wear during start up & shut down
- No test data for rotordynamic force coefficients
- Thermal management issues
- Predictive models lack validation. Difficulties in modeling + dry-friction damping + effects of temperature on material properties and components' expansion.

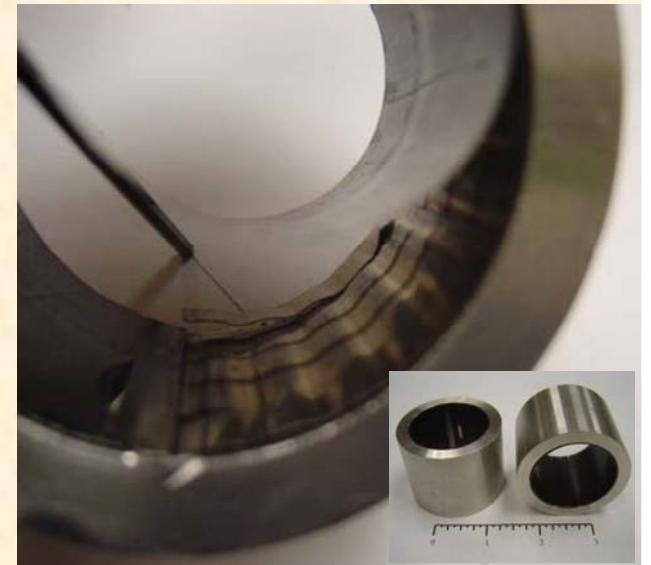
Applications: ACMs, micro gas turbines, turbo expanders

SOW – Main Objective



To develop a detailed, physics-based computational model of gas-lubricated foil journal bearings including thermal effects to predict bearing performance.

The result of this work shall include a fully tested and experimentally verified design tool for predicting gas foil journal bearing torque, load, gas film thickness, pressure, flow field, temperature distribution, thermal deformation, foil deflections, stiffness, damping, and any other important parameters.



References **Foil Bearings**

- ASME GT2011-46767** De Santiago, O., and San Andrés, L., 2011, "Parametric Study of Bump Foil Gas Bearings for Industrial Applications"
- ASME GT2011-45763** San Andrés, L., and Ryu, K., 2011, "On the Nonlinear Dynamics of Rotor-Foil Bearing Systems: Effects of Shaft Acceleration, Mass Imbalance and Bearing Mechanical Energy Dissipation."
- ASME GT2010-22508**
NASA/TM 2010-216354 Howard, S., and San Andrés, L., 2011, "A New Analysis Tool Assessment for Rotordynamic Modeling of Gas Foil Bearings," ASME J. Eng. Gas Turbines and Power, v 133
- ASME GT2010-22981** San Andrés, L., Ryu, K., and Kim, T-H, 2011, "Thermal Management and Rotordynamic Performance of a Hot Rotor-Gas Foil Bearings System. Part 2: Predictions versus Test Data," ASME J. Eng. Gas Turbines and Power, v 133
- ASME GT2010-22981** San Andrés, L., Ryu, K., and Kim, T-H, 2011, "Thermal Management and Rotordynamic Performance of a Hot Rotor-Gas Foil Bearings System. Part 1: Measurements," ASME J. Eng. Gas Turbines and Power, v 133
- J Eng Gas Turbines & Power** San Andrés, L., Ryu, K., and Kim, T.H., 2011, "Identification of Structural Stiffness and Energy Dissipation parameters in a 2nd Generation Foil Bearing; Effect of Shaft Temperature", ASME J. Eng. Gas Turbines Power, vol. 133 (March) , pp. 032501
- 8th IFToMM Int. Conf. on Rotordynamics** San Andrés, L., Camero, J., Muller, S., Chirathadam, T., and Ryu, K., 2010, "Measurements of Drag Torque, Lift Off Speed, and Structural Parameters in a 1st Generation Floating Gas Foil Bearing," Seoul, S. Korea (Sept.)
- ASME GT2009-59920** San Andrés, L., Kim, T.H., Ryu, K., Chirathadam, T. A., Hagen, K., Martinez, A., Rice, B., Niedbalski, N., Hung, W., and Johnson, M., 2009, "Gas Bearing Technology for Oil-Free Microturbomachinery – Research Experience for Undergraduate (REU) Program at Texas A&M University
- AHS 2009 paper** Kim, T. H., and San Andrés, L., 2010, "Thermohydrodynamic Model Predictions and Performance Measurements of Bump-Type Foil Bearing for Oil-Free Turboshaft Engines in Rotorcraft Propulsion Systems," ASME J. of Tribology, v132
- ASME GT2009-59919** San Andrés, L., and Kim, T.H., 2010, "Thermohydrodynamic Analysis of Bump Type gas Foil Bearings: A Model Anchored to Test Data," ASME J. Eng. Gas Turbines and Power, v 132

References Foil Bearings

- IJTC2008-71195** Kim, T.H., and San Andrés, L., 2009, "Effects of a Mechanical Preload on the Dynamic Force Response of Gas Foil Bearings - Measurements and Model Predictions," Tribology Transactions, v52
- ASME GT2008-50571**
IJTC2007-44047 Kim, T. H., and San Andrés, L., 2009, "Effect of Side End Pressurization on the Dynamic Performance of Gas Foil Bearings – A Model Anchored to Test Data," ASME J. Eng. Gas Turbines and Power, v131. **2008 Best PAPER Rotordynamics IGTI**
- ASME GT2007-27249** San Andrés, L., and Kim, T.H., 2009, "Analysis of Gas Foil Bearings Integrating FE Top Foil Models," Tribology International, v42
- J of Tribology** Kim, T.H., Breedlove, A., and San Andrés, L., 2009, "Characterization of Foil Bearing Structure at Increasing Temperatures: Static Load and Dynamic Force Performance," ASME Journal of Tribology, v 131(3)
- Tribology International** San Andrés, L., and **Kim, T.H.**, 2008, "Forced Nonlinear Response of Gas Foil Bearing Supported Rotors," Tribology International, **41**(8), pp. 704-715.
- Kim, T-H**, and L., San Andrés, 2007, "Analysis of Gas Foil Bearings with Piecewise Linear Elastic Supports." Tribology International, **40**, pp. 1239-1245.
- AIAA-2007-5094** San Andrés, L., and T.H. Kim, 2007, "Issues on Instability and Force Nonlinearity in Gas Foil Bearing Supported Rotors," 43rd AIAA/ASME/SAE/ASEE Joint Propulsion Conference, Cincinnati, OH, July 9-11
- ASME GT2005-68486** Kim, T.H., and L. San Andrés, 2008, "Heavily Loaded Gas Foil Bearings: a Model Anchored to Test Data," ASME J. Eng. Gas Turbines and Power, v130
- ASME GT2006-91238** San Andrés, L., D. Rubio, and T.H. Kim, 2007, "Rotordynamic Performance of a Rotor Supported on Bump Type Foil Gas Bearings: Experiments and Predictions," ASME J. Eng. Gas Turbines and Power, v129
- ASME GT2005-68384** **Rubio, D.**, and L. San Andrés, 2007, "Structural Stiffness, Dry-Friction Coefficient and Equivalent Viscous Damping in a Bump-Type Foil Gas Bearing," ASME J. Eng. Gas Turbines and Power, v 129 **2005 Best PAPER Rotordynamics IGTI Structures and Dynamics Committee**
- ASME GT2004-53611** San Andrés, L., and D. Rubio, 2006, "Bump-Type Foil Bearing Structural Stiffness: Experiments and Predictions," ASME J. Eng. Gas Turbines and Power, v128

References **Metal mesh foil bearings**

- ASME GT2011-45274** San Andrés, L., and Chirathadam, T., 2011, "Metal Mesh Foil Bearings: Effect of Excitation Frequency on Rotordynamic Force Coefficients"
- ASME GT2010-22440** San Andrés, L., and Chirathadam T.A., 2010, "Identification of Rotordynamic Force Coefficients of a Metal Mesh Foil Bearing Using Impact Load Excitations."
- ASME GT2009-59315** San Andrés, L., Chirathadam, T. A., and Kim, T.H., 2009, "Measurements of Structural Stiffness and Damping Coefficients in a Metal Mesh Foil Bearing."
- AHS Paper** San Andrés, L., Kim, T.H., Chirathadam, T.A., and Ryu, K., 2009, "Measurements of Drag Torque, Lift-Off Journal Speed and Temperature in a Metal Mesh Foil Bearing," American Helicopter Society 65th Annual Forum, Grapevine, Texas, May 27-29
- Other**
- Journal of Tribology** **Kim, T.H.**, and L. San Andrés, 2006, "Limits for High Speed Operation of Gas Foil Bearings," ASME Journal of Tribology, **128**, pp. 670-673
- ASME DETC2007-34136** Gjika, K., C. Groves, L. San Andrés, and G. LaRue, 2007, "Nonlinear Dynamic Behavior of Turbocharger Rotor-Bearing Systems with Hydrodynamic Oil Film and Squeeze Film Damper in Series: Prediction and Experiment."

Topic

- Statement of Work & Sources for Presentation
- **Objectives and accomplished work in 07-08**
Computational model. Validation with published data. Rotordynamic measurements at TAMU
- Objectives and accomplished work in 2008-09
 - Description of test rig and foil bearings at TAMU
 - Effect of temperature on bearing temperatures, coastdown speed and rotor motions
 - Effect of cooling flow on bearing and shaft temperatures. Validation of computational model
- * The computational code
 - Graphical User Interface. Further predictions
- GFB thermal management tests and preds.
- Closure & added value

Research Objectives (2007-08)

THD model for prediction of GFB performance

- Perform physical analysis, derive governing equations, and implement numerical solution.
- **Develop GUI for User ready use**
- Compare GFB predictions to limited published test data (NASA mainly)
- **Revamp existing test rig with cartridge heater, acquire new bearings, machine new rotor**
- Perform structural tests on bearings and measure rotordynamic response for increasing shaft temperatures

Scheduled Timeline & completion

Luis San Andres

MS student

Tae Ho Kim

UG worker

Task	Q1	Q2	Q3	Q4	Q5	Q6	Q7	Q8
Computational analysis GFBS								
Development physical model for thermal transport in foil bearings								
Implementation thermal model (Finite Element Based) and coupling to existing STRUCTURAL MODEL								
Integration of thermal model with GFB FD computational code (gas film)								
Predictions of GFB performance for parametric studies							→	
Comparison of GFB predictions to measured performance from TAMU test rig								→
Nonlinear analysis GFBS								
Development simple NONLINEAR physical model for foil bearings								
Prediction of performance and comparisons to available rotordynamic test data								→
Test rig for identification of FB structure (High Temperature)								
Planning of modification, selection of instrumentation and cartridge heater, design of insulation cover								
Reception of parts and assembly of components, troubleshooting, connection to static loader and shaker			→					
Measurements of load & bearing deflection for increasing shaft temperatures (max 500 C), identification of FB structural parameters								
Rotordynamic-GFBs Test rig (High Temperature)								
Planning of modifications to existing, selection of instrumentation and cartridge heater, design of insulation cover and rotor								
Reception of parts and assembly of components, troubleshooting, connection to static loader and shaker								→
Rotordynamic Measurements for increasing shaft temperatures (max 500 C), identification of GFB synchronous force coefficients								

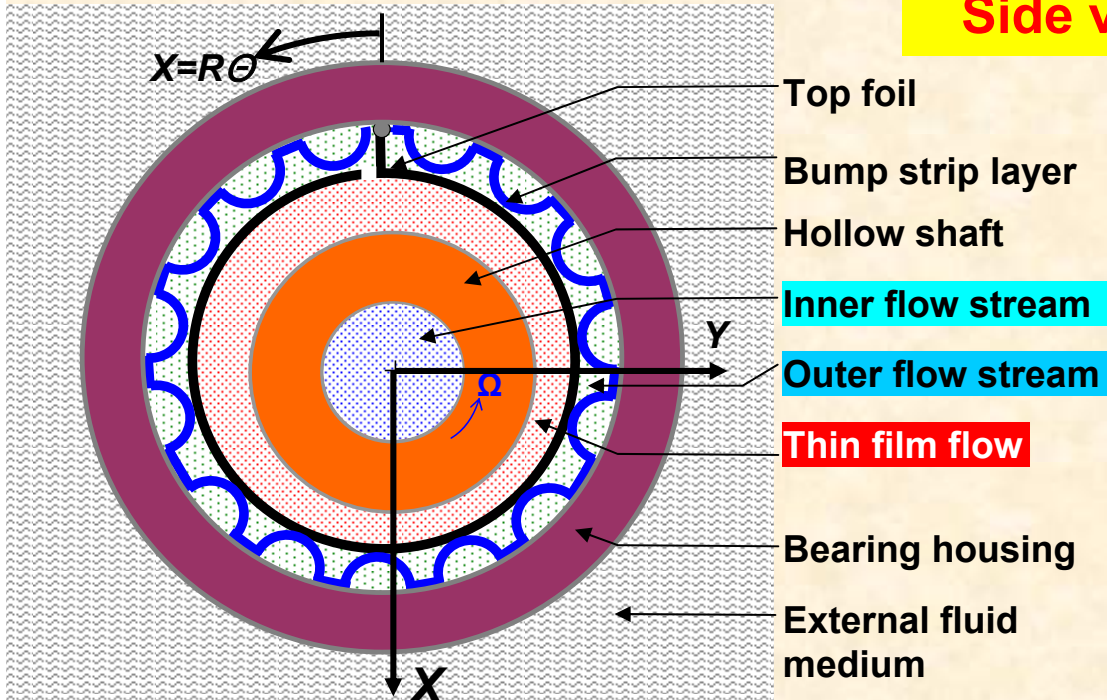
Accomplishments: Proposed & Actual

Task	Planned & Actual	comment
Thermohydrodynamic Analysis of GFBS		
Physical model for thermal transport in foil bearings. Integration of thermal model with GFB FD computational code (gas film). Prediction of GFB performance: parametric study	✓	Analysis completed. Code delivered on June 10, 2009
Validation of GFB predictions with measured temperatures from NASA & TAMU published research	✓	See Q4 & Q7 reports
Nonlinear structural analysis of GFBS	✓	
Development simple NONLINEAR physical model for foil bearings. Prediction of performance and comparisons to rotordynamic test data		Implementation in XLTRC2 for ready rotordynamic analyses
Test rig for identification of FB structure (High Temperature)	✓	
Design & construction; selection & procurement of instrumentation and bearings; assembly, troubleshooting and operation at high temperature. Measurements of static load performance & comparison to predictions		See Q4, Q7 reports
Rotordynamic-GFBs Test rig (High Temperature)	✓	
Design & construction; selection & procurement of instrumentation and bearings; assembly, troubleshooting and operation at high temperature rotor-bearing test rig. Measurements of temperatures and rotordynamic performance with Foster-Miller GFBs completed (see Q7). Tests with MiTi® bearings at higher temperatures in progress. Validation of computational model also in progress.	100%	Completed Dec 2010

1st & 2nd Years

Thermohydrodynamic model in a GFB

Side view of GFB with hollow shaft



- Ideal gas with density, $\rho = P / \mathcal{R}_g T$

- Gas viscosity, $\mu = \alpha_v T$

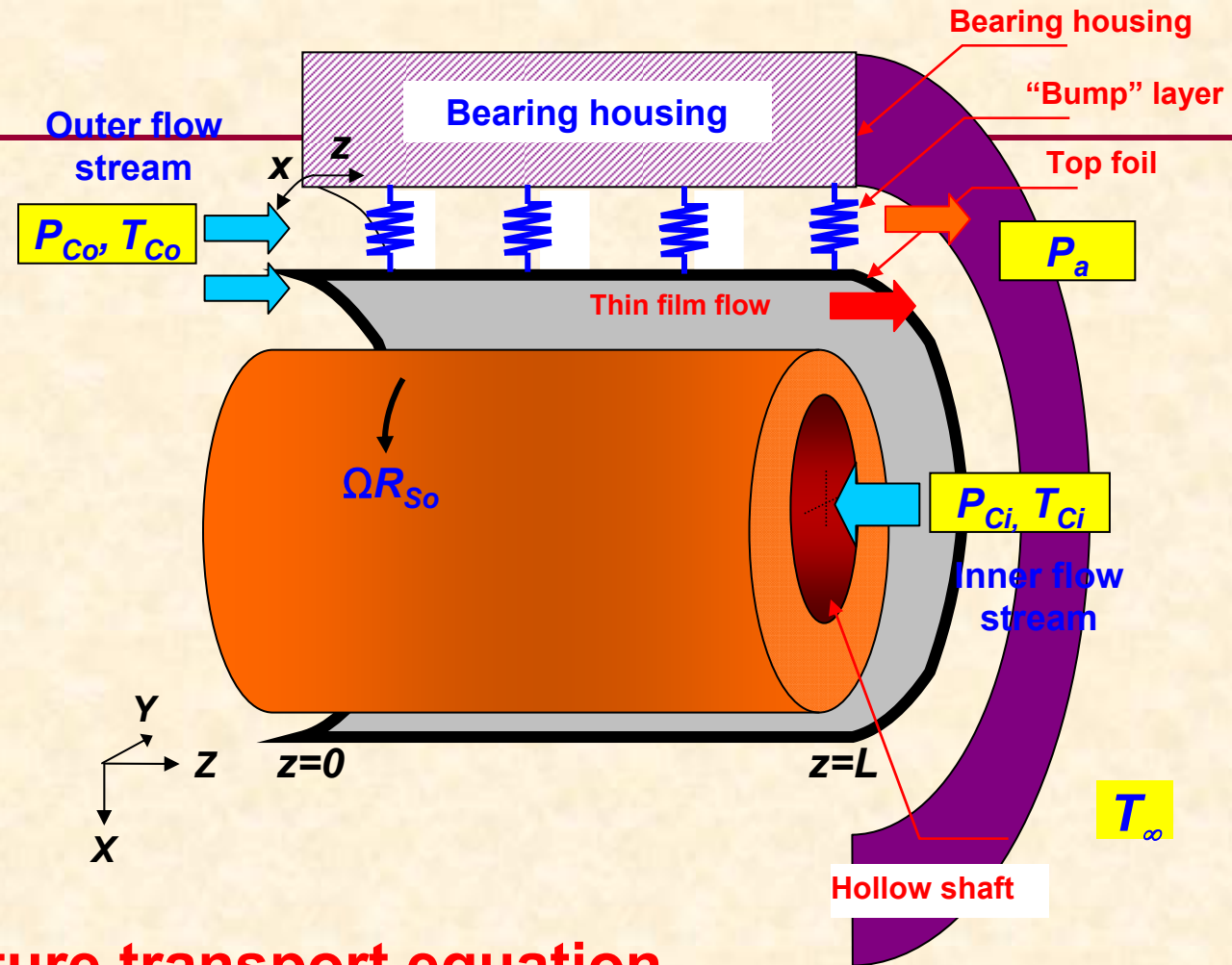
- Gas Specific heat (c_p) and thermal conductivity (κ_g) at an effective temperature

Reynolds equation in thin film

$$\frac{\partial}{\partial x} \left(\frac{h_f^3 P_f}{12 \mu_f \mathcal{R}_g T_f} \frac{\partial P_f}{\partial x} \right) + \frac{\partial}{\partial z} \left(\frac{h_f^3 P_f}{12 \mu_f \mathcal{R}_g T_f} \frac{\partial P_f}{\partial z} \right) = U_{m(z)} \frac{\partial}{\partial x} \left(\frac{P_f h_f}{\mathcal{R}_g T_f} \right)$$

THD model

GFB with cooling flows
(inner and/or outer)



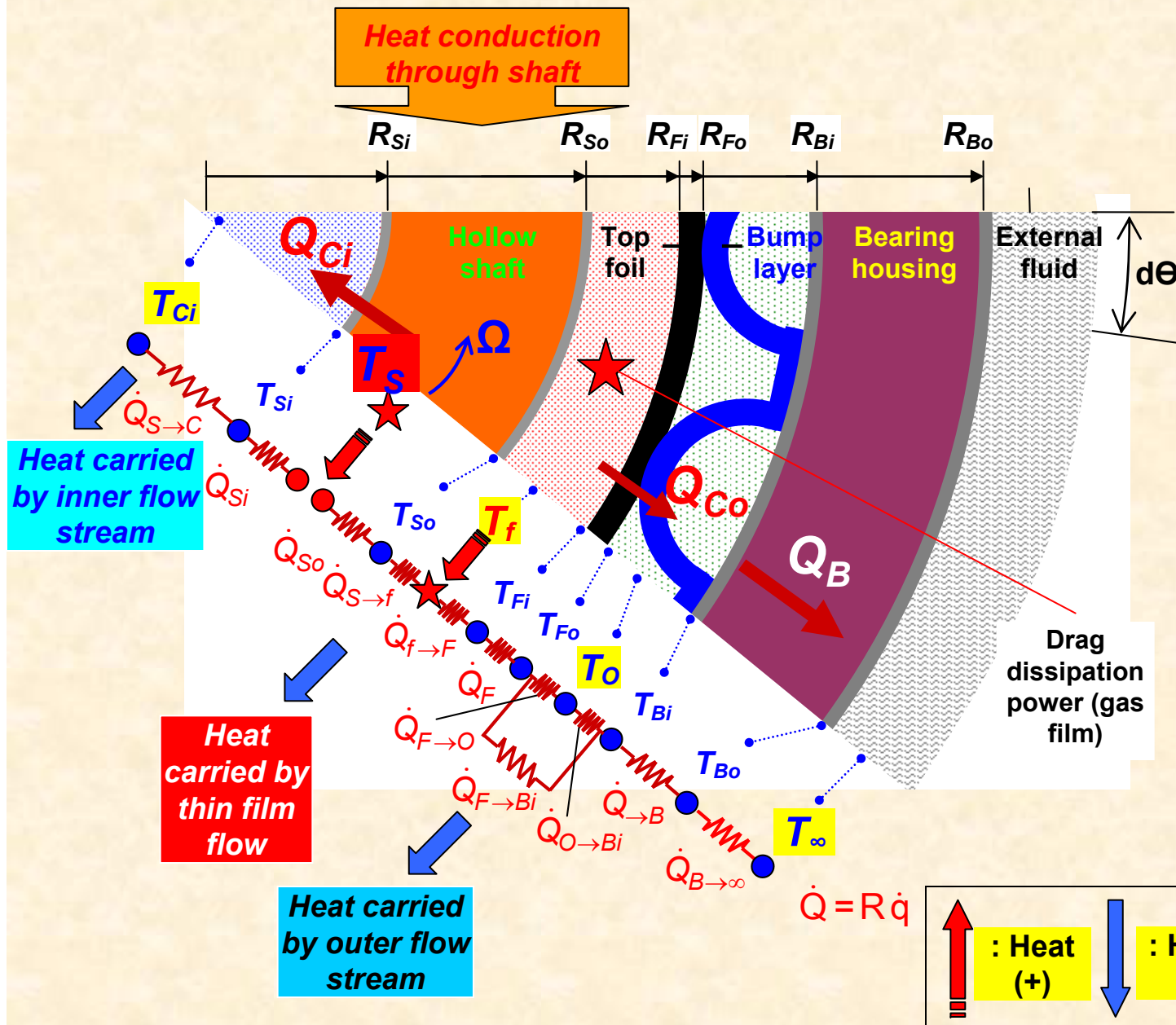
Bulk-flow temperature transport equation

$$c_{p_f} \left(\frac{\partial(\rho_f h_f U_f T_f)}{\partial x} + \frac{\partial(\rho_f h_f W_f T_f)}{\partial z} \right) + \bar{h}_{fF} (T_f - T_{F_i}) - \bar{h}_{Sf} (T_{S_o} - T_f)$$

$$= \left(U_f h_f \frac{\partial P_f}{\partial x} + W_f h_f \frac{\partial P_f}{\partial z} \right) + \frac{12\mu_f}{h_f} \left\{ W_f^2 + \frac{1}{3} U_m + (U_f - U_m)^2 \right\}$$

Convection of heat
by fluid flow +
diffusion to
bounding surfaces
= compression
work + dissipated
energy

Heat flow paths in rotor - GFB system



Heat flows & thermal resistances in a GFB & hollow shaft

Heat conducted into bearing

Cooling gas streams carry away heat

THD Model Validation

Published data

Generation I GFB with single top foil and bump strip layer

Parameters	Value / comment	
Bearing cartridge		
Bearing inner radius	25 mm	Ref. [7]
Bearing length	41 mm	Ref. [7]
Bearing cartridge thickness	5 mm	Assumed
<i>Nominal</i> radial clearance	20 μm	Assumed
Top foil and bump strip layer		
Top foil thickness	127 μm	Ref. [21]
Bump foil thickness	127 μm	Ref. [21]
Bump half length	1.778 mm	Assumed
Bump pitch	4.064 mm	Assumed
Bump height	0.580 mm	Assumed
Number of bumps x strips	39 x 1	Assumed
Bump foil Young's modulus	200 GPa	
Bump foil Poisson's ratio	0.31	
Bump foil stiffness	10.4 GN/m ³	

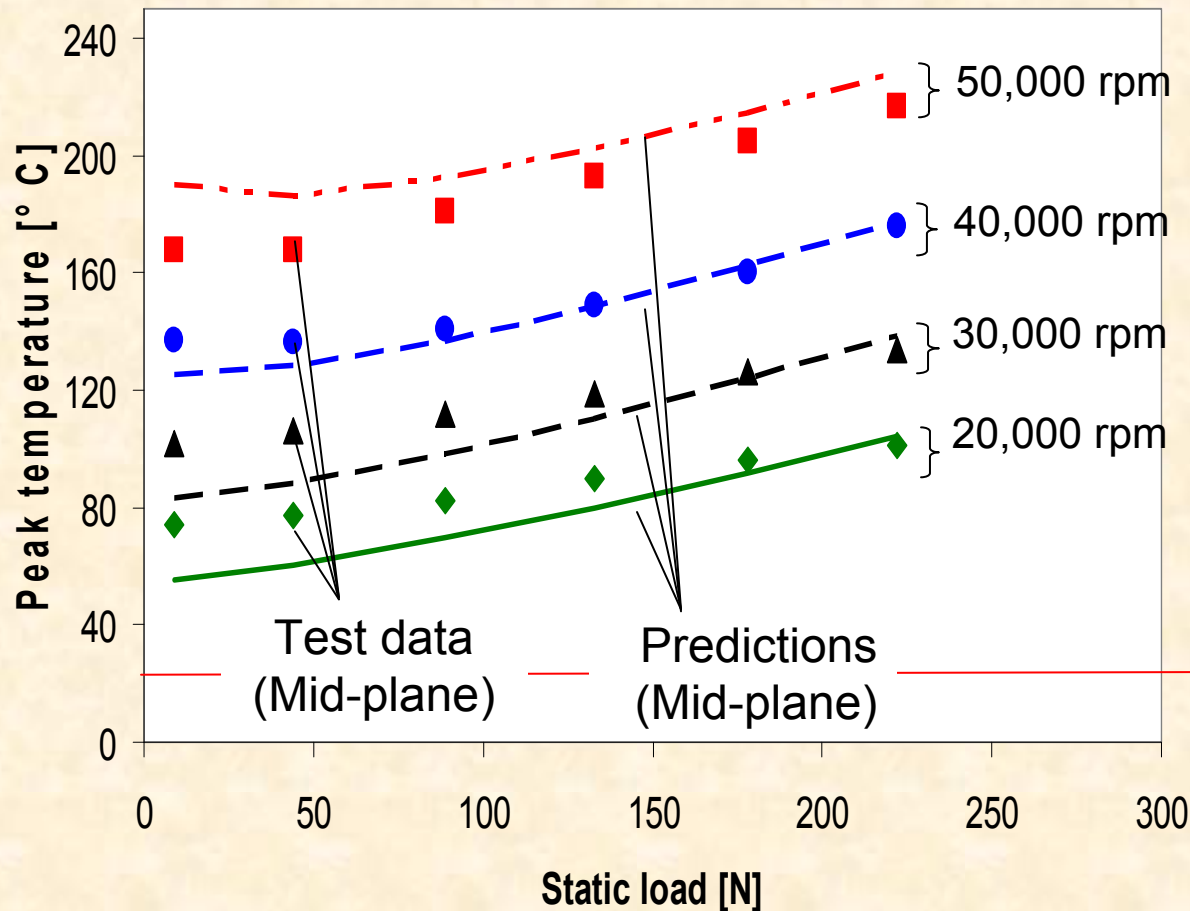
Parameters	Value
Gas properties at 21 °C	
Gas Constant	287 J/(kg·°K)
Viscosity	10 ⁻⁵ Pa·s
Conductivity	0.0257 W/m°K
Density	1.164 kg/m ³
Specific heat	1,020 J/kg°K
Ambient pressure	1.014 x 10 ⁵ Pa

Gas viscosity & density & conductivity, foil Young's modulus, and clearance change with temperature.

Radil and Zeszotek, 2004
Dykas and Howard, 2004

Peak film temperature

Predictions & test data



Supply air (T_{Supply}),
shaft (T_S), and
bearing OD (T_B)
temperatures at 21 °C.

$T_{Supply} = 21^\circ\text{C}$

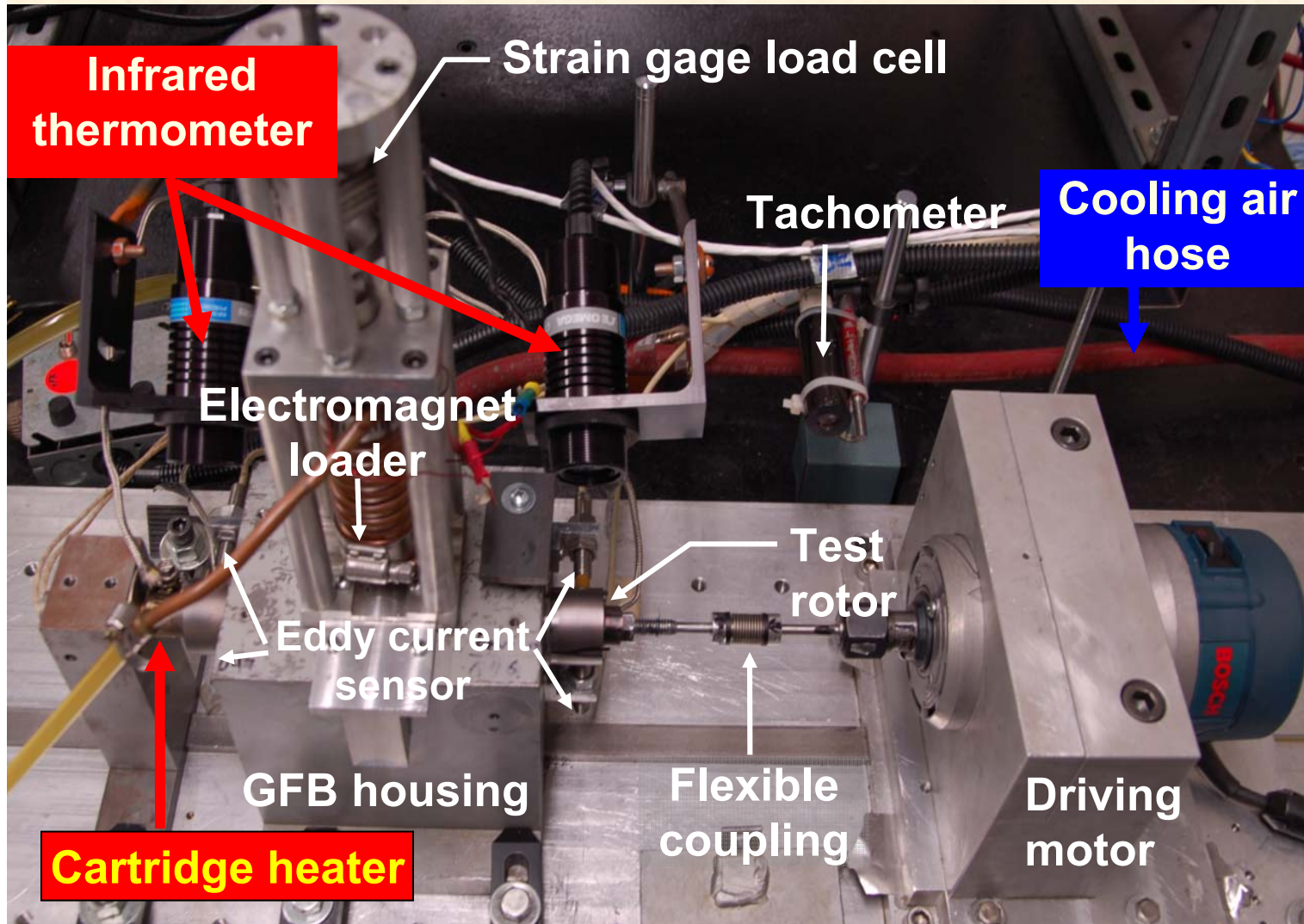
Predictions & test data Radil and Zeszotek, 2004

Read more in **ASME**
Paper GT2009-59919

Film temperature + higher than ambient, even for small load of 9 N.
Good agreement preds with test data

2008 rotor-GFB test rig

Max. temp. 130 °C



Drive motor
(25 krpm).

Cartridge
heater max.
temperature:
300F

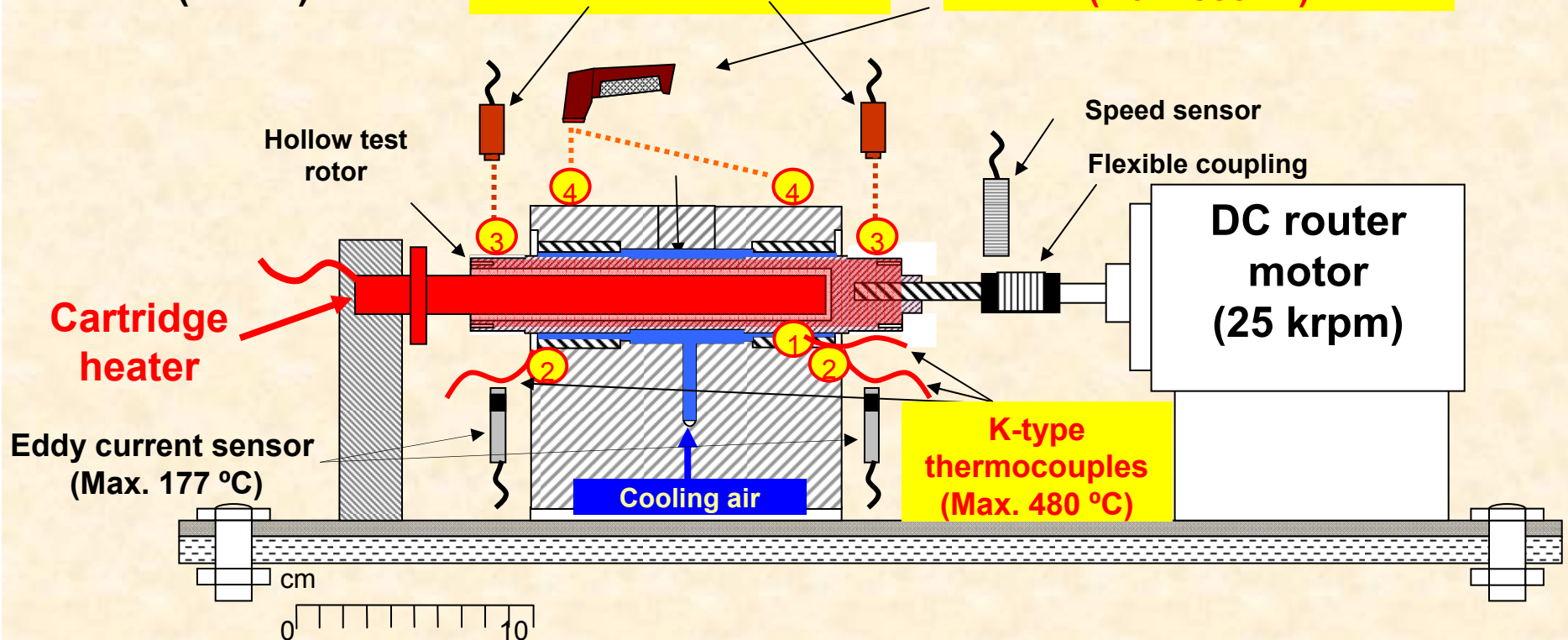
Air flow meter
(Max. 100
L/min at 14
psig)

2008 hot rotor-GFB test rig

Ambient temp. (T_a)
~ 22 °C (71 °F)

Infrared Thermometer
(Max. 540 °C)

Infrared Thermometer gun
(Max. 500 °C)



- ① Bearing sleeve temperature (at five locations along circumference)
- ② Bearing outer surface temperature (Drive and bearing and free end bearing)
- ③ Rotor surface temperature (Drive end and free end)
- ④ Bearing support (housing) surface temperature (Drive end and free end)

Numbers in circles show locations of temperature measurement.

THD Model Validation

Bearings at TAMU

Parameter [mm]	Foster-Miller (2 nd gen.)	KIST (1st gen.)	MiT (2 nd gen.)
Bearing cartridge			
Outer diameter	50.85	50.80	44.575
Inner diameter	39.36	37.95	37.921
Top foil and bump strip layer			
Top foil axial length	38.2	38.1	25.4
Top foil thickness	0.100	0.120	0.127
Bump foil thickness	0.100	0.120	0.102
Number of Bumps	25 × 5 axial	26 × 1 axial	24 × 3 axial
Bump pitch	4.581	4.300	4.640
Bump length	3.742	2.100	3.950
Bump height	0.468	0.540	0.510
Bump arc radius	5.581	4.161	4.079
Bump arc angle [deg]	68	59	58

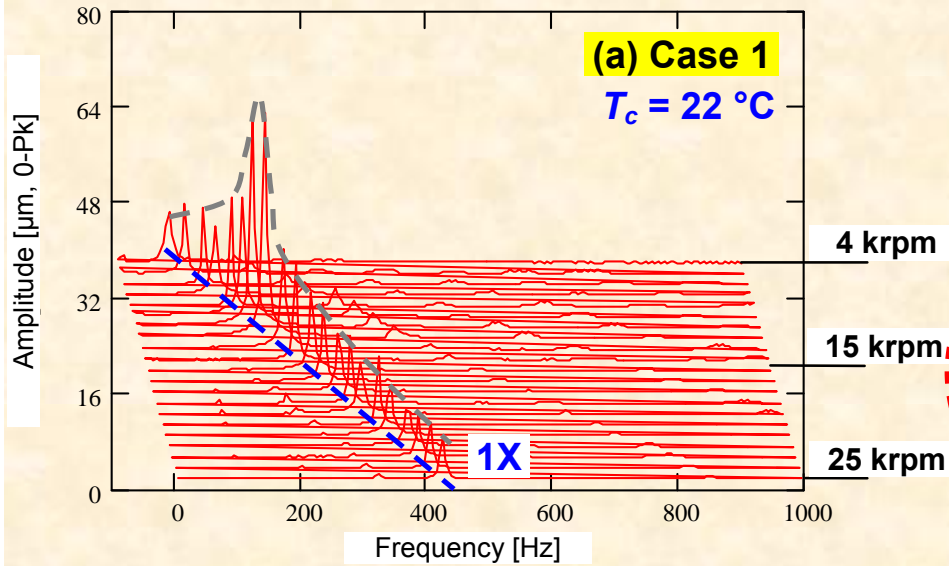
Elastic Modulus 214 GPa,
Poisson ratio=0.29

**Foster-Miller FB with Teflon®
coating (Generation II)**

Waterfall plots: coastdown responses

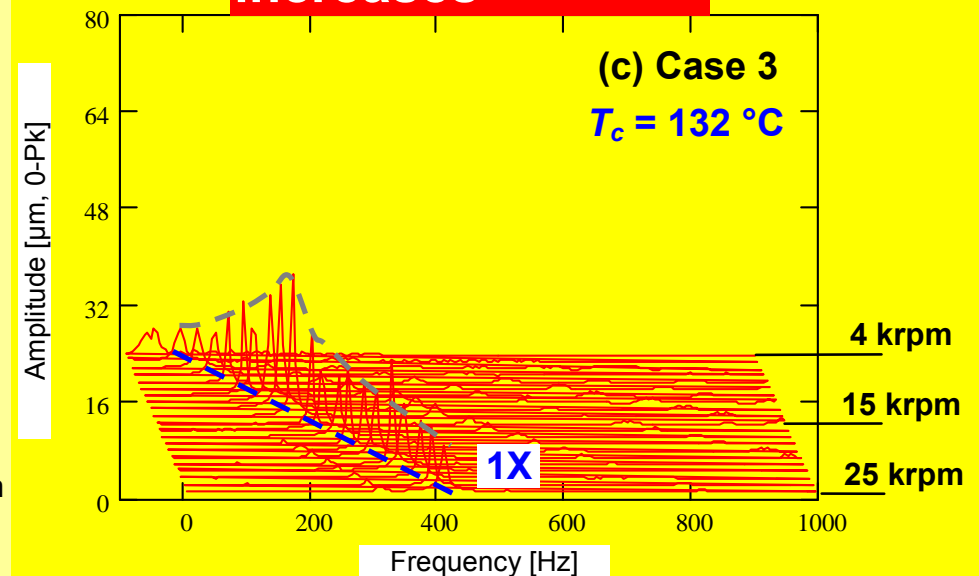
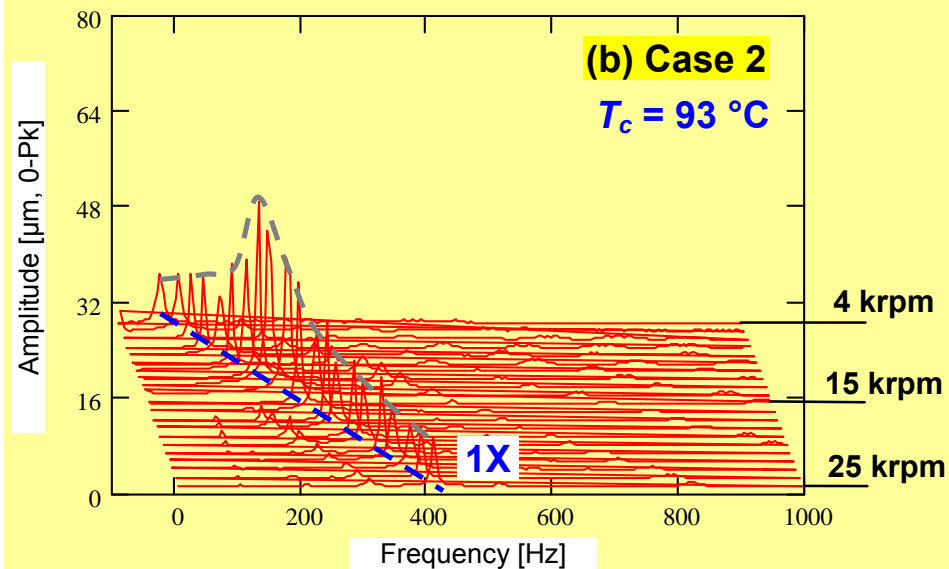
Case 1-3 without cooling flow, $T_a \sim 22^\circ\text{C}$, and $T_{hs} = 22^\circ\text{C}$, 93°C , and 132°C

FE – vertical plane



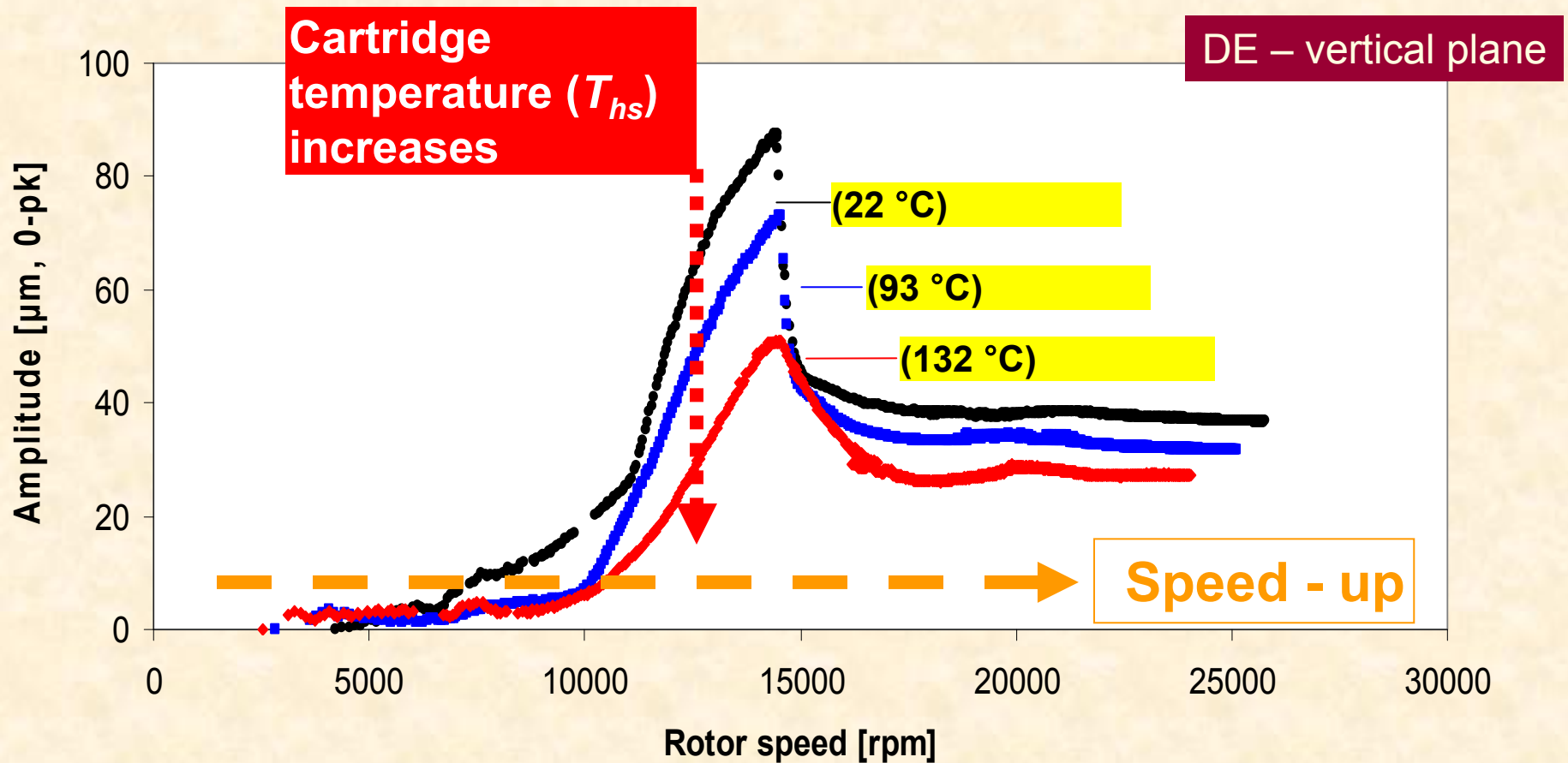
1X component dominant, i.e.,
no subsynchronous motion,
during coastdown tests

Cartridge
temperature (T_{hs})
increases



Rotor speed up 1X response

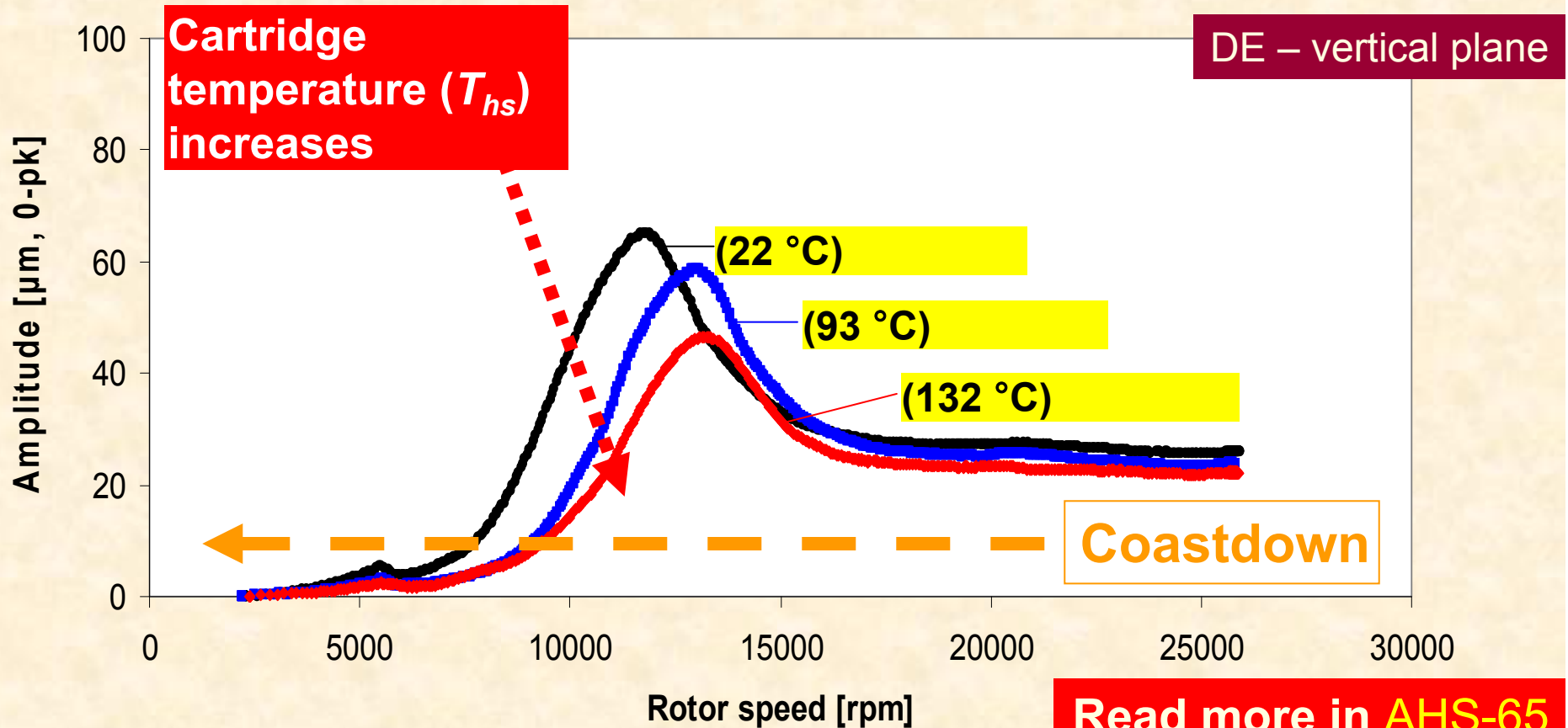
W/o cooling flow, $T_a \sim 22^\circ\text{C}$, and $T_{hs} = 22^\circ\text{C}, 93^\circ\text{C} \text{ \& } 132^\circ\text{C}$



Above critical speed ~ 14.5 krpm, amplitude drops. A nonlinearity! As T_{hs} increases, the peak amplitude decreases.

Rotor coastdown 1X response

W/o cooling flow, $T_a \sim 22^\circ\text{C}$, and $T_{hs} = 22^\circ\text{C}$, 93°C , and 132°C



Read more in [AHS-65](#)
2009 Paper

As T_{hs} increases, critical speed raises by ~ 2 krpm and the peak amplitude decreases. Nonlinearity absent!

Topic

- Statement of Work & Sources for Presentation
- Objectives and accomplished work in 07-08

Computational model. Validation with published data.
Rotordynamic measurements at TAMU

- **Objectives and accomplished work in 2008-09**

Description of test rig and foil bearings at TAMU

**Effect of temperature on bearing temperatures,
coastdown speed and rotor motions**

**Effect of cooling flow on bearing and shaft
temperatures. Validation of computational model**

- * The computational code

Graphical User Interface. Further predictions

- GFB thermal management tests and preds.
- Closure & added value

Research Objectives 2008-09

Model validation with TAMU FB test data

- Complete test rig using cartridge heater for high temperature operation (up to 360C)
- Measure rotordynamic performance during speed coastdown from 30 krpm and for increasing shaft temperatures
- Quantify effect of side flow on cooling bearings (max. 150 LPM per bearing)
- Benchmark model predictions

THD Model Validation

Bearings at TAMU

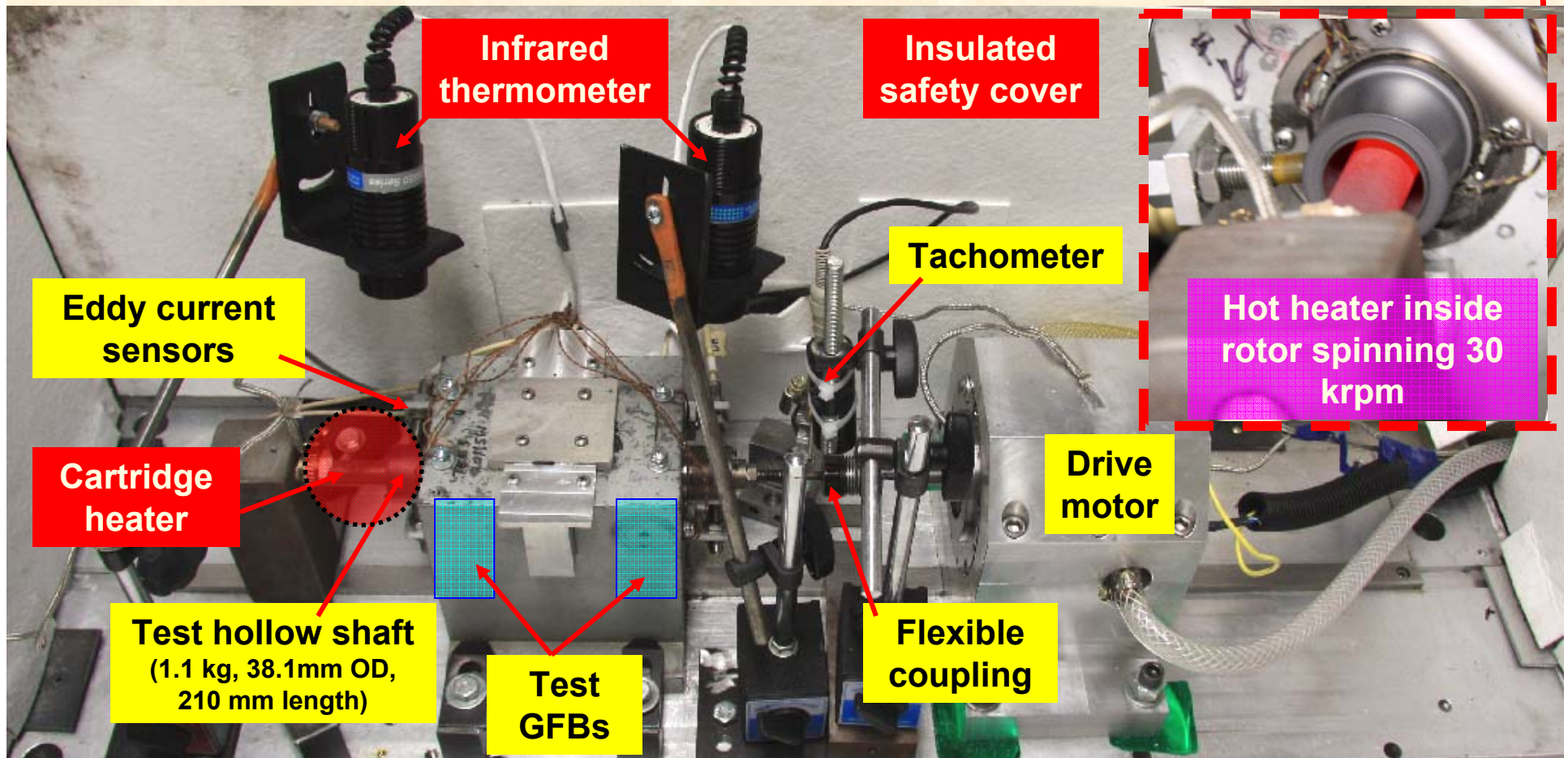
Parameter [mm]	Foster-Miller (2 nd gen.)	KIST (1st gen.)	MiT (2 nd gen.)
Bearing cartridge			
Outer diameter	50.85	50.80	44.575
Inner diameter	39.36	37.95	37.921
Top foil and bump strip layer			
Top foil axial length	38.2	38.1	25.4
Top foil thickness	0.100	0.120	0.127
Bump foil thickness	0.100	0.120	0.102
Number of Bumps	25 × 5 axial	26 × 1 axial	24 × 3 axial
Bump pitch	4.581	4.300	4.640
Bump length	3.742	2.100	3.950
Bump height	0.468	0.540	0.510
Bump arc radius	5.581	4.161	4.079
Bump arc angle [deg]	68	59	58

Elastic Modulus 214 GPa,
Poisson ratio=0.29

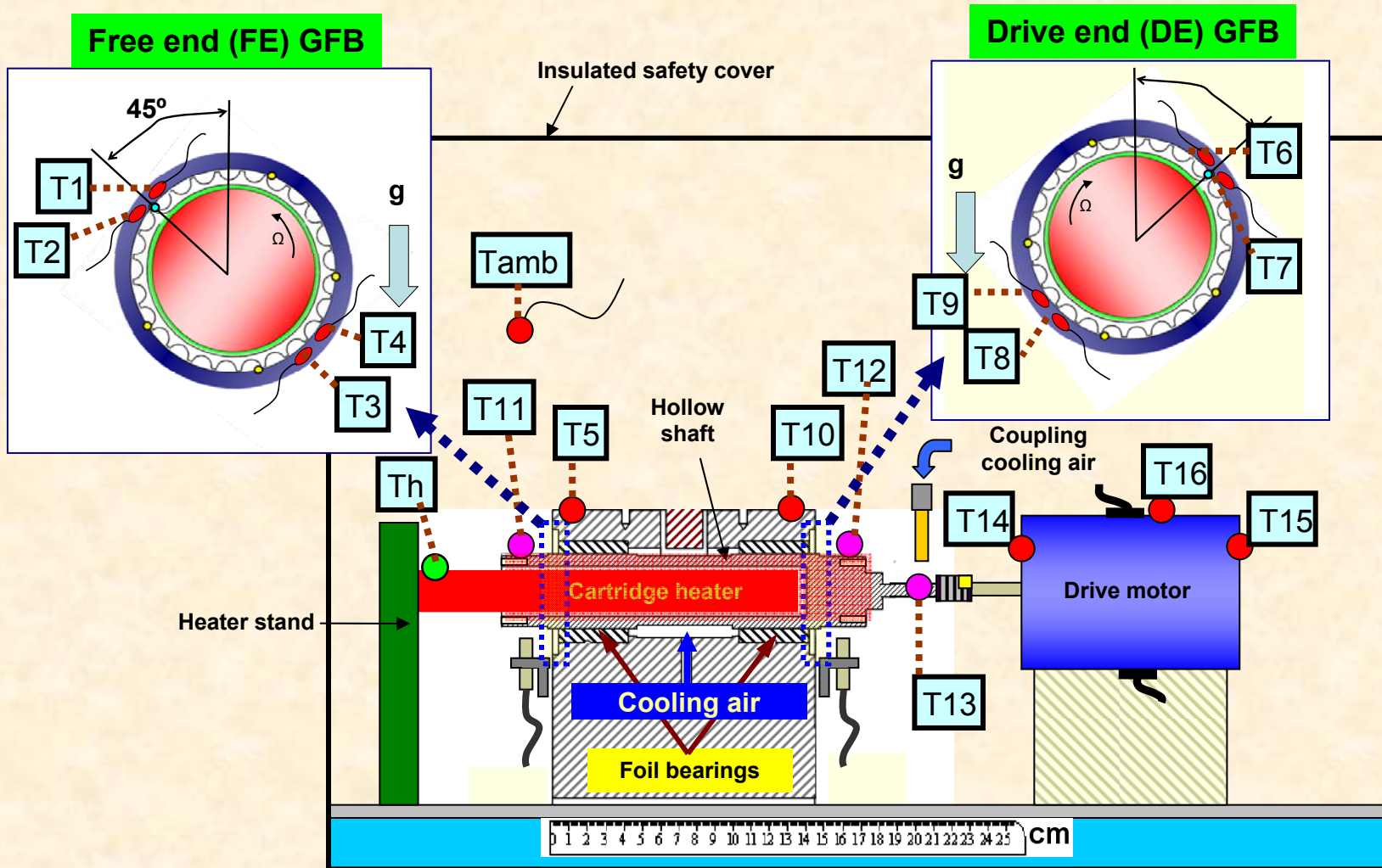
2009 hot rotor-GFB test rig

Max. 360 °C

Instrumentation for high temperature. Insulation casing
Gas flow meter (Max. 500 LPM). Drive motor (max. 65 krpm)

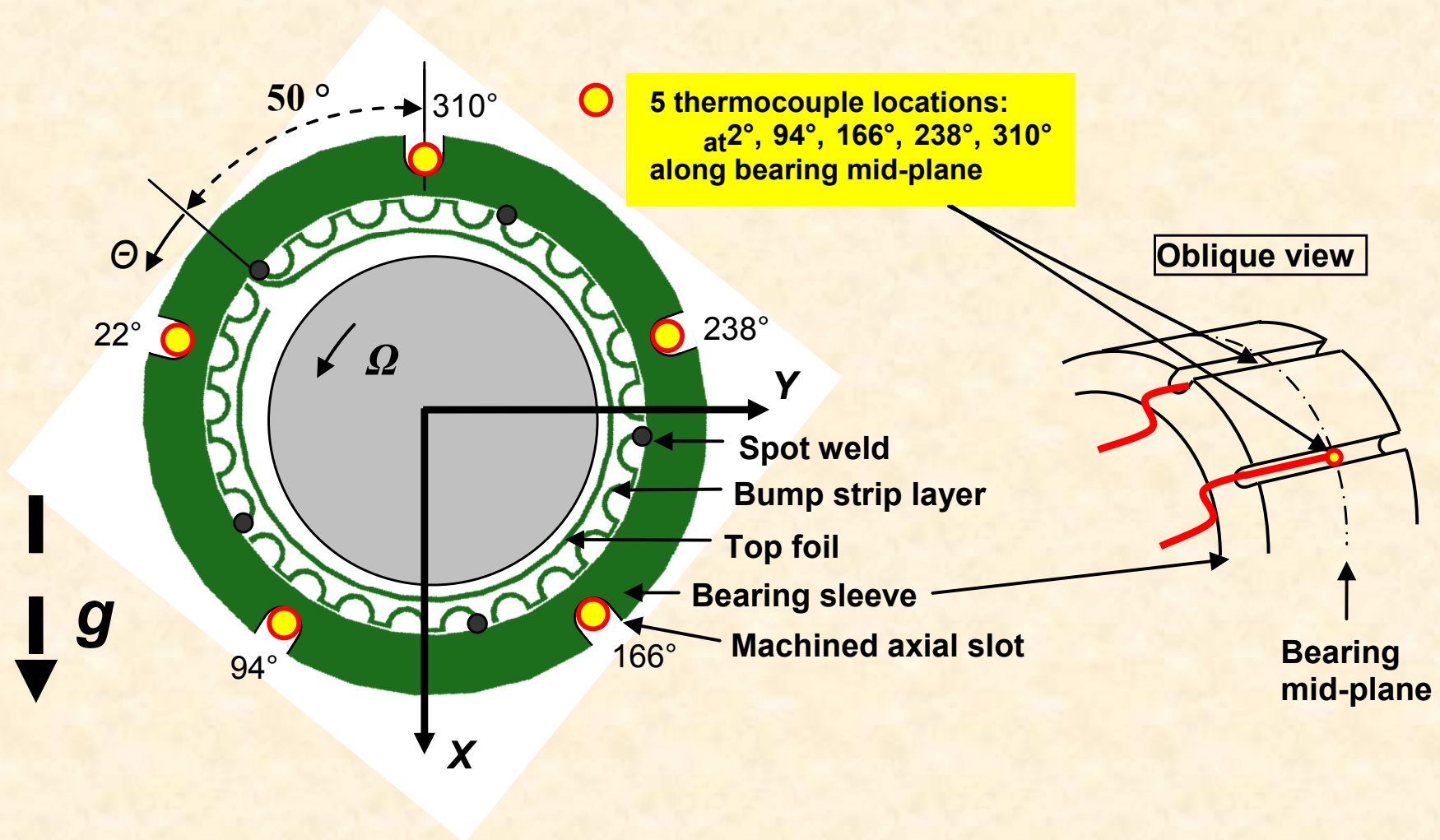


Thermocouples in test rotor-GFB rig



Overall 15 thermocouples for GFB cartridge outboard, Bearing support housing surface, Drive motor, Test rig ambient, and Cartridge heater temperatures
Two noncontact infrared thermometers for rotor surface temperature

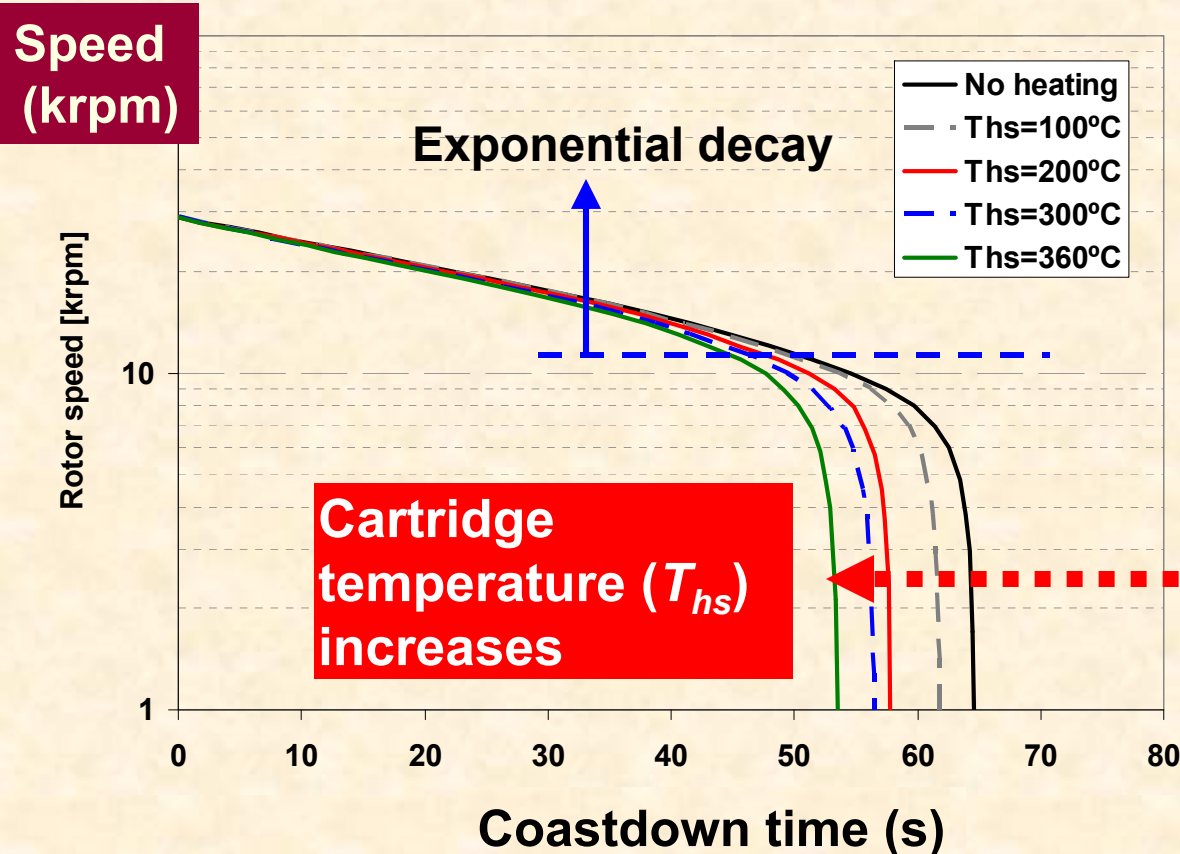
Thermocouples in test GFB



Foster-Miller FB uncoated (Generation II)

five (5) thermocouples placed within machined axial slots.

Time to coast down rotor Effect of shaft temperature

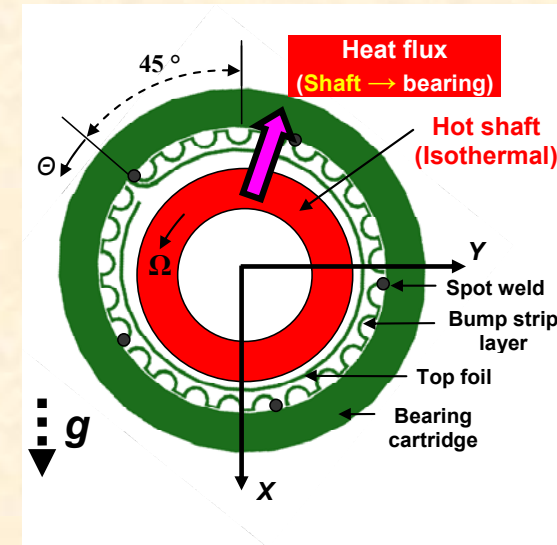
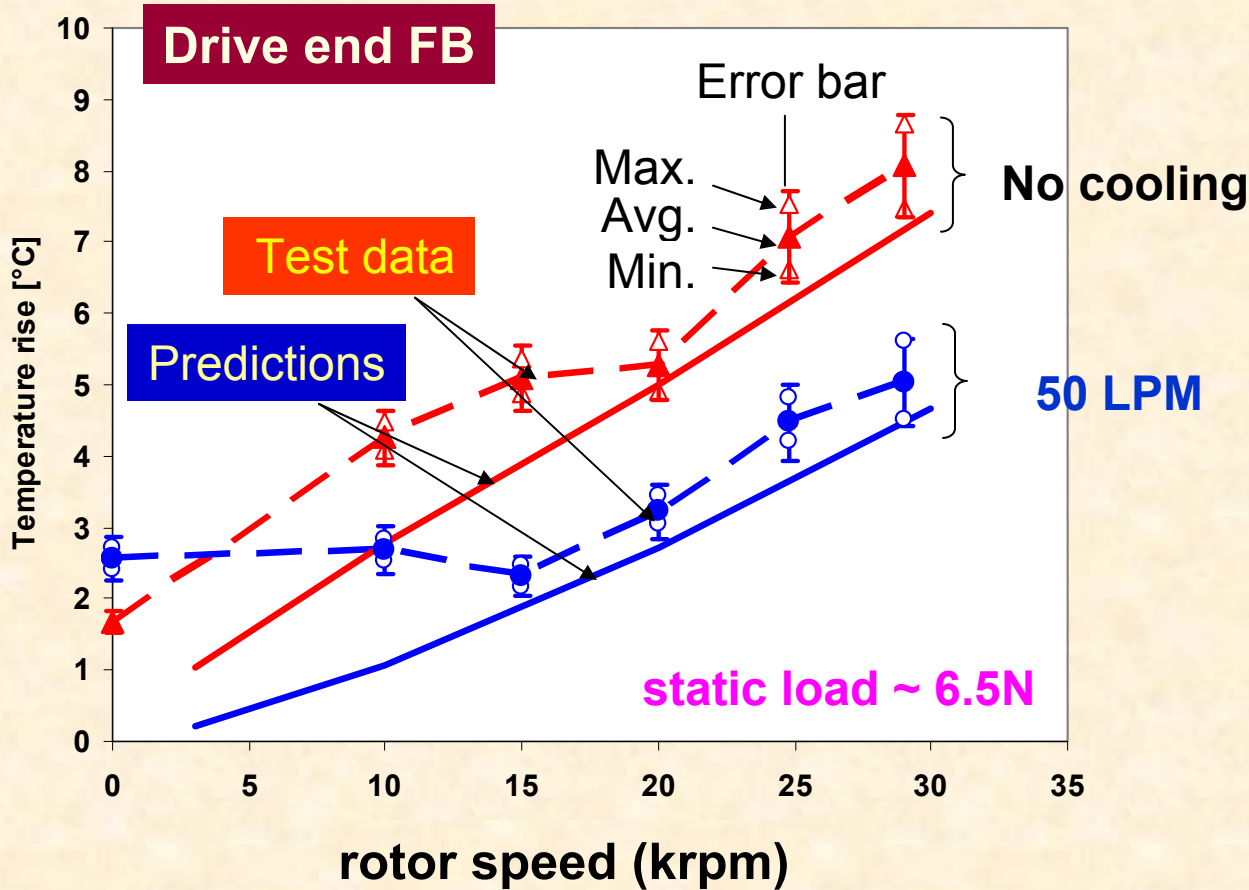


Baseline,
Heater up to 360C.
No forced cooling

Long time to coastdown :
very low viscous drag
(no contact between rotor and bearings)

Test Data Coastdown time lesser as rotor heats (reduced clearance)

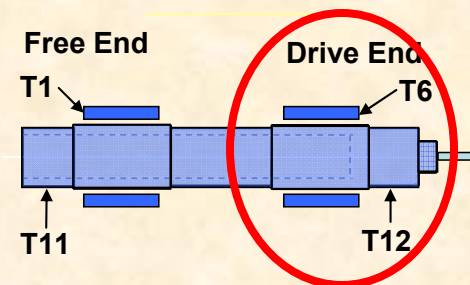
Bearing outboard temperature predictions & test data



Room temperature 21 °C.

Heater OFF
w/o and w low cooling

Rotor speed : 30 krpm

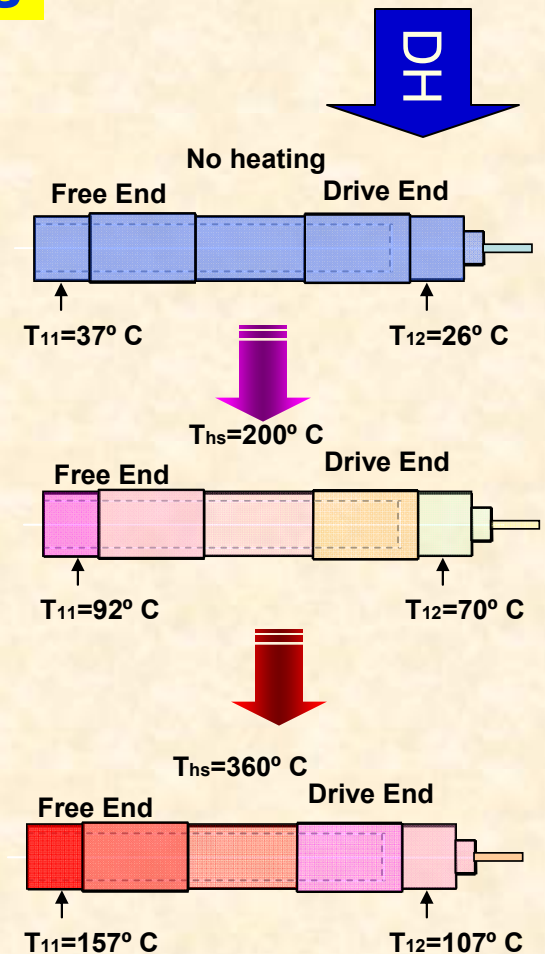
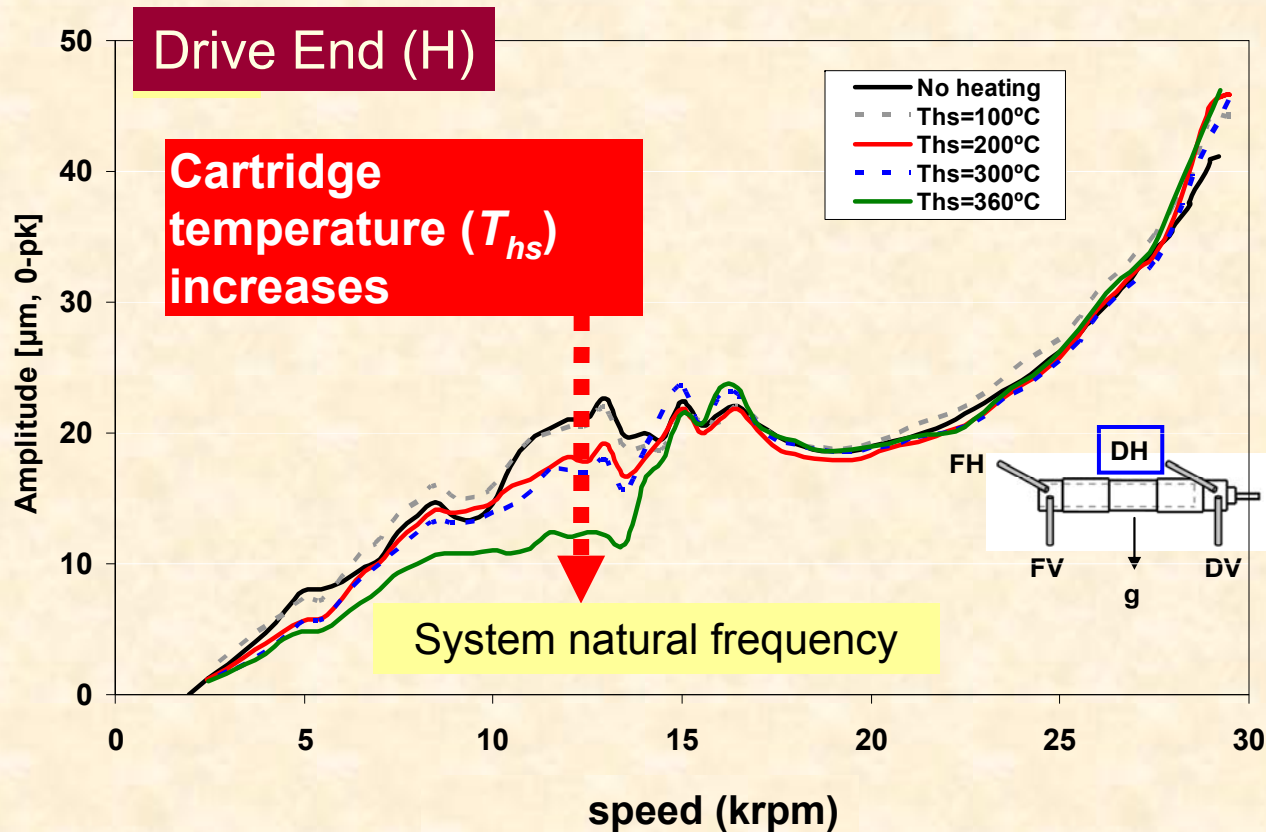


Test data & predictions

FB OD temperature rises with rotor speed and decreases with forced cooling stream ~ 50 LPM. Predictions agree with test data

1X response as rotor heats Tests

Baseline. Heater to 360C. No forced cooling

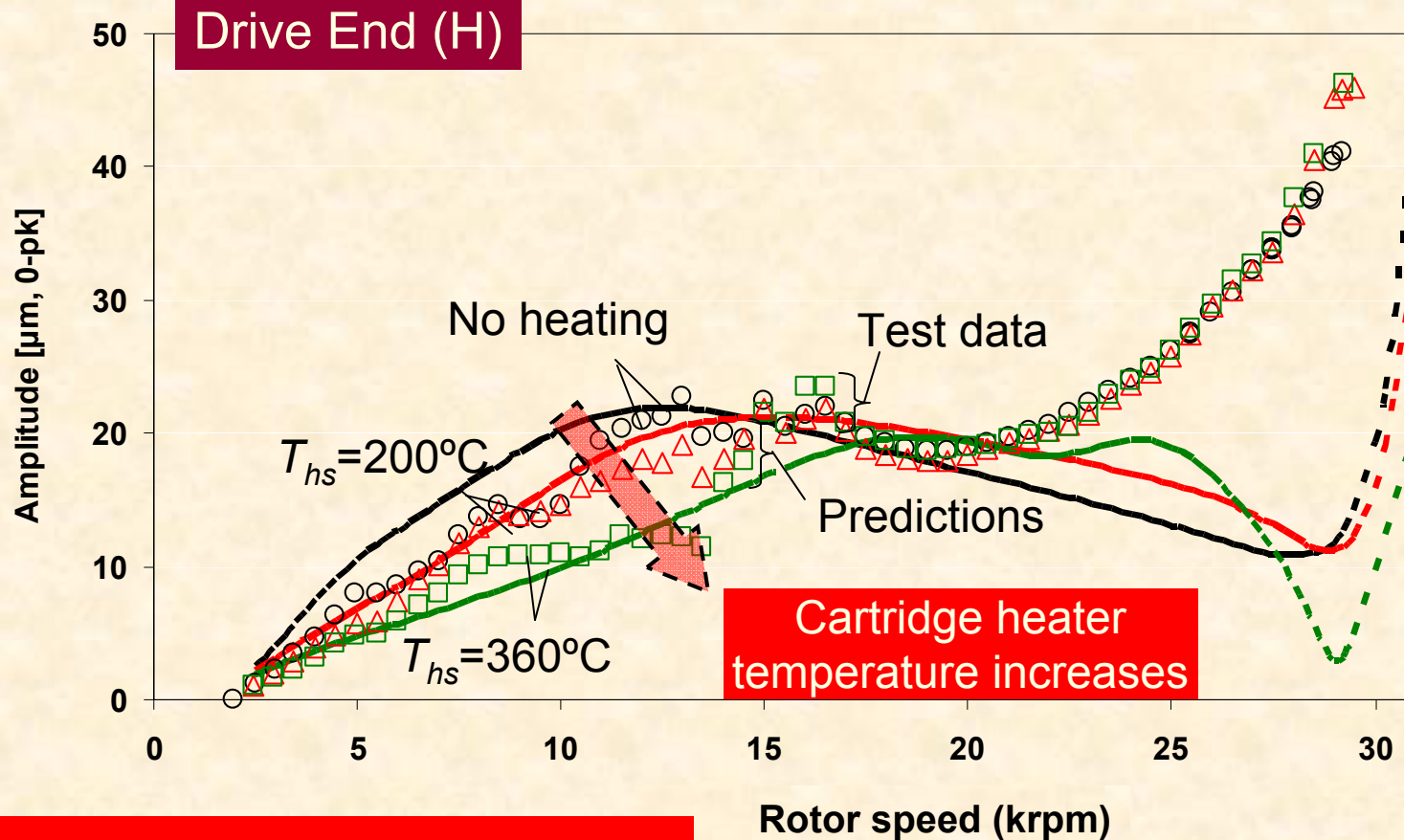


Test Data

As heater T increases to 360°C , peak motion amplitude decreases in speed range 7 krpm to 15 krpm

1X rotor response predictions & tests

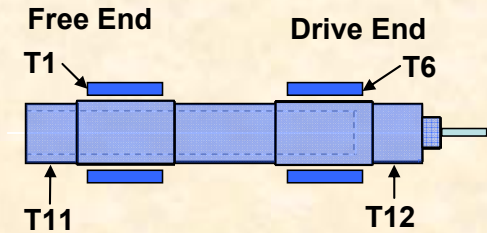
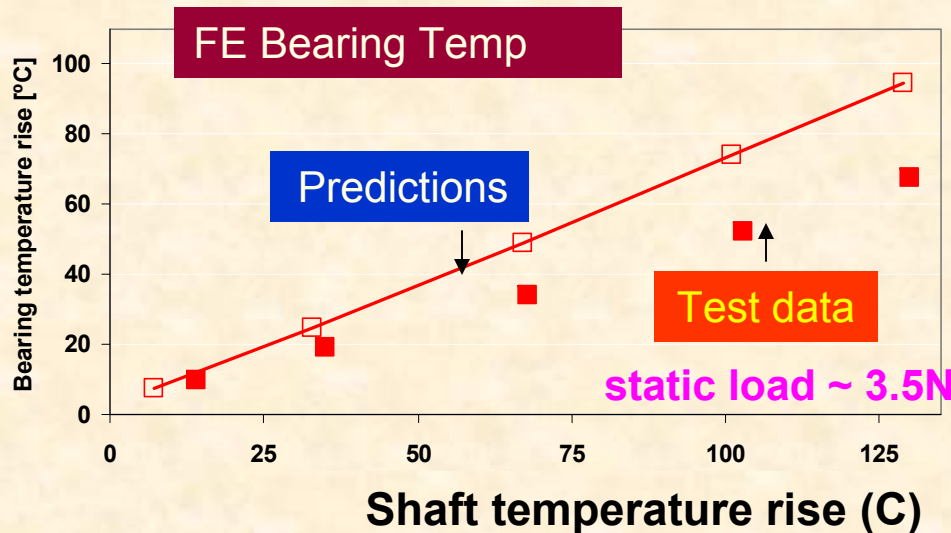
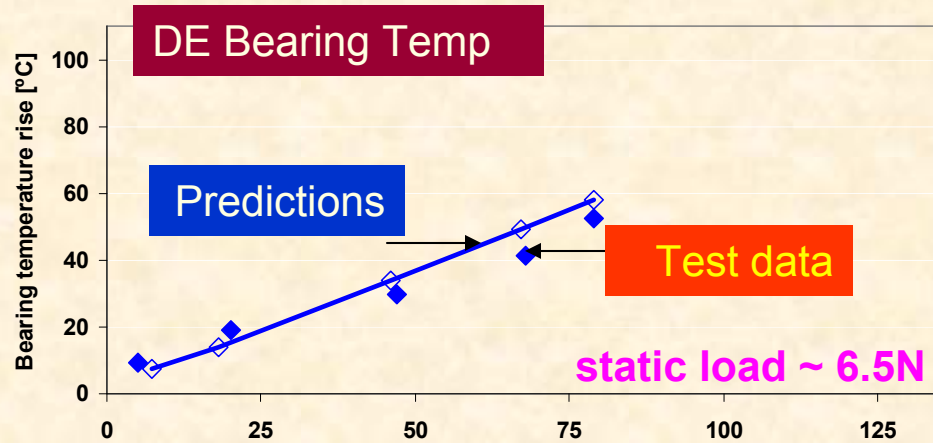
Baseline. Heater to 360C. No forced cooling



Test data & predictions

As heater temperature raises, rotor amplitude decreases for speed < 15 krpm & the critical speed increases from 14 krpm to 17 krpm

Bearing outboard temperature predictions & tests



Supply air (T_{Supply}) ~ 21 °C.

Heater up to 360C.

No cooling flow

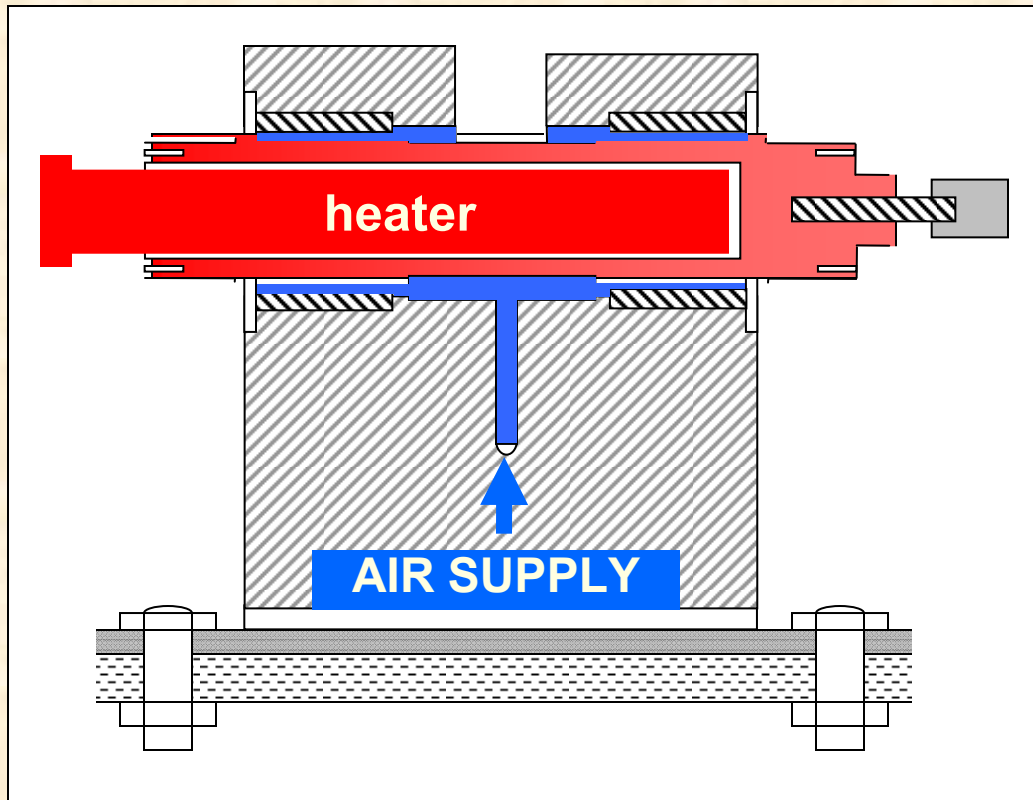
Rotor speed : 30 krpm

Test data & predictions

FB cartridge temperature increases linearly with shaft temperature

Cooling gas flow into GFBs

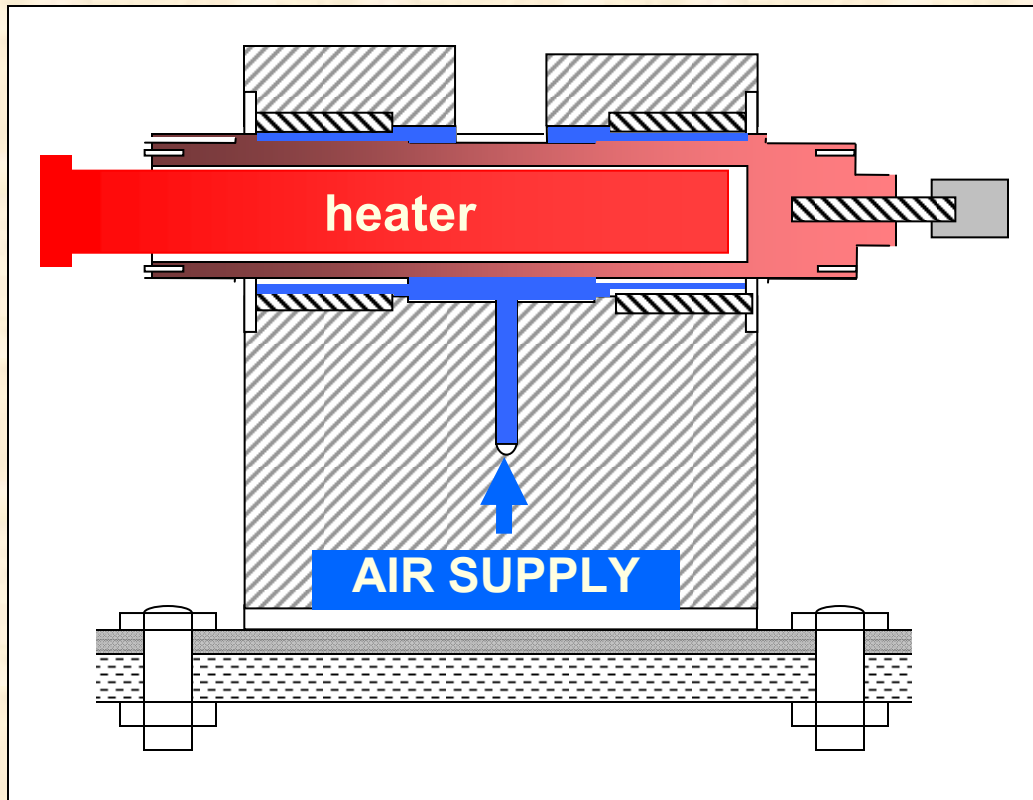
Gas pressure Max. 100 psi



Cooling flow needed for thermal management: to remove heat from shear drag or to reduce thermal gradients in **hot/cold** engine sections

Cooling gas flow into GFBs

Gas pressure Max. 100 psi




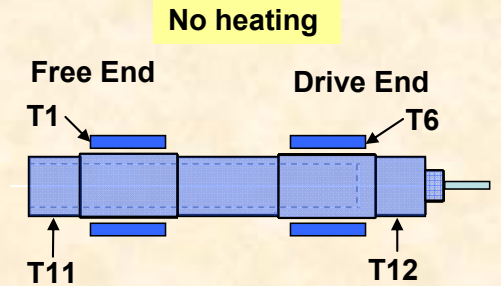
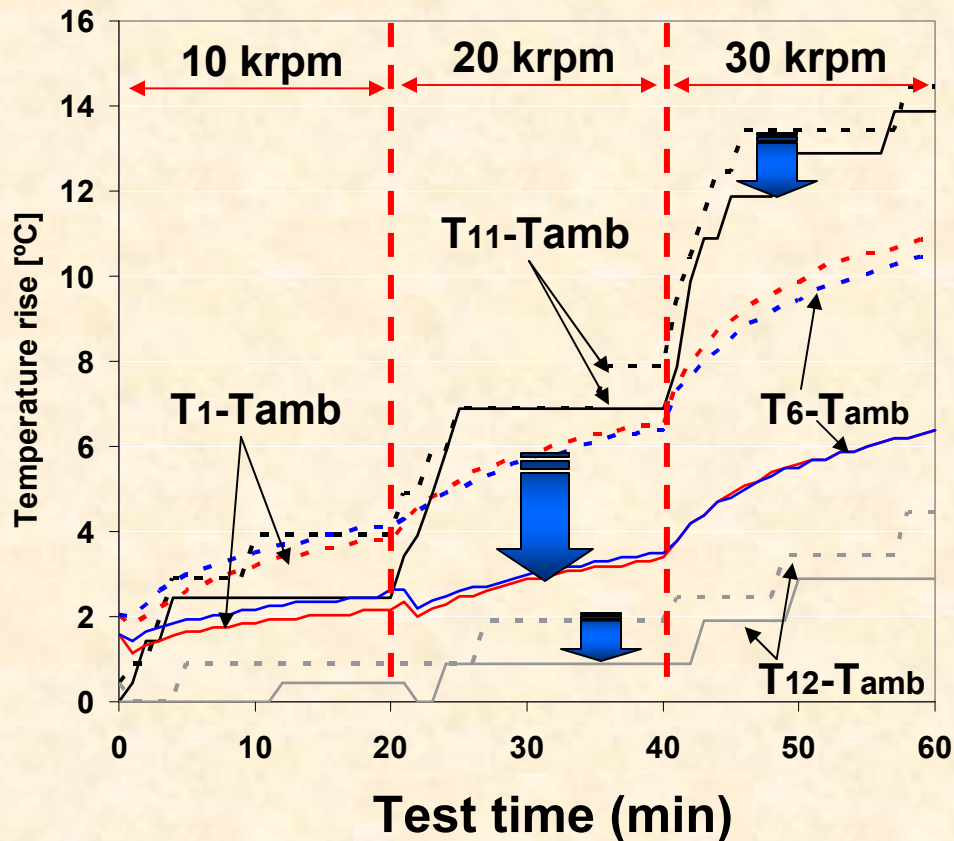
Heater warms unevenly rotor.

Side cooling cools unevenly rotor and also heater

Heating of rotor Effect of rotor speed and side cooling

Baseline imbalance, **No side flow & 50 L/min**

 : Temp. drop due to 50L/min cooling flow



Bearing cartridge and rotor temperatures increase steadily with time

Rotor speed : 10, 20, 30 krpm

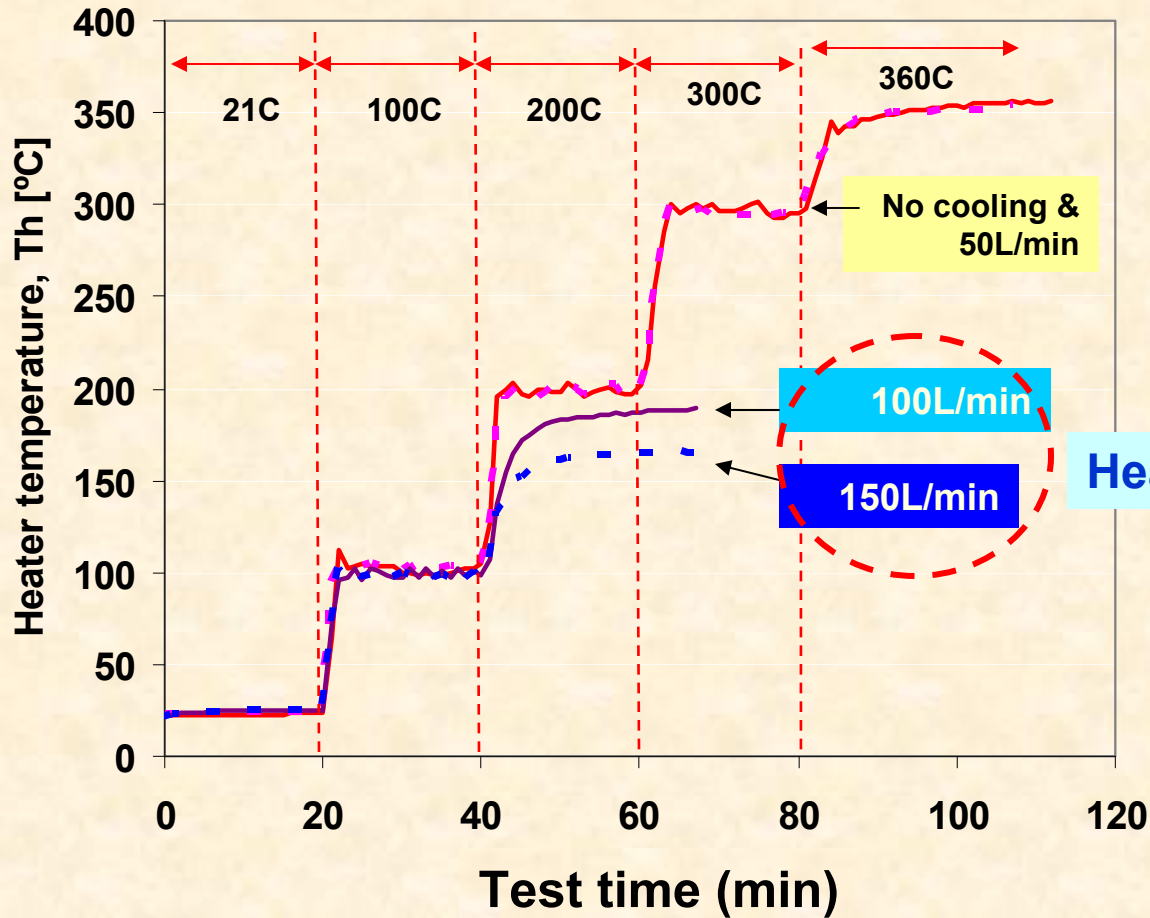
Rotor speed makes rotor and bearings hotter

Cooling flow removes heat from shear dissipation in rotor, most effective at high speed

Test Data Heater OFF

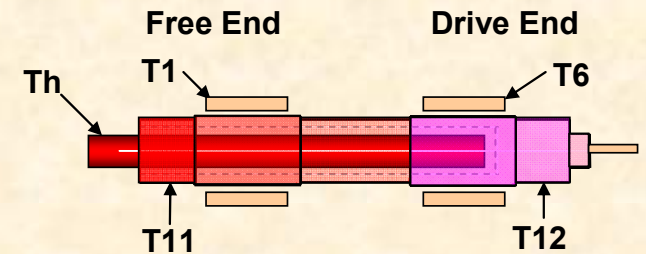
Heater temperature Effect of cooling flow

Heater temperature increases



Heater up to 360C
w/o & w cooling flows

Rotor speed : 30 krpm

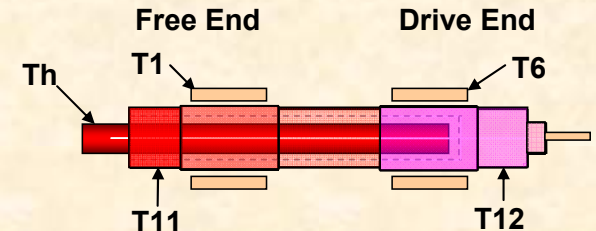
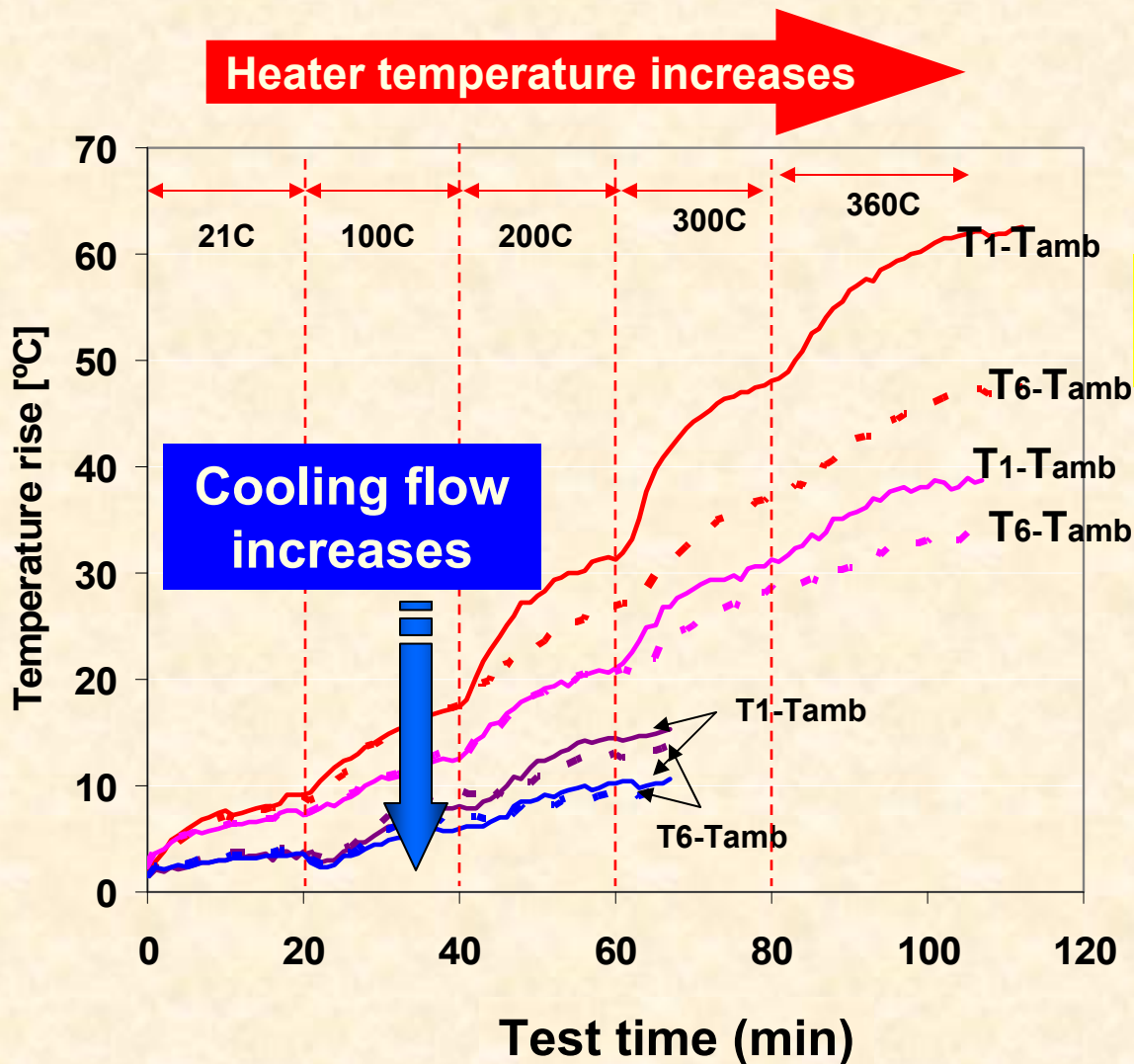


Heater power is limited

Test Data Cooling > 100 LPM cools both rotor & HEATER!

Bearings OD temperatures

Effect of cooling flow



High temp. (heater up to 360C).
Cooling flow up to 150 L/min

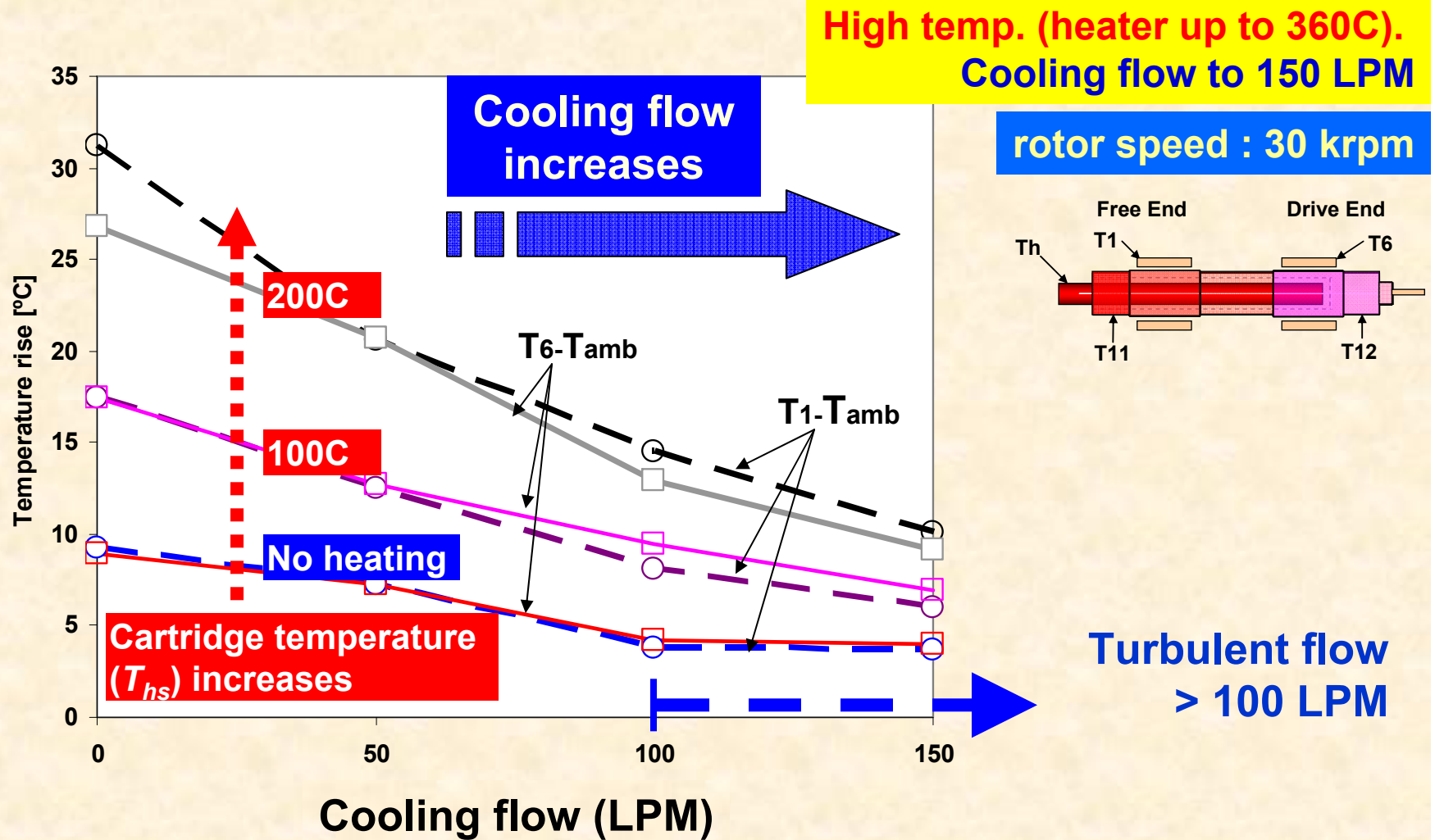
rotor speed : 30 krpm

Test Data

Cooling effective > 100 LPM and when heater at highest temperature

Bearing cartridge temperature

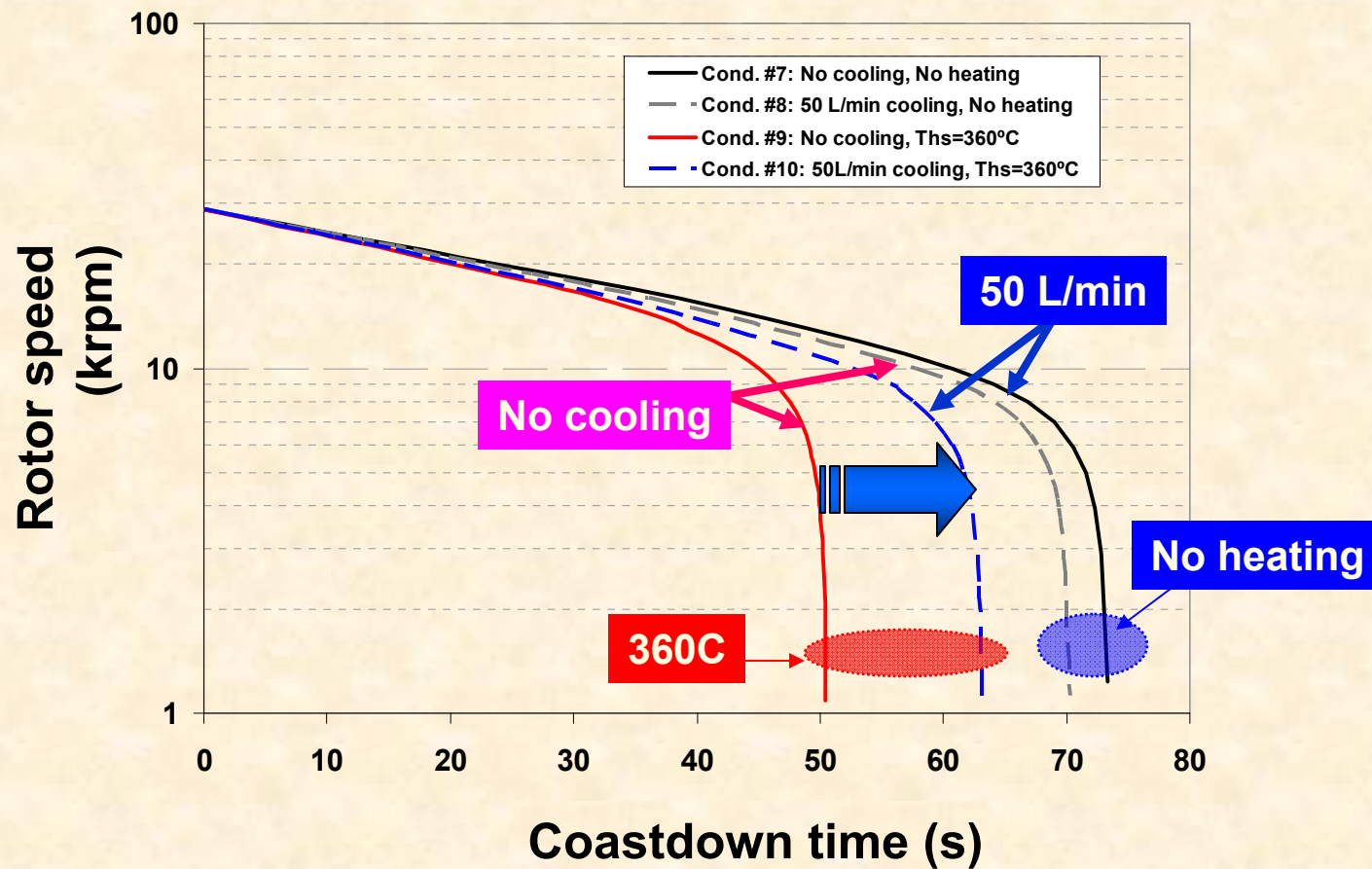
Effect of cooling flow



Test Data

Bearing OD temperature decreases with cooling flow

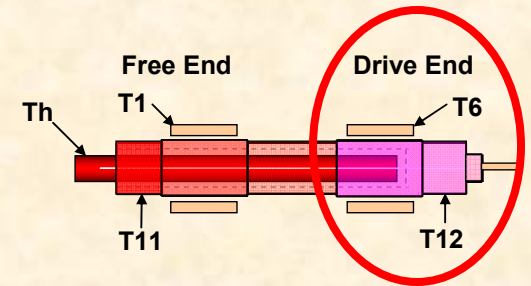
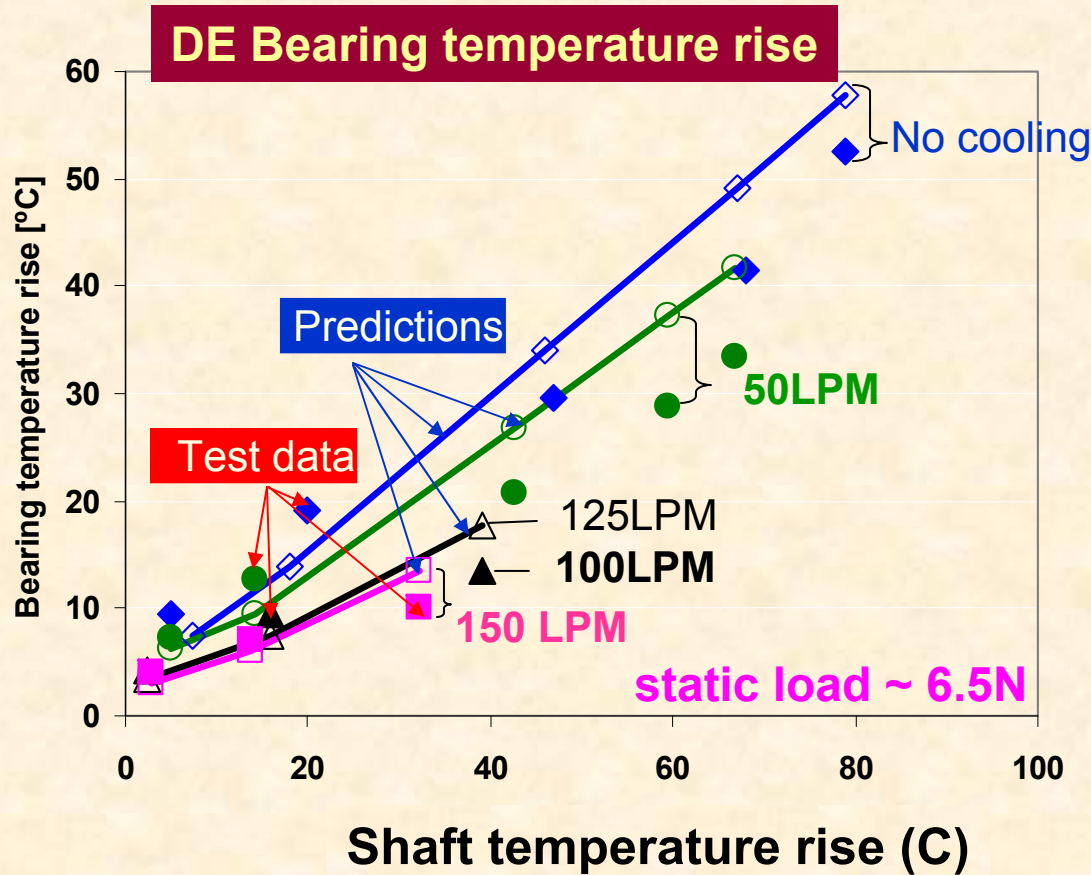
Time to coast down rotor Effect of cooling flow



Test Data Coastdown time down by 20% (13 s) with cooling at 50 LPM

Bearing cartridge temperature

Predictions & tests



Test data & predictions

As cooling flow rate increases, FB cartridge temperature decreases. Predictions agree with test data.

Post-test condition of rotor and GFBs

Before operation

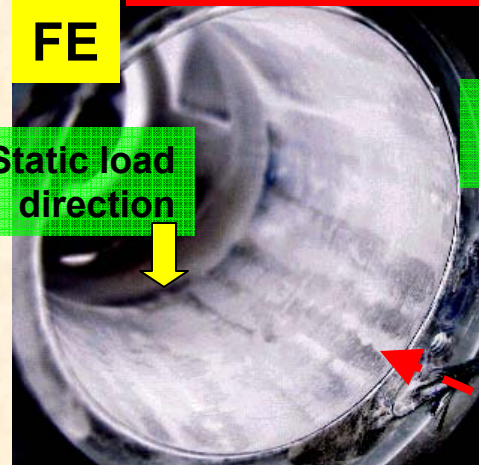


UNCOATED top foil !

After extensive heating with rotor spinning

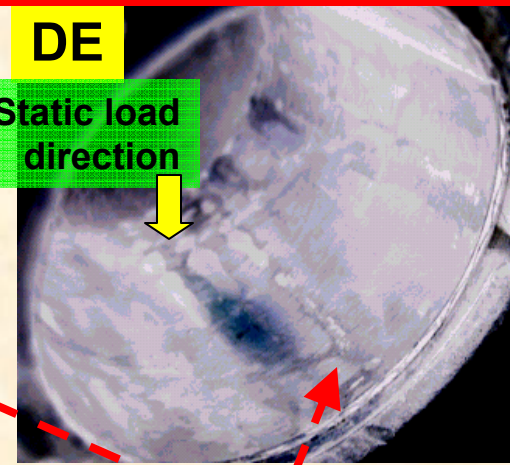
FE

Static load direction



DE

Static load direction



Wear marks on top foils are at side edges

Before operation



FE

DE

After extensive hearing with rotor spinning tests



Rotor shows polishing marks at bearing locations. Deep wear marks at outboard edges

Test data & predictions

- **Amplitudes of rotor synchronous motion proportional to added imbalances.**
- **For operation with hot shaft, amplitude of rotor motion drops while crossing (rigid body mode) critical speed.**
- **As rotor and bearing temperatures increase, air becomes more viscous and bearing clearances decrease; hence coastdown time decreases.**
- **Thermal management with axial cooling streams is beneficial at high temperatures and with large flow rates ensuring turbulent flow conditions.**
- **Test foil bearings continue to survive high temperature & high vibration operation!**

Topic

- Statement of Work & Sources for Presentation
- Objectives and accomplished work in 07-08

Computational model. Validation with published data.
Rotordynamic measurements at TAMU

- Objectives and accomplished work in 2008-09

Description of test rig and foil bearings at TAMU

Effect of temperature on bearing temperatures,
coastdown speed and rotor motions

Effect of cooling flow on bearing and shaft
temperatures. Validation of computational model

* The computational code

Graphical User Interface. Further predictions

- GFB thermal management tests and preds.
- Closure & added value

The computational program

- **Windows XP OS and MS Excel 2003 (minimum requirements)**
- **Fortran 99 Executables for FE underspring structure and gas film analyses. Prediction of forced – static & dynamic- performance.**
- **Excel® Graphical User Interface (US and SI physical units). Input & output (graphical)**
- **Compatible with XLTRC² and XLROTOR codes**

Code: XL_GFB_THD

Delivered on June 2009

Graphical User Interface

XL GFB TH™ Spreadsheet for hydrodynamic foil GAS bearings

Version 1.0. Copyright 2009 by Texas A&M University. All rights reserved. Dr. Luis San Andres & Dr. Tae Ho Kim

NOTE to USER : Enter input values in gray cells. Yellow cells show output values.

Provide information for COOLING STREAMS, AMBIENT CONDITIONS, and BEARING CARTRIDGE/SHAFT TEMPERATURES AND MATERIALS. Select gas and shaft/bearing materials in dropdowns to see their material properties at 21 deg C.

PHYSICAL MODEL

SI

Hot hollow shaft - gas foil bearing model
with (1) OUTER COOLING STREAM flowing through thin film region and underneath top foil and with (2) INNER COOLING STREAM flowing through hollow shaft

1. Run Shaft_Bearing Models

SELECT COOLING STREAM GAS

Cooling Streams		
Viscosity at Tambient	0.01932	c-Poise
Density at Tambient	1.1614	kg/m ³
Specific Heat	1007	J/(kg-K)
Thermal Conductivity	0.0243	W/(m-K)
Gas Constant	287	J/(kg-K)

Outer Cooling Stream

Outer stream flow rate	150	LPM
Outer stream temperature	21	deg C

Cooling streams

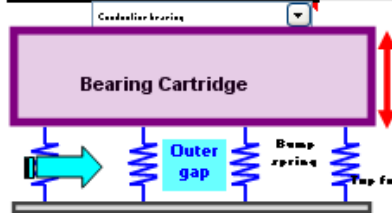
Inner Cooling Stream

Inner stream flow rate	0	LPM
Inner stream temperature	21	deg C

INPUT OPERATING CONDITIONS

Ambient pressure	1.013	bar
Ambient temperature	21	deg C

Bearing cartridge temperature option	
Cartridge temperature	50 deg C



Shaft temperature option	
Shaft temperature	150 deg C

SELECT BEARING & SHAFT MATERIAL

Bearing cartridge		
Wall thickness, t_b	6	mm
Elastic modulus, E_b	200	Gpa
Poisson's ratio, ν_b	0.284	
Density, ρ_b	7300	kg/m ³
Thermal Expansion Coefficient, S_b	1.73E-05	1/deg K
Thermal Conductivity, k_b	16.3	W/(m-K)
Specific Heat, c_b	473	J/(kg-K)
Expansion ?	2	

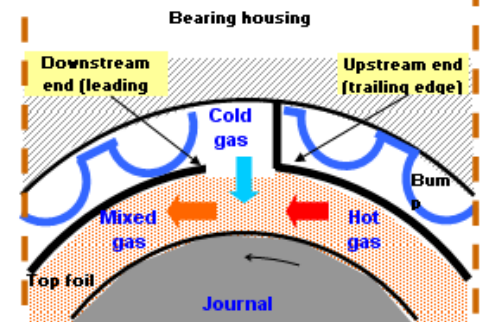
Hollow shaft		
Wall thickness, t_s	6.4	mm
Elastic modulus, E_s	210	Gpa
Poisson's ratio, ν_s	0.3	
Density, ρ_s	8003	kg/m ³
Thermal Expansion Coefficient, S_s	1.22E-05	1/deg K
Thermal Conductivity, k_s	42.7	W/(m-K)
Specific Heat, c_s	473	J/(kg-K)

SELECT TOP & BUMP FOIL MATERIAL

NOTE to USER : Enter THERMAL MIXING PARAMETER ($0 < \lambda < 1$, empirical value).

Thermal mixing conditions
at gap between top foil trailing edge and leading edge

INPUT OPERATING CONDITIONS



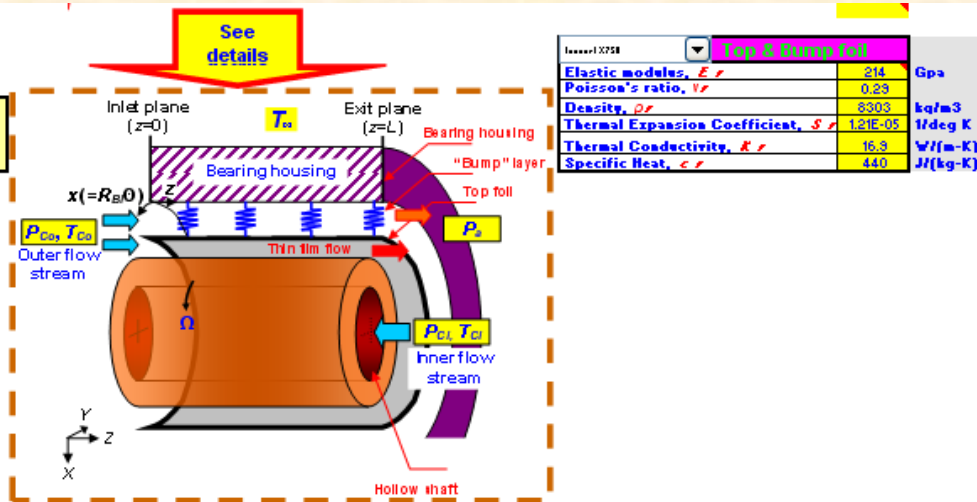
Thermal Mixing Parameter	
Mixing Parameter, λ	0.65

Thermal mixing parameter λ (<1): Empirical.
Low values: Cold gas feed conditions.
 $\lambda \sim 1$: little replenishment of fresh gas

Worksheet: Shaft & Bearing models (I)

Graphical User Interface

Modify Tables 1 and 2 below, if need more materials for gas, bearing, shaft and foil



Inconel X750		Top & Bump foil	
Elastic modulus, E	214	Gpa	
Poisson's ratio, ν	0.29		
Density, ρ	8303	kg/m ³	
Thermal Expansion Coefficient, α	1.21E-05	1/deg K	
Thermal Conductivity, k	16.3	W/(m-K)	
Specific Heat, c_p	440	J/(kg-K)	

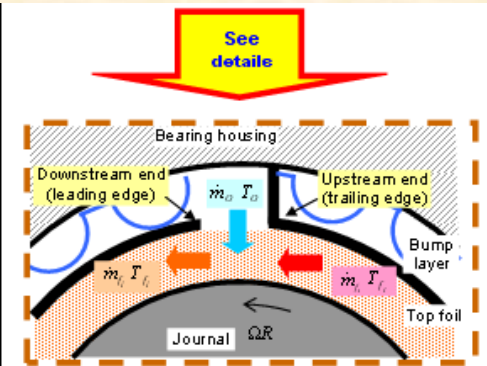


Table 1. DATABASE (COMMON COOLING GAS MATERIAL PROPERTIES)

	Viscosity at Tambient: Viscosity $(\mu)=A \cdot T \cdot \text{deg K} + B$			Thermal Conductivity at Tambient: $k=C \cdot T \cdot \text{deg K} + D$			Specific Heat at Tambient: $\text{Specific heat } (J)=E \cdot T \cdot \text{deg K} + F$			Gas Constant	Density	Temperature
	21 deg C	A	B	21 deg C	C	D	21 deg C	E	F			
Air	1.93E-02	4.00E-08	*****	0.0243	7.00E-05	0.0042	1007	0.1602	953.08	287	1.1614	21
Helium	2.00E-02	4.00E-08	*****	0.149	7.00E-05	0.0042	5188	0.1602	953.08	2077	0.1637	21
Carbon Dioxide	7.03E-02	4.00E-08	*****	0.087	7.00E-05	0.0042	839	0.1602	953.08	189	1.98	21
Nitrogen	1.80E-02	4.00E-08	*****	0.026	7.00E-05	0.0042	1040	0.1602	953.08	297	1.1468	21
Other												

Table 2. DATABASE (COMMON SHAFT & BEARING CARTRIDGE & FOIL MATERIALS)

	Elastic modulus at Tambient: $E_{\text{modulus}}(T)=A \cdot T \cdot \text{deg K} + B$			Poisson's ratio	Density	Thermal Expansion Coefficient	Thermal Conductivity	Specific Heat
	21 deg C	A	B					
Inconel 718	209	-0.0605	226	0.284	8220	1.30E-05	11.4	473
Inconel X750	214	-0.0677	234	0.29	8303	1.21E-05	16.3	440
Stainless Steel 304	200	-0.0729	221	0.284	7900	1.73E-05	16.3	473
Stainless Steel 4140	210	-0.064924	234	0.3	8003	1.22E-05	42.7	473
Other								

◀ ▶ README TYPICAL notation Shaft Bearing Models Top Foil and Bump Models FOIL GAS BEARING Radial Temperature Temperature field CenterlineFILM ▶

Worksheet: Shaft & Bearing models (II)

Graphical User Interface

XL GFB TH™ Spreadsheet for hydrodynamic foil GAS bearings
Version 1.0. Copyright 2009 by Texas A&M University. All rights reserved. Dr. Luis San Andres & Dr. Tae Ho Kim

Box 8

NOTE to USER: Run "Bump_stiffness", Enter Bump type, and then run "FE_2D Analysis" to build the SUB-FOIL STRUCTURE MODEL of GAS FOIL BEARINGS. Enter input values in gray cells. Yellow cells show output

BUMP GEOMETRY		
Enter INPUT values		
Bump foil thickness, t_b	1.02E-04	meters
Bump pitch, s_0	4.57E-03	meters
Bump half length, l_0	2.03E-03	meters
Bump height, h_b	3.81E-04	meters
Bump foil elastic modulus, E_b	214.00	GPa
Bump foil Poisson's ratio, ν_b	0.29	
Friction coefficient, μ_f	0.0	
Bump type - STIFFNESS PER UNIT AREA (Iordanoff's formula, 1999)		
1. Bump stiffness (free-free end bump), K_{ff}	3.17E+09	N/m ³
2. Bump stiffness (welded-free end bump), K_{fp}	7.15E+09	N/m ³
Structural loss factor, γ	0.2	

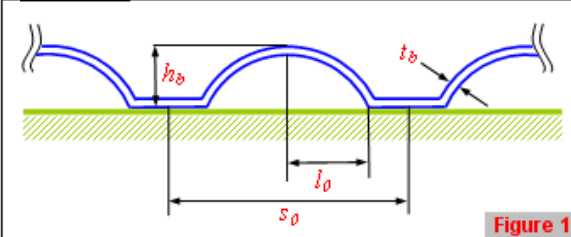
TOP FOIL MATERIAL PROPERTIES		
Enter INPUT values		
Foil Arc Diameter (= Rotor outer diameter, D)	3.81E-02	meters
Foil Arc Length, L_e	350	deg
Top foil width (=Axial length), W_e	3.81E-02	meters
Number of Bumps, N_b	25	
Foil thickness, T_e	1.02E-04	meters
Material elastic modulus, E_e	214.00	GPa
Material Poisson's ratio, ν_e	0.29	
Stiffening factor (circumferential direction), S_{fc}	4	
No. of elements between bumps, N_{int}	3	
No of elements in the cir. direction, N_{cz}	75	
No of elements in the axial direction, N_{cy}	12	

Box 10

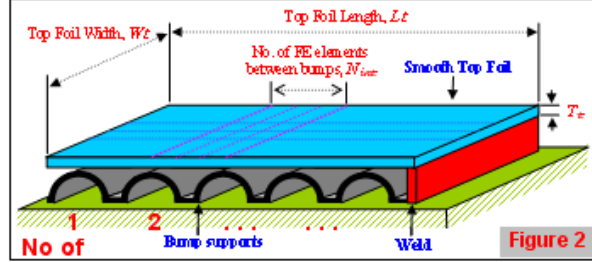
Box 9

Enter BUMP Type	
BUMP STIFFNESS MATRIX	
Bump No.	Bump type
1	1
2	1
3	1
4	1
5	2
6	1
7	1
8	1
9	1
10	2
11	1
12	1
13	1
14	1
15	2
16	1
17	1
18	1
19	1
20	2
21	1
22	1
23	1
24	1
25	2

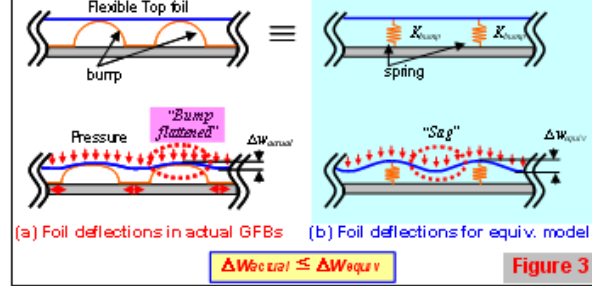
BUMP GEOMETRY



TOP FOIL MODEL



ACTUAL AND EQUIVALENT TOP FOIL MODEL BEHAVIORS



◀ ▶ ⏪ ⏩ README / TYPICAL notation / Shaft Bearing Models / Top Foil and Bump Models / FOIL GAS BEARING / RadialTemperature / Temperature field / Cent

Worksheet: Top Foil and Bump Models

Graphical User Interface

XL GFB TH™ Spreadsheet for hydrodynamic foil GAS bearings
 Version 1.0. Copyright 2009 by Texas A&M University. All rights reserved. Dr. Luis San Andres & Dr. Tae Ho Kim
 TEE8 project # 32525/33600/ME funded by NASA
 Interface to Program:XLGFBHT
 EDIT "DUMP.TXT" after program execution to VERIFY calculations & convergence.

Thermohydrodynamic MODEL

Bearing Geometry Rotor Outer Diameter: 3.81E-02 meters Axial Length: 3.81E-02 meters Radial Clearance: 3.50E-05 meters Number of shims: 0 TOP Foil - arc length: 350.00 deg TOP Foil - leading edge: 45.00 deg Shim thickness: 0.00 meters Offset (Avg location of sh): 0.00 deg		Lubricant Fluid Properties Ambient Pressure: 1.013 bar Ambient Temperature: 21.0 deg C Properties at 21 deg C Viscosity at Tambient: 1.93E-02 c-Poise Density at Tambient: 1.16 kg/m3 Specific Heat: 1007.0 J/(kg-K) Thermal Conductivity: 0.02 W/(m-K) Gas Constant: 287 J/(kg-K)		CONVERGENCE PARAMETERS Max Iterations - film ls: 500 error press-temp film ls: 1.00E-05		Select - Analysis Type Vary Load Select - Option Foil Detach DETACH
GRID RATIO (circ/Axi) 0.98 No. Circ. Grid Points: 76 No. Axial Grid Points: 13		Frequency Analysis Option Constant Shaft Rpm: 30000 rpm Spectral Analysis		4. Run FOIL_GAS_BEAR		

NOTE to USER: Enter input values in gray cells.
 "Run FOIL_GFB_BEAR" predicts GAS FOIL BEARING static and dynamic force performance and temperature field.
 Yellow cells show output values.

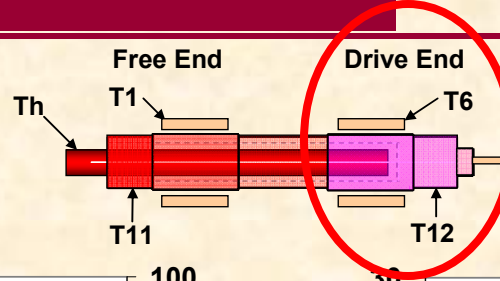
Enter INPUT values					FOIL Bearing force coefficients										IMPEDANCES (R: real, I: im)		
ex_input [mm]	ey_input [mm]	Load-X [N]	Load-Y [N]	Speed [rpm]	Kstructure [N/m]	Kxx [N/m]	Kxy [N/m]	Kyx [N/m]	Kyy [N/m]	Cxx [N-s/m]	Cxy [N-s/m]	Cyx [N-s/m]	Cyy [N-s/m]	R-XX [N/m]	R-XY	R-YX	
		6.50	0.00	10000	2.37E+06	3.33E+06	6.12E+05	-1.18E+06	3.33E+06	3227.6	-1868.5	879.3	3676.8	3.33E+06	6.12E+05	-1.18E+06	
		6.50	0.00	20000	2.37E+06	5.53E+06	-6.09E+05	-1.29E+06	5.53E+06	1619.4	-1110.6	621.5	1913.9	5.53E+06	-6.09E+05	-1.29E+06	
		6.50	0.00	30000	2.37E+06	6.93E+06	-1.14E+06	-1.18E+06	6.72E+06	938.6	-661.0	457.3	1188.0	6.93E+06	-1.14E+06	-1.18E+06	
		6.50	0.00	40000	2.37E+06	7.98E+06	-1.31E+06	-1.10E+06	7.76E+06	606.0	-439.6	356.4	815.2	7.98E+06	-1.31E+06	-1.10E+06	

FOIL Bearing static load performance parameters																
Speed [rpm]	ex [mm]	ey [mm]	Eccentricity [mm]	eccentricity ratio	Angle [deg]	Minimum film [mm]	Peak film temperature [degC]	Fx Reaction [N]	Fy Reaction [N]	Force [N]	Specific load [bar]	Max pressure [bar]	Torque [N-m]	Power Loss [kW]	Keq [N/m]	
10000.00	38.41	1.38	3.00	3.30	65.33	15.48	124.3	-6.5	-0.1	6.5	0.04	1.11	1.68E-03	1.76E-03	2.93E+06	
20000.00	38.41	0.16	1.64	1.65	84.26	16.76	125.1	-6.4	0.0	6.4	0.04	1.13	3.26E-03	6.82E-03	5.17E+06	
30000.00	38.41	-0.10	1.14	1.14	84.80	16.76	126.4	-6.5	0.1	6.5	0.04	1.18	4.81E-03	1.51E-02	6.71E+06	
40000.00	38.41	-0.22	0.82	0.85	74.68	16.32	128.4	-6.5	0.1	6.5	0.05	1.23	6.39E-03	2.68E-02	7.87E+06	

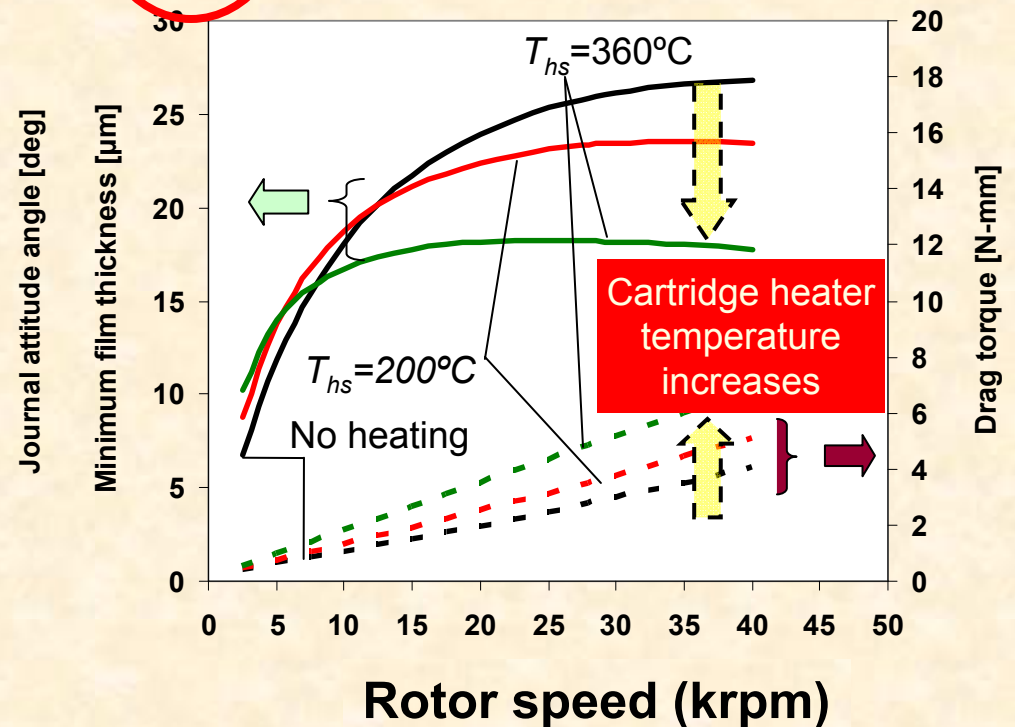
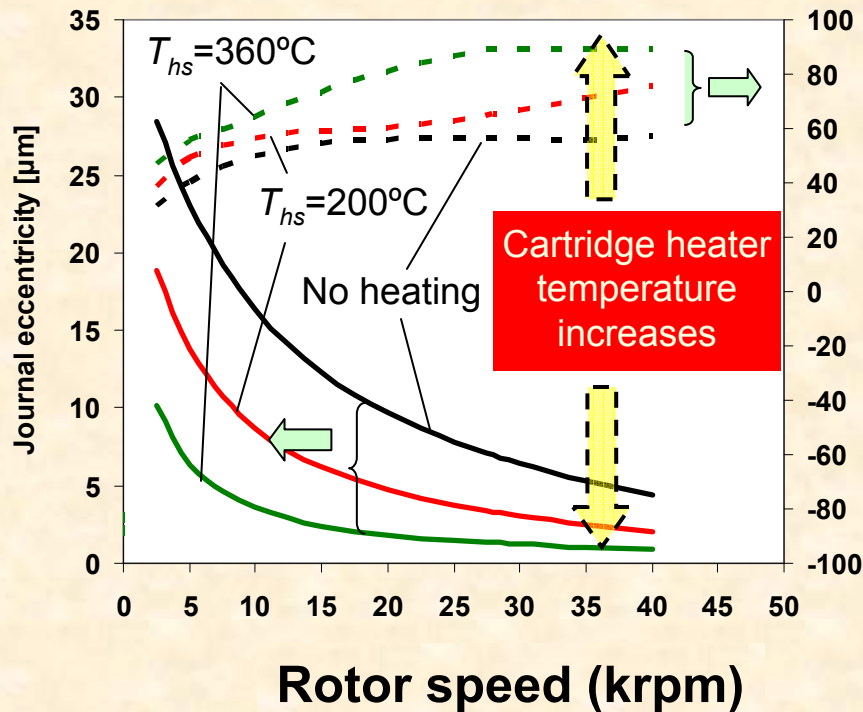
Worksheet: Foil Bearing (Operation and Results)

Static load parameters Predictions

Drive End FB



static load ~ 6.5 N
No cooling flow



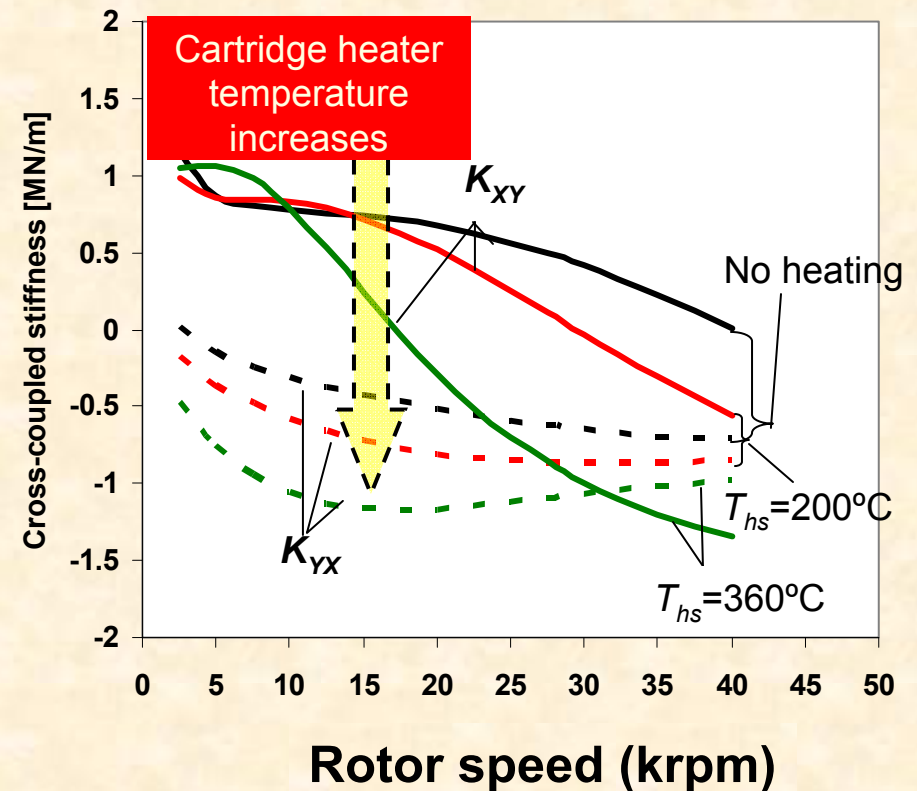
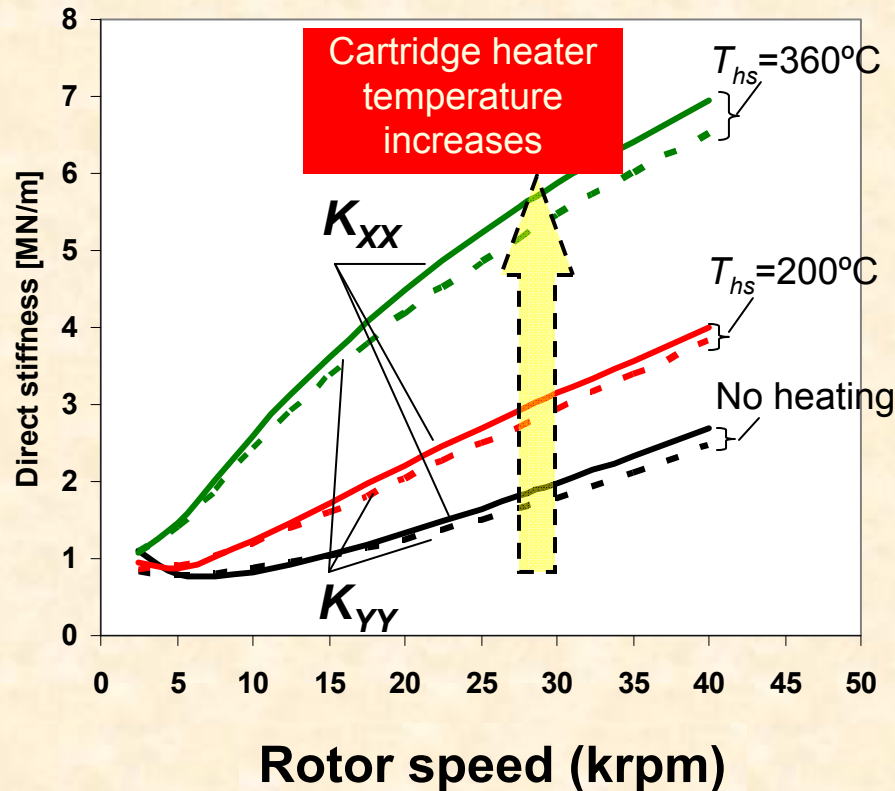
Predictions

As temperature increases, journal attitude angle and drag torque increase but journal eccentricity and minimum film thickness decrease due to reduction in operating clearance

Bearing stiffnesses Predictions

Drive End FB

static load ~ 6.5 N
No cooling flow



Predictions

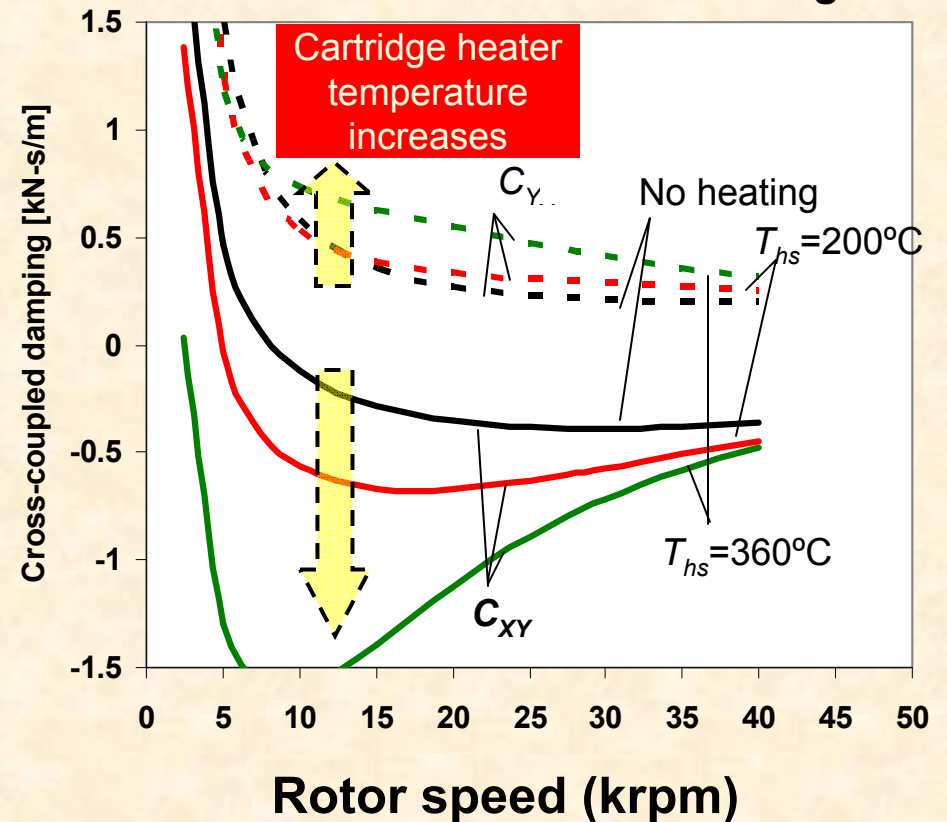
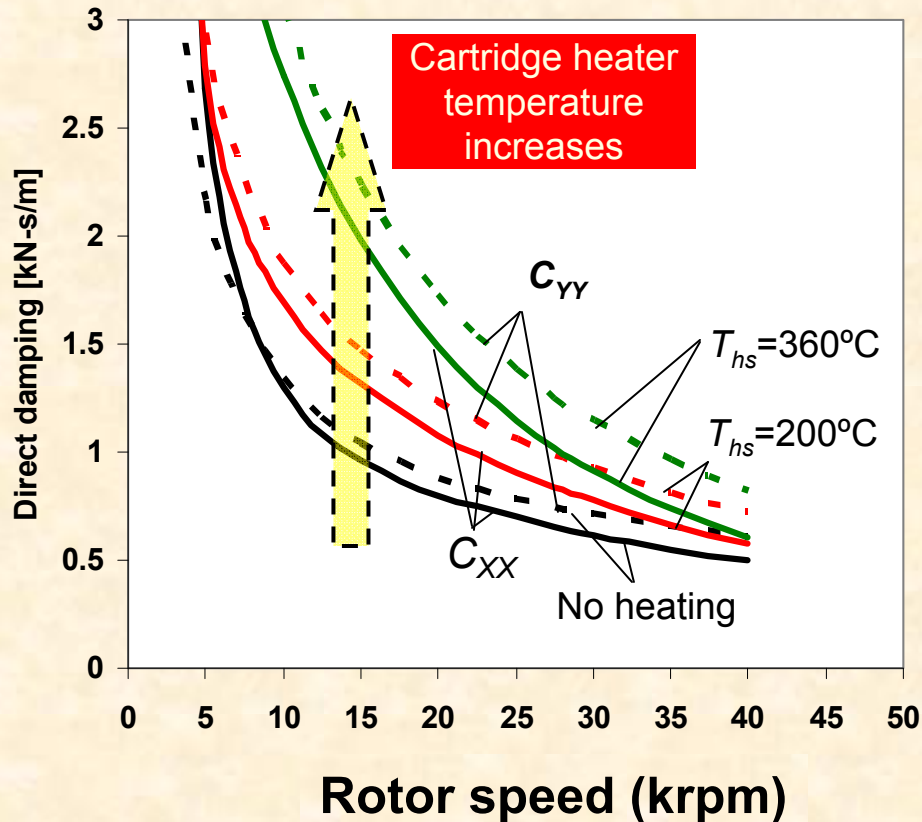
As temperature increases, stiffnesses (K_{XX} , K_{YY}) increase significantly, while difference ($K_{XY}-K_{YX}$) increases slightly at low rotor speeds and decreases at high rotor speeds

Bearing damping

Predictions

Drive End FB

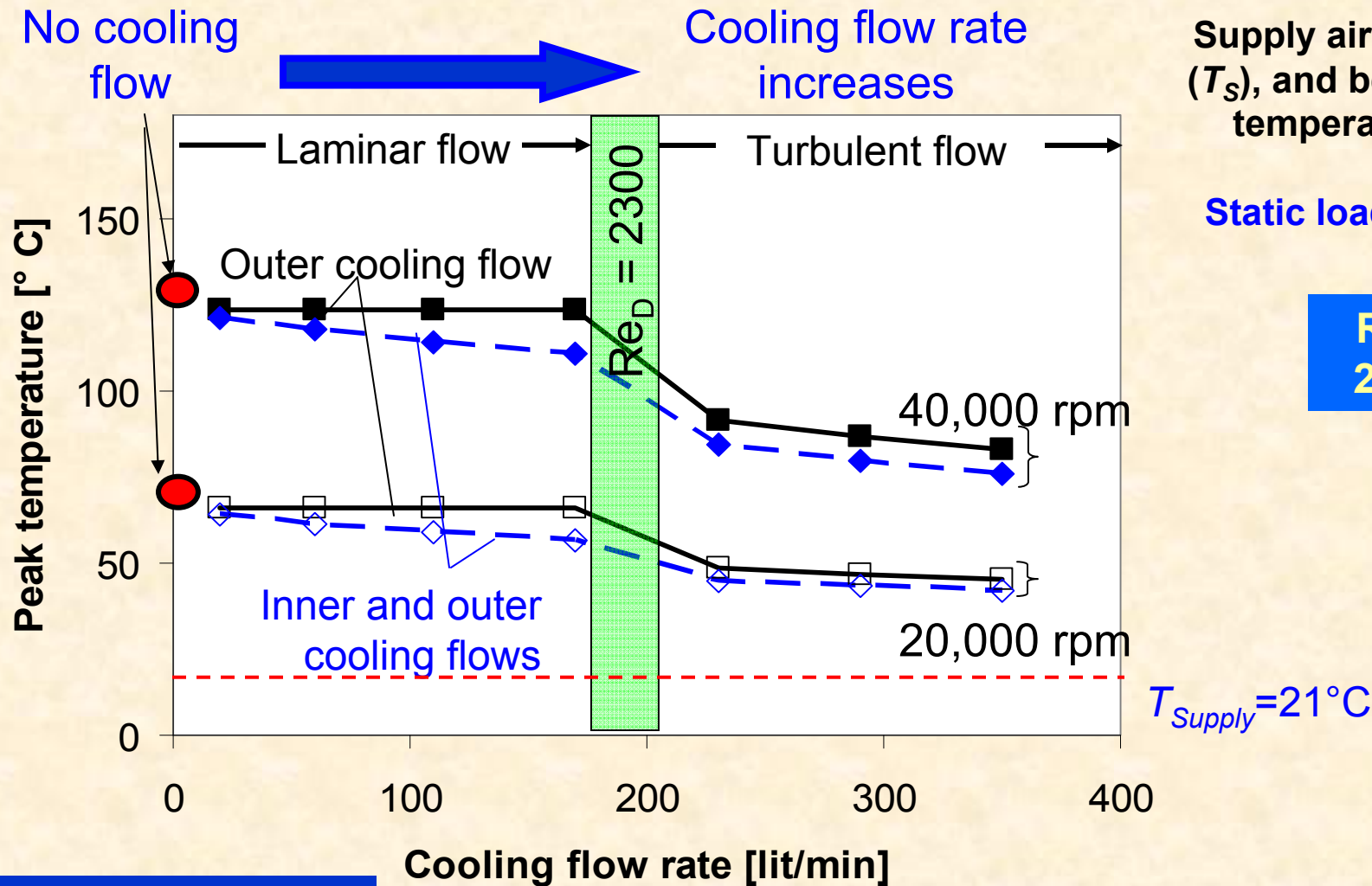
static load ~ 6.5 N
No cooling flow



Predictions

As temperature increases, damping (C_{XX} , C_{YY}) increase. Cross damping (C_{XY} , C_{YX}) change little above 30 krpm.

Predictions on effect of cooling flow

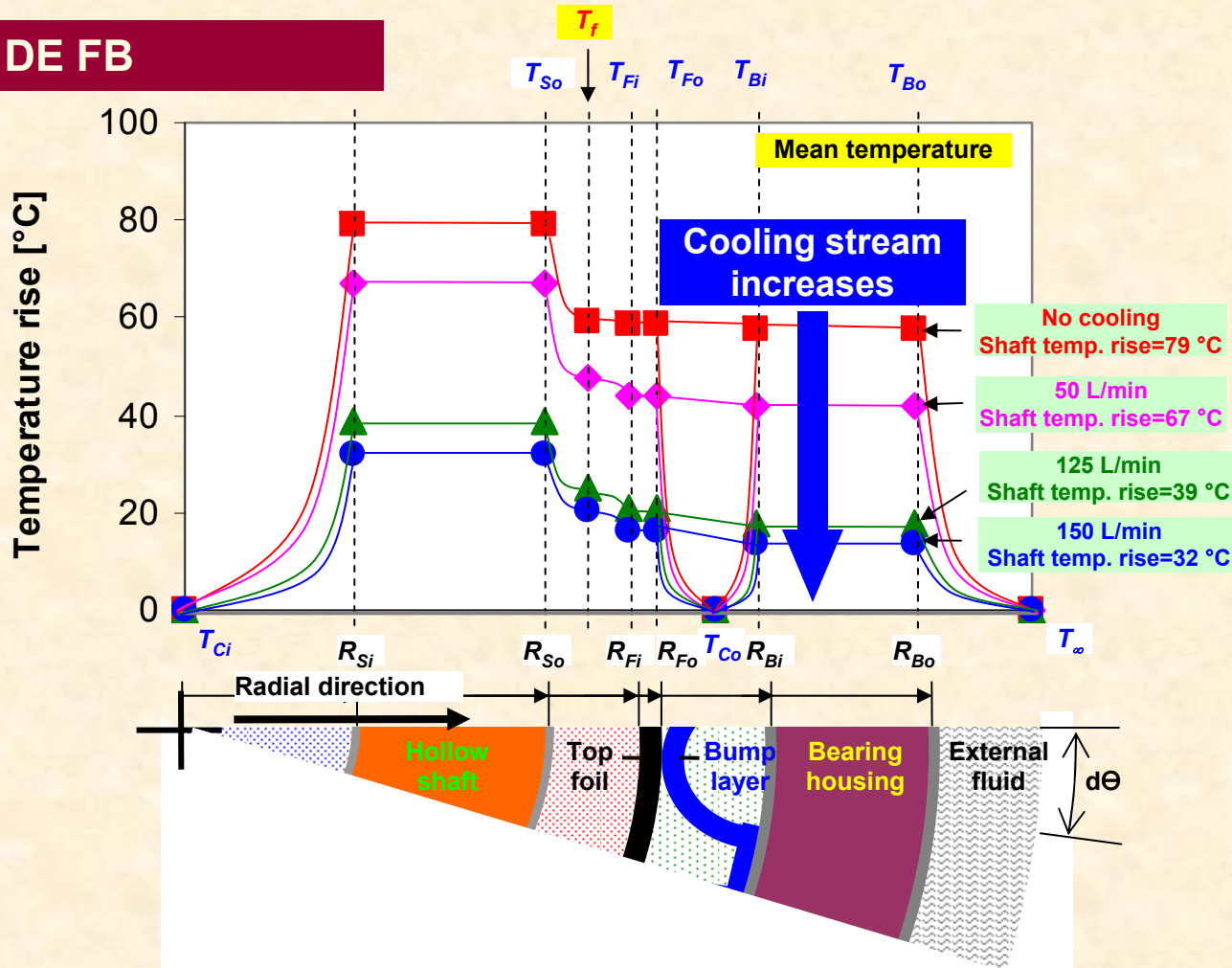


Predictions

Peak temperature drops with strength of cooling stream. **Sudden drop at ~ 200 lit/min b/c of transition from laminar to turbulent flow**

Predictions radial temperature Model

DE FB



Natural convection on exposed surfaces of bearing OD and shaft ID

w/o & w cooling flow

Rotor speed : 30 krpm

Model predictions

With forced cooling, GFB operates 50 °C cooler. Outer cooling stream is most effective in removing heat

Topic

- Statement of Work & Sources for Presentation
- Objectives and accomplished work in 07-08

Computational model. Validation with published data.
Rotordynamic measurements at TAMU

- Objectives and accomplished work in 2008-09

Description of test rig and foil bearings at TAMU
Effect of temperature on bearing temperatures,
coastdown speed and rotor motions
Effect of cooling flow on bearing and shaft
temperatures. Validation of computational model

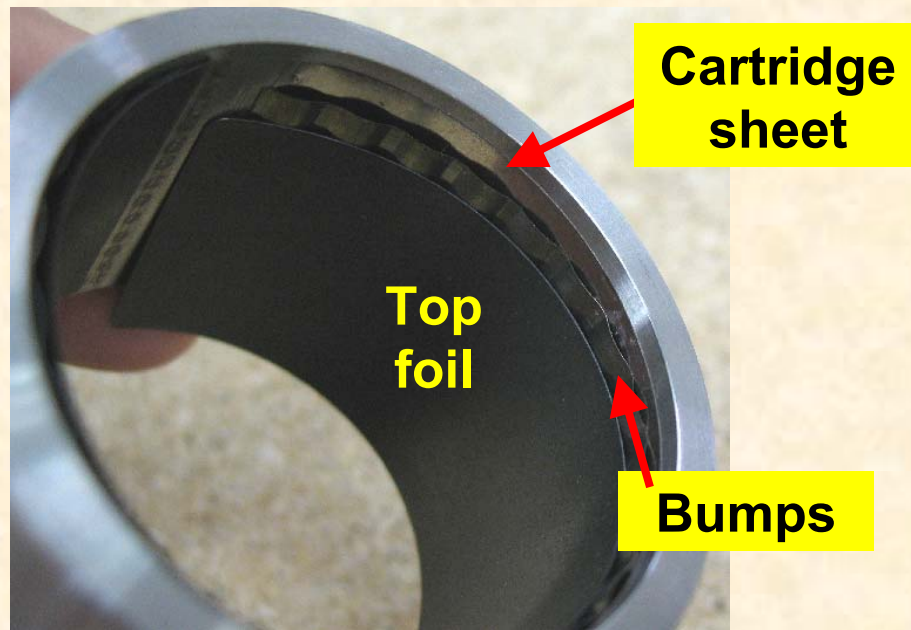
- * The computational code

Graphical User Interface. Further predictions

- **Work with MiTi Bearings**

- **Ch** San Andrés, L., Ryu, K., and Kim, T.H., 2011, "Identification of Structural Stiffness and Energy Dissipation parameters in a 2nd Generation Foil Bearing; Effect of Shaft Temperature", ASME J. Eng. Gas Turbines Power, vol. 133 (March) , pp. 032501

MiTi Korolon® foil bearing



FB nominal dimensions

Parameter [Dimension]	Symbol	Value
Cartridge inner diameter [mm]	D	37.98
Cartridge outer diameter [mm]	D_o	44.64
Axial bearing length [mm]	L	25.40
Number of bumps	N_B	24× 3
Bump pitch [mm]	s	4.318
Bump length [mm]	$2l_o$	3.302
Bump foil thickness [mm]	t	0.102
Bump height [mm]	h	0.394
Top foil thickness [mm]	t_T	0.127
Bump arc radius [mm]	r_B	5.08
Bearing Top foil inner diameter [mm]	D_T	38.135
Shaft diameter [mm]	D_J	36.84
Nominal radial clearance [mm]	C	0.160

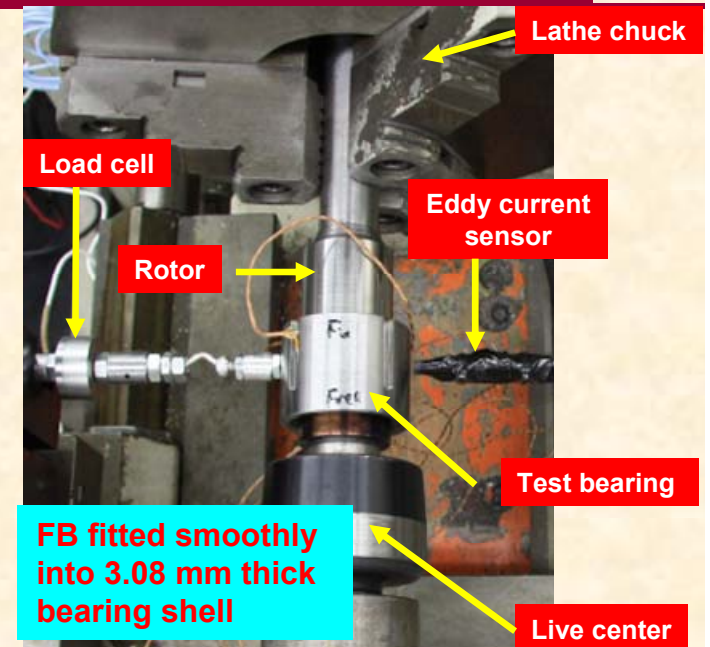
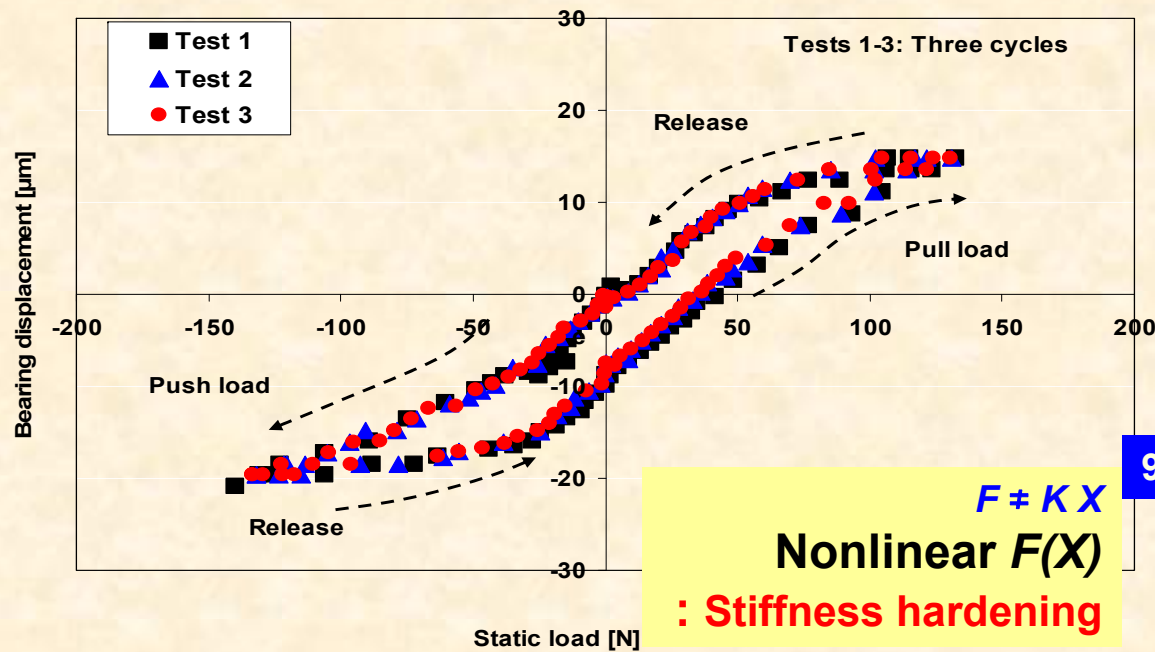
Two generation II GFBs

Three (axial) bump strip layers,
each with 24 bumps.

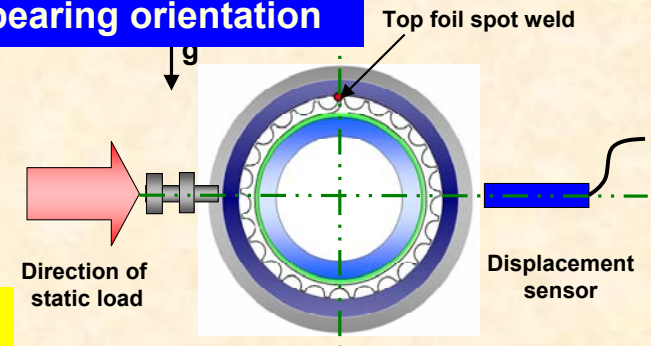
Korolon® 800 coating
(up to 800°F) on top foil surface.

MiTi® FB deflection versus static load

Room temperature tests



90° bearing orientation



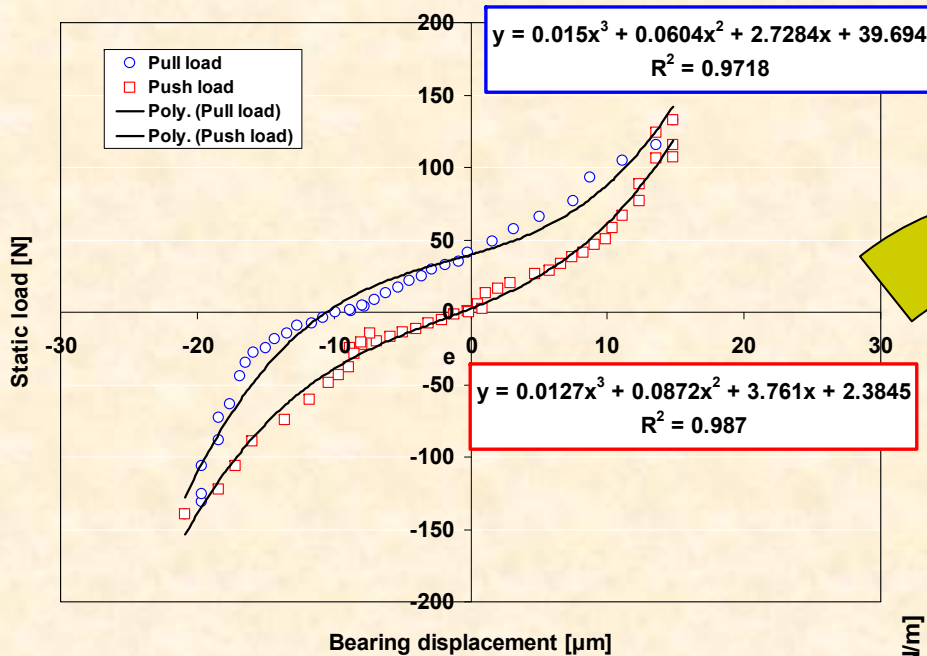
Shaft OD 36.56 mm: Highly preloaded FB

Large hysteresis loop : Mechanical energy dissipation

due to dry-friction between top foil contacting bumps and bump strip layers contacting bearing cartridge sheet

MiTi® FB structural stiffness

Room temperature tests

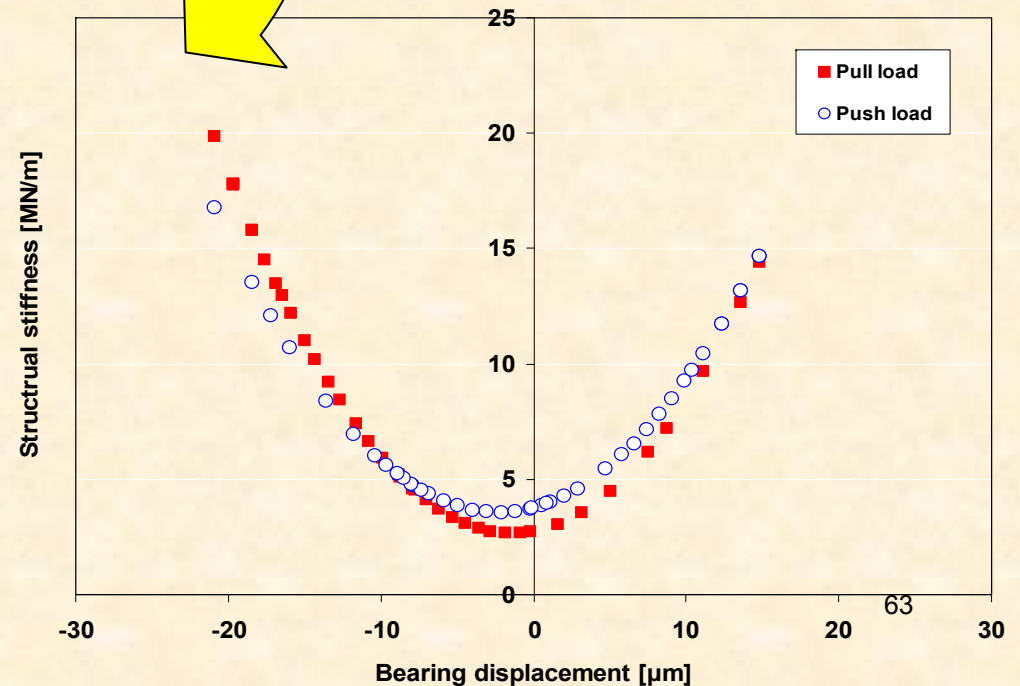


Cubic polynomial curve fit over span of applied loads

$$F = F_0 + K_1X + K_2X^2 + K_3X^3$$

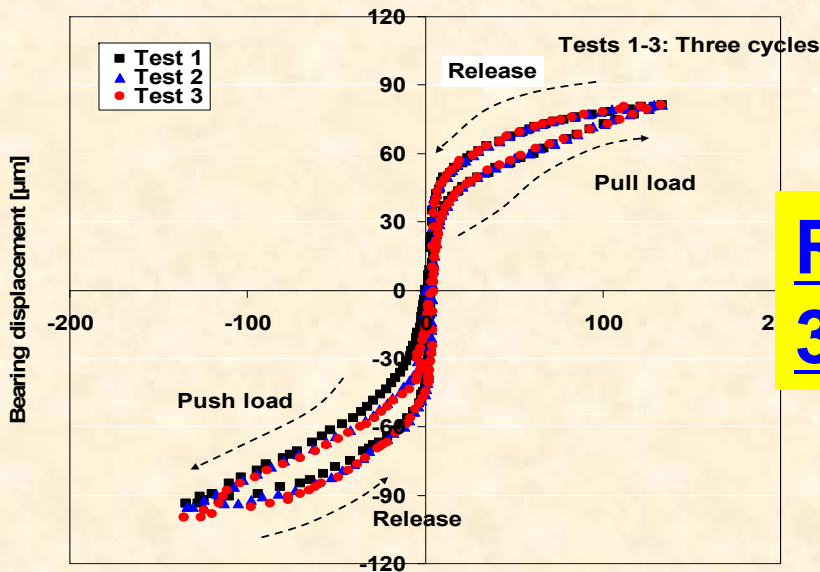
$$K = K_1 + 2K_2X + 3K_3X^2$$

Distinctive hardening effect as FB deflection increases

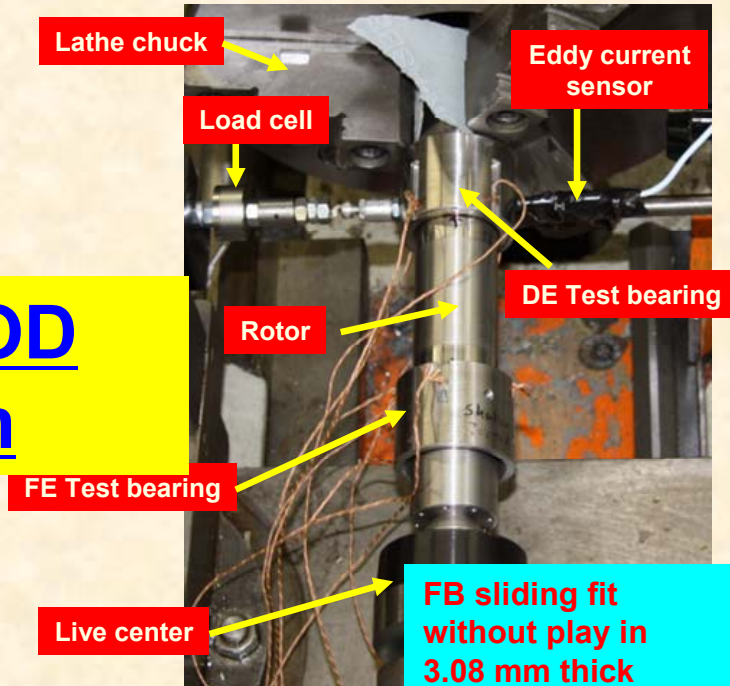


MiTi® FB deflection versus static load

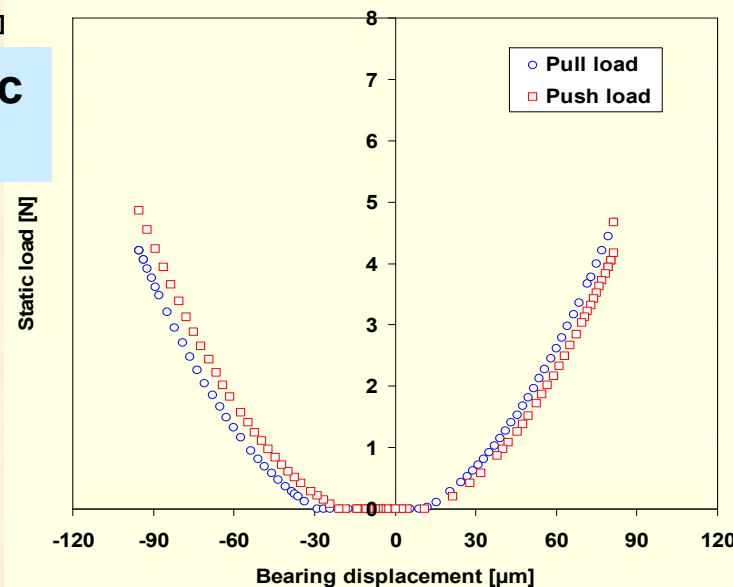
Room temperature tests



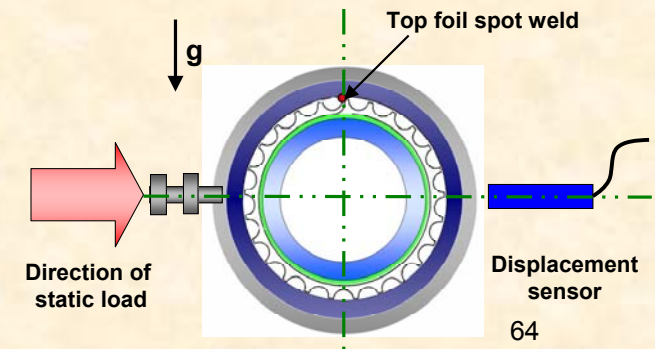
ROTOR OD
36.46 mm



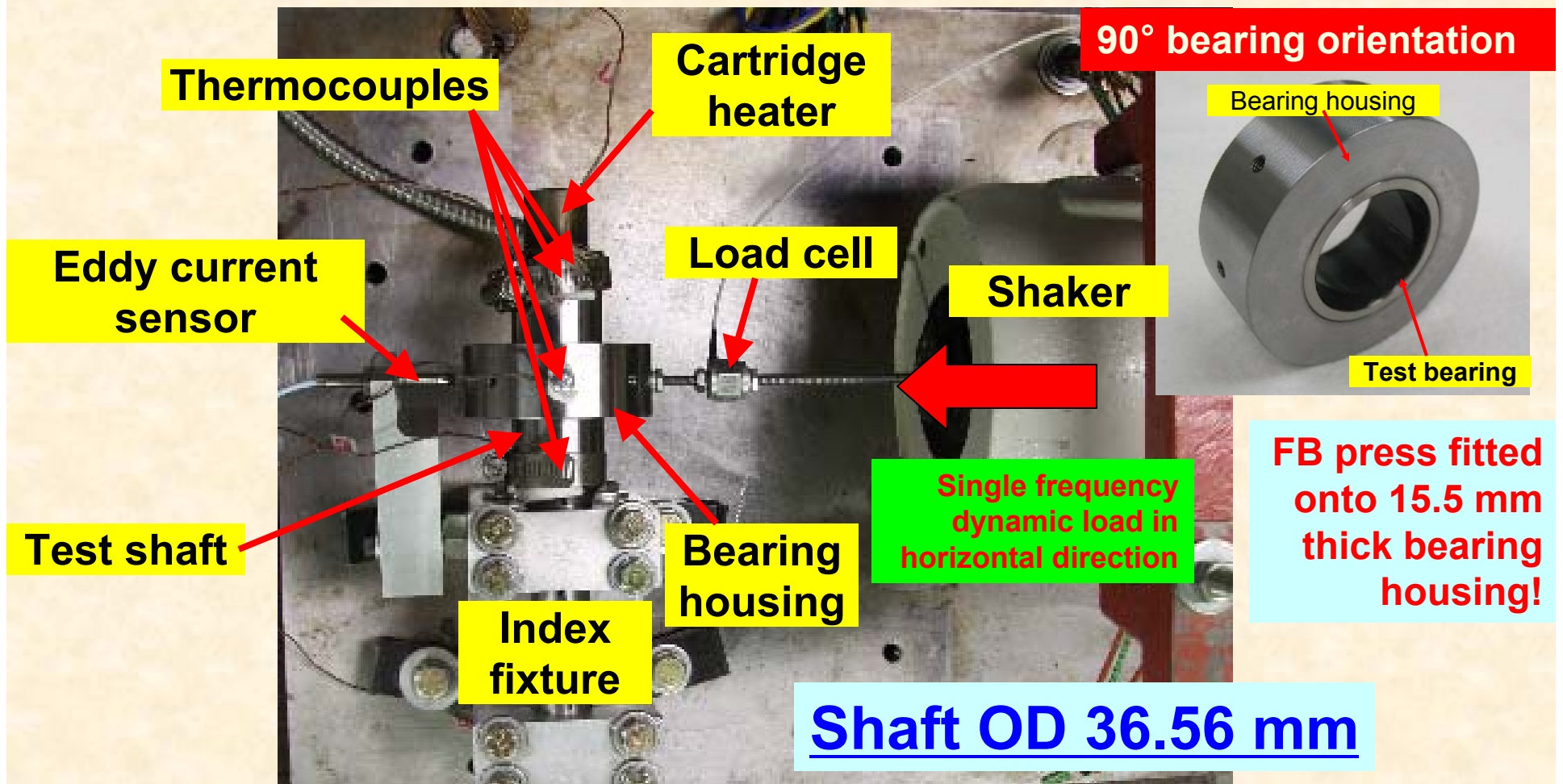
Identified from Cubic polynomial curve fit



90° bearing orientation



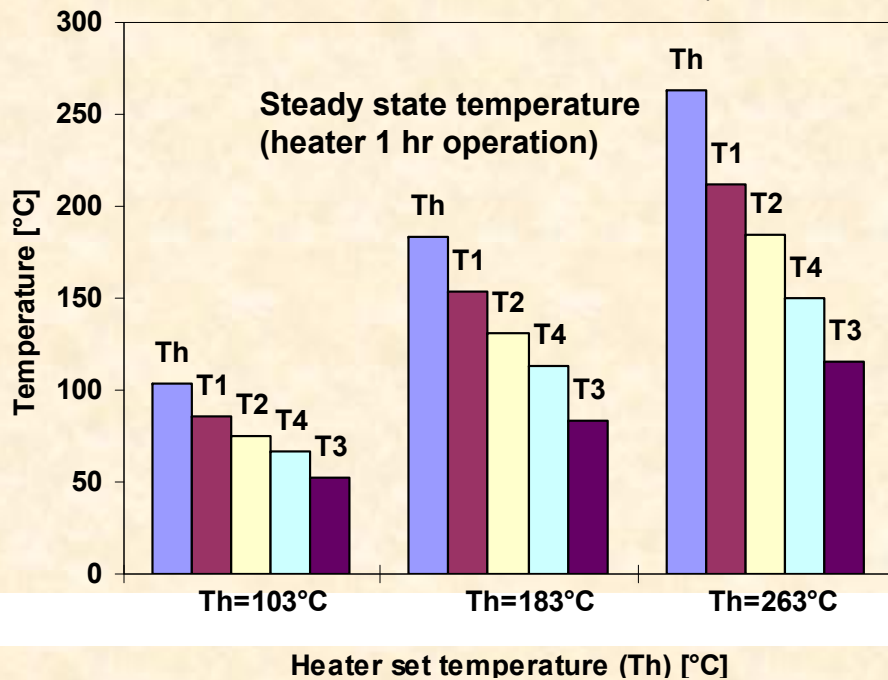
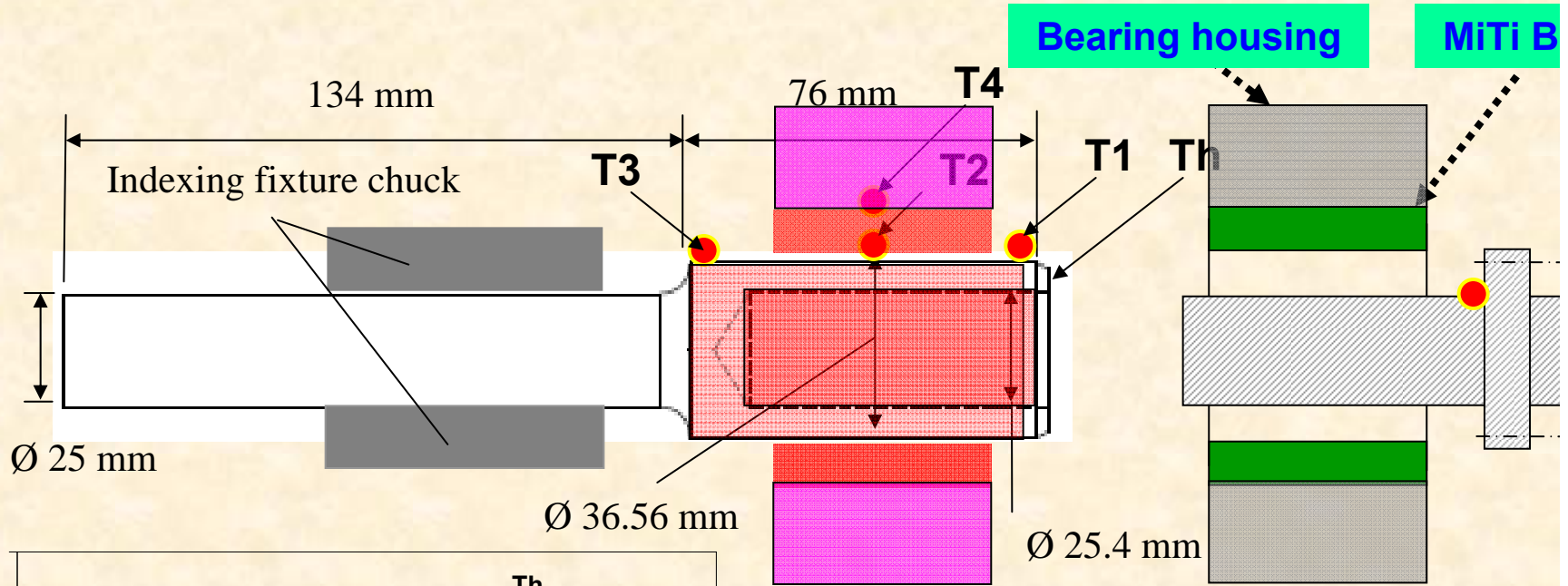
MiTi® FB test setup for dynamic loads



FB Displacement controlled [μm]	7.4, 11.1, 14.8, and 18.5
Frequency Range, Hz	50-200 (increment: 25 Hz)
Shaft Temperature, °C	23, 103, 183, and 263
Bearing Mass M, kg	0.785 (load cell + attachment hardware)

Uncoated rigid, non-rotating, hollow shaft supported on FB.

Shaft heating using electric heater

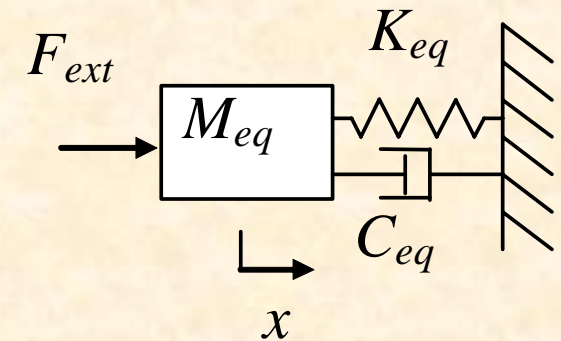


Significant temperature gradient along shaft axis.
Cartridge heater warms unevenly shaft

Parameter Identification (no shaft rotation)

Equivalent Test System: 1DOF

K stiffness, C_{eq} viscous damping OR γ loss factor



$$M \ddot{x} + K x + C_{eq} \dot{x} = F_{(t)}$$

$$F(t) = F_o e^{i\omega t} \quad x(t) = \bar{X} e^{i\omega t}$$

← Harmonic force & displacements

$$Z = \frac{F_o}{\bar{X}} = (K - \omega^2 M) + i \omega C_{eq}$$

← Impedance Function

$$E_{dis} = \pi \omega C_{eq} |\bar{X}|^2$$

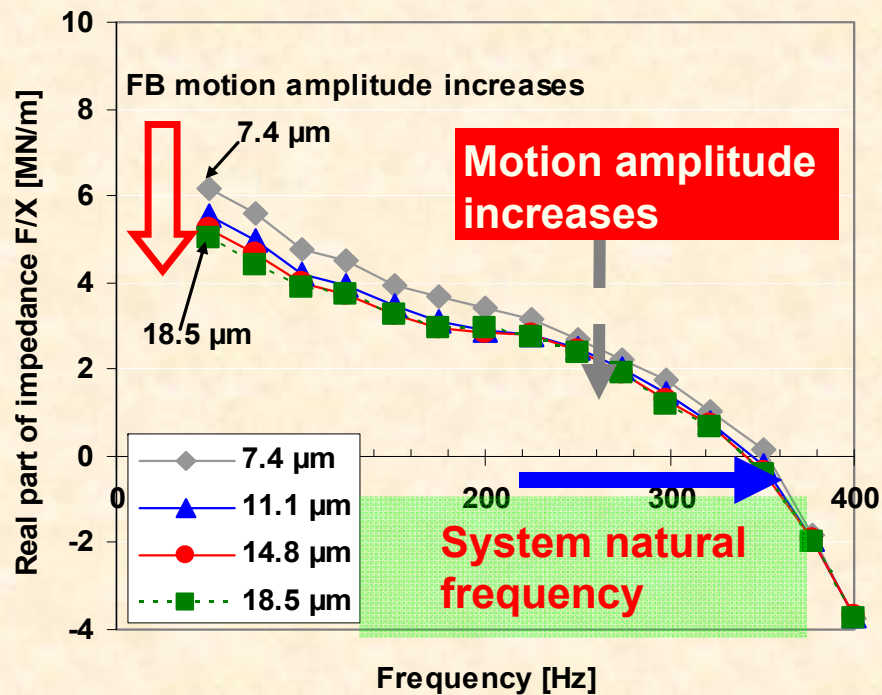
← Viscous Dissipation or dry-friction Energy

$$E_{dis} = \pi \gamma K |\bar{X}|^2$$

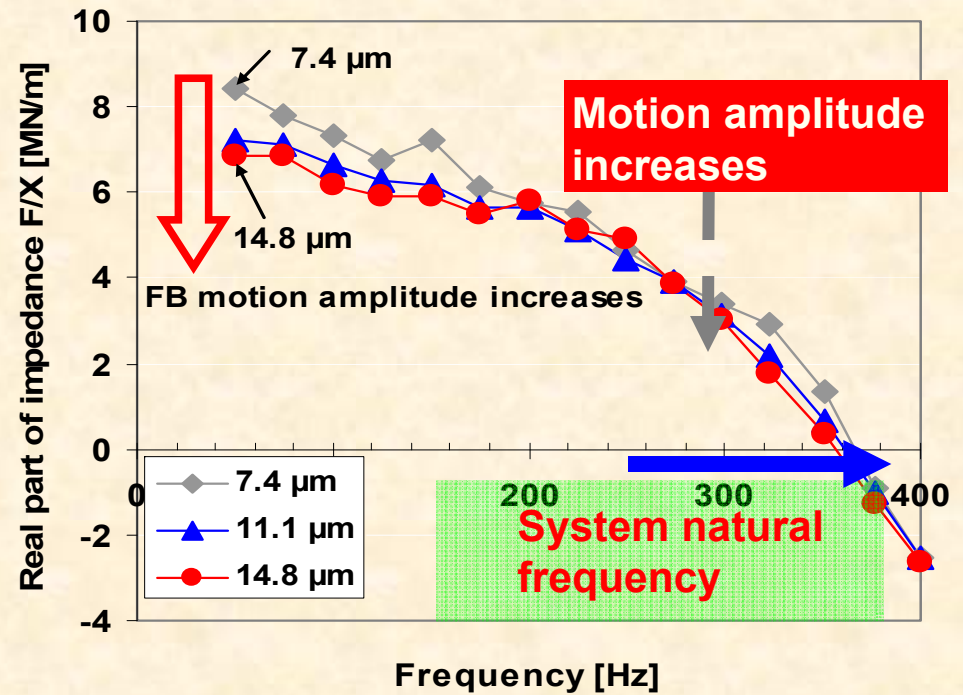
Effect of temperature on dynamic stiffness

$$\operatorname{Re}\left(\frac{F_o}{\bar{X}}\right) = (K - \omega^2 M)$$

$T_h = 23^\circ\text{C}$



$T_h = 263^\circ\text{C}$



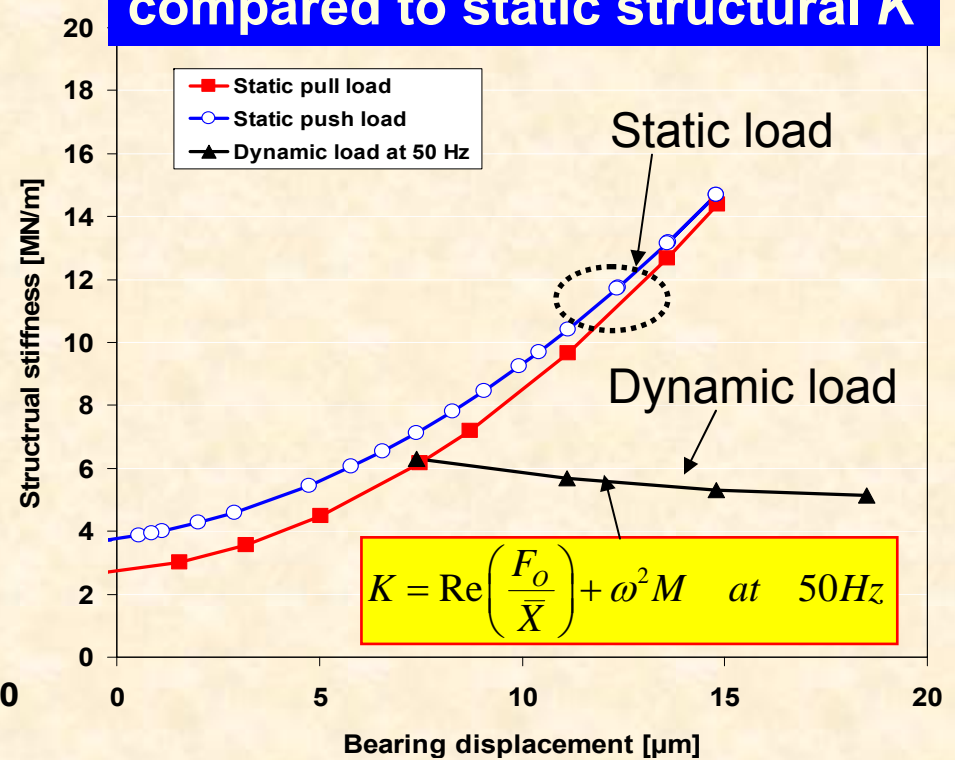
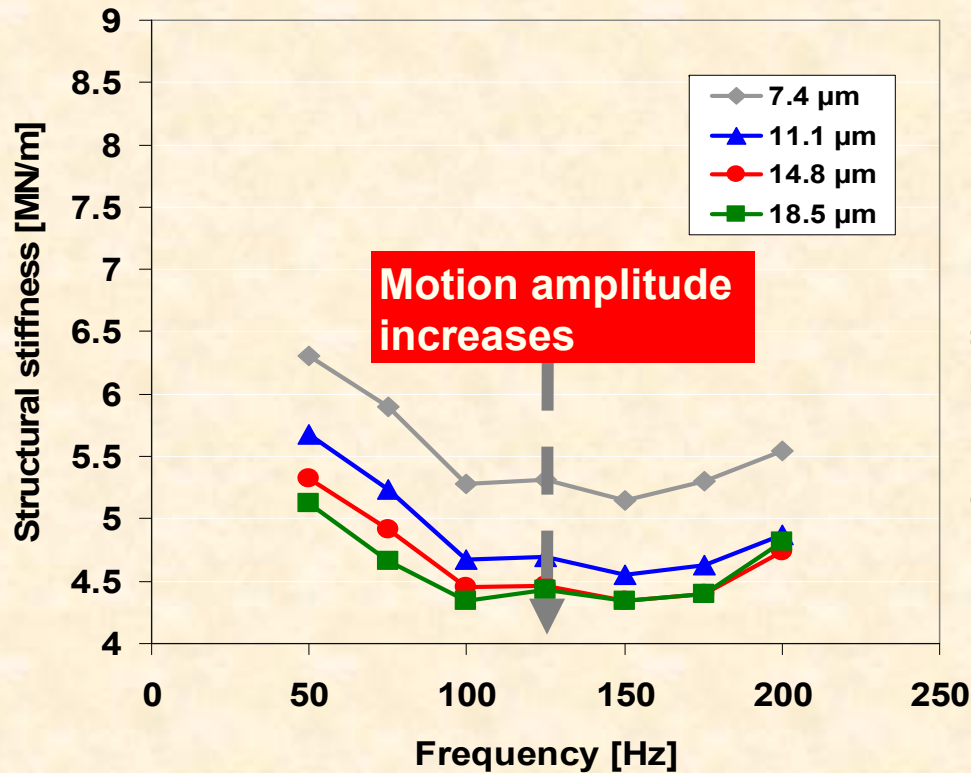
Real (F/X) decreases with FB motion amplitude & increases with shaft temperature.

Effect of temperature on structural stiffness

$$K = \text{Re}\left(\frac{F_o}{\bar{X}}\right) + \omega^2 M$$

$T_h = 23^\circ\text{C}$, 90° bearing orientation

Dynamic structural K compared to static structural K



At larger FB deflections, static K is larger than dynamic K

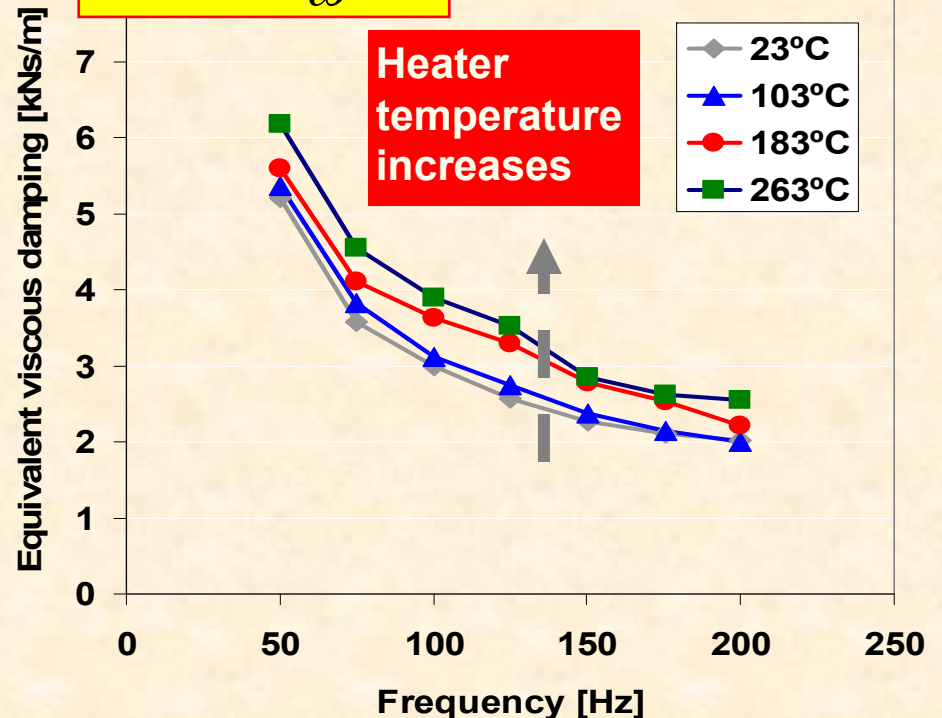
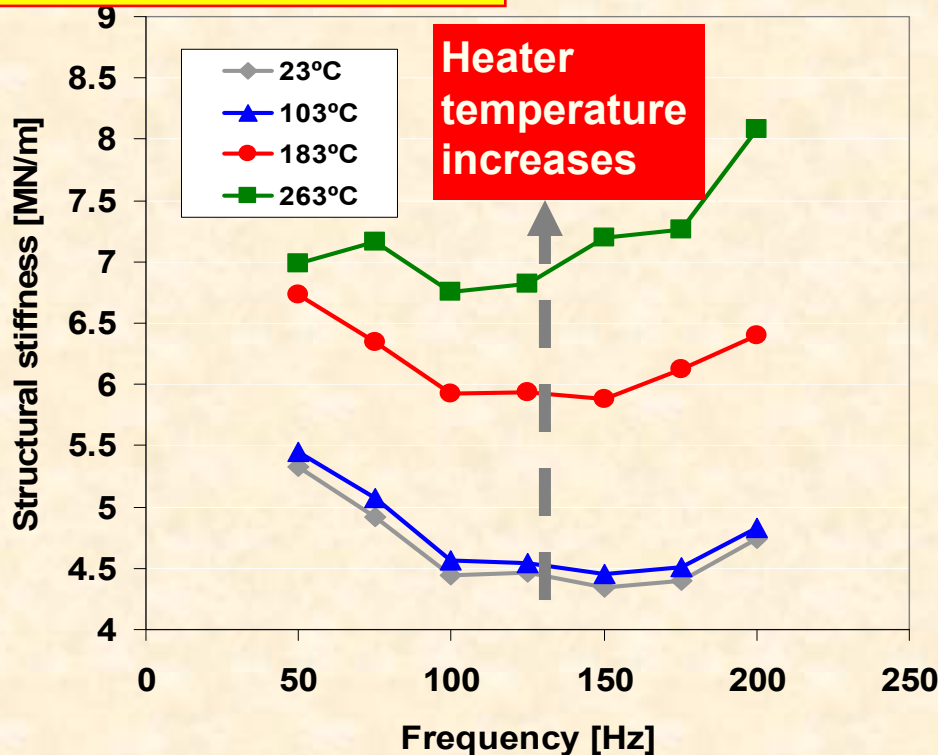
Highly preloaded FB: K decreases as FB motion amplitude increases due to decrease in # of active bumps

Effect of temperature on stiffness & damping

$$K = \operatorname{Re}\left(\frac{F_o}{\bar{X}}\right) + \omega^2 M$$

$$C_{eq} = \frac{\operatorname{Im}\left(\frac{F_o}{\bar{X}}\right)}{\omega}$$

FB motion
amplitude: 14.8 μm



FB stiffness and viscous damping increase with shaft temperature and decrease with excitation frequency.

TEST FB cartridge OD is constrained within bearing housing.

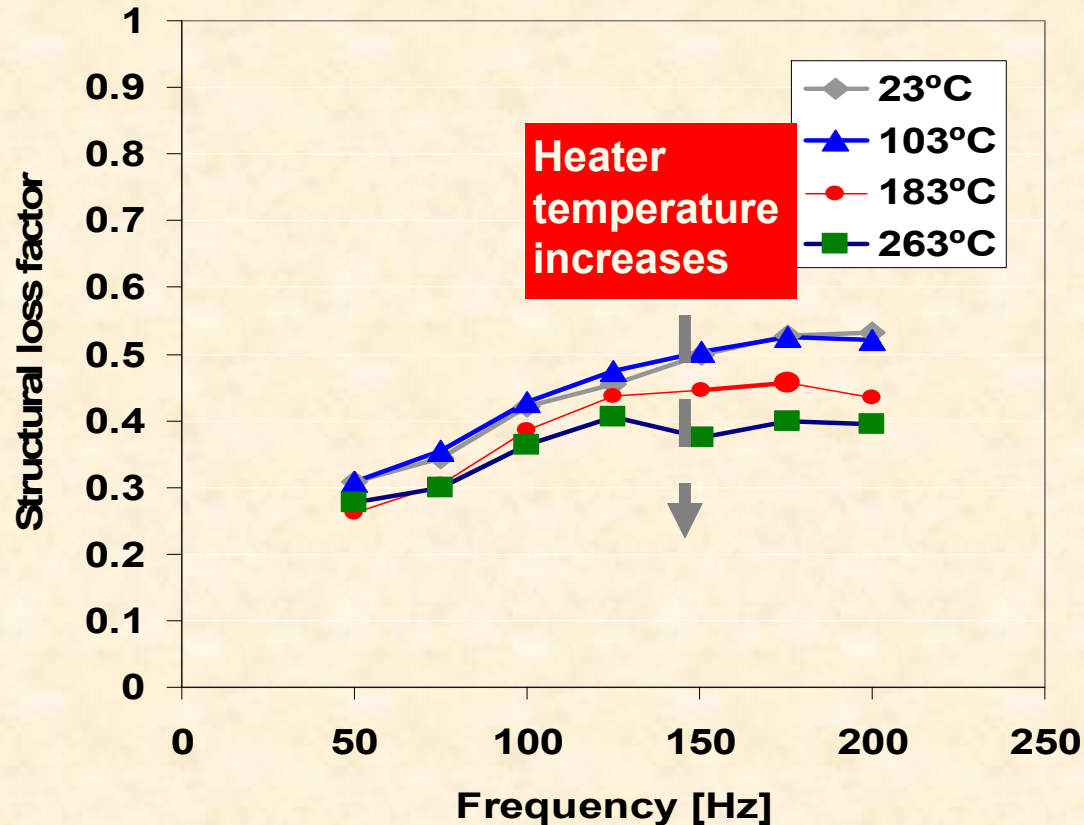
FB radial clearance decreases as shaft temperature raises!

Effect of temperature on loss factor γ

Structural (material) loss factor best represents energy dissipation in FB

FB motion amplitude: 14.8 μm

$$\gamma = \frac{C_{eq} \omega}{K}$$



The FB loss factor increases with excitation frequency and decreases slightly with shaft temperature. More damping expected in rotordynamic measurements



Texas A&M University
Mechanical Engineering Department

Nov. 23, 2010



EFFECT OF COOLING FLOW ON THE OPERATION OF A HOT ROTOR-GAS FOIL BEARING SYSTEM

Ph. D. Final Exam

Keun Ryu

Chair of Advisory Committee: Dr. Luis San Andrés

**This material is based upon work supported by NASA GRC and the TAMU
Turbomachinery Research Consortium (TRC)**

Objective

Quantify effect of cooling flow and shaft temperature on the rotordynamic performance of a GFB supported rotor. Investigate adequate thermal management strategies using forced cooling flow into the GFBs

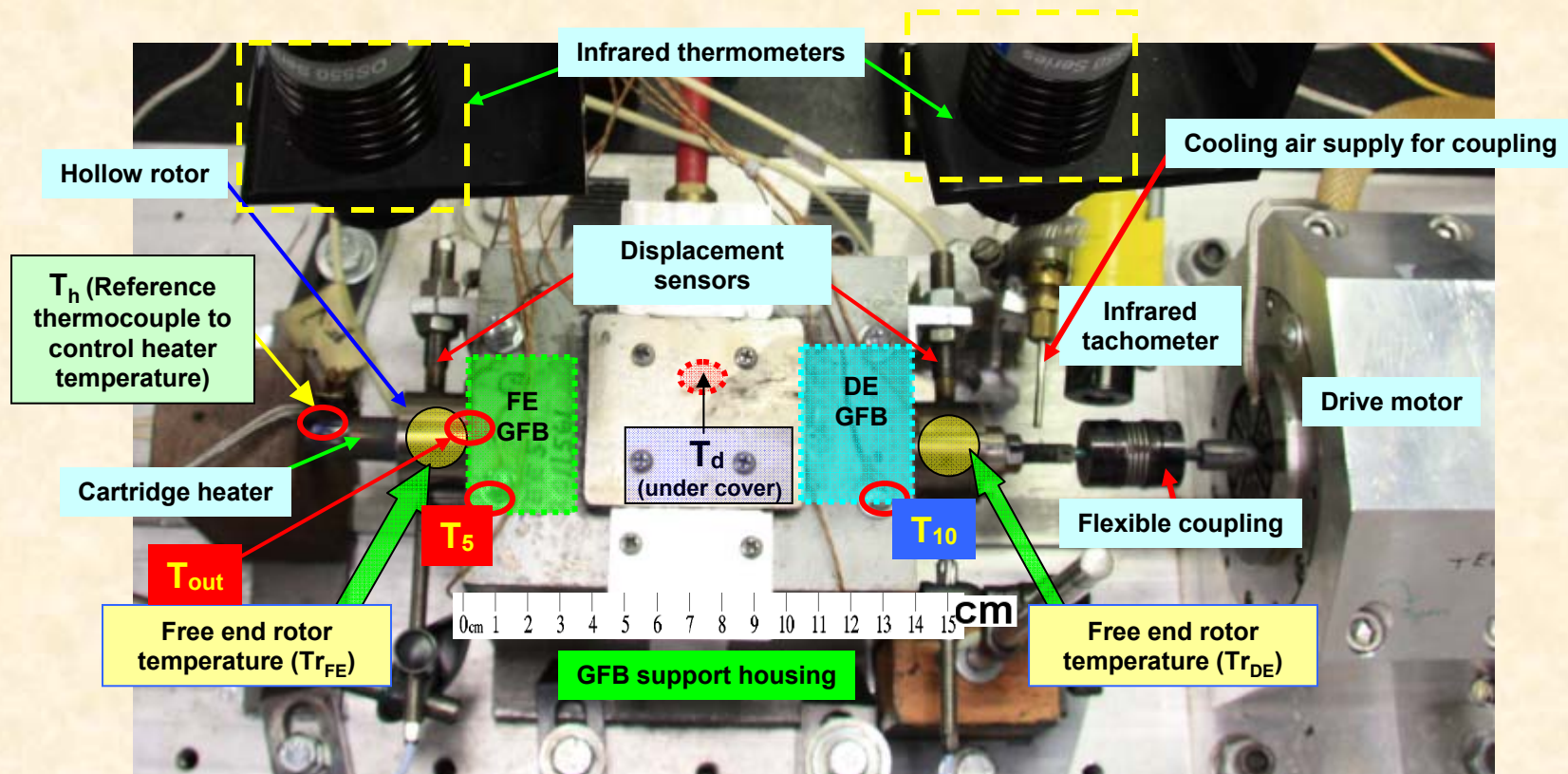
Research tasks

- **Revamp a GFB rotordynamic test rig for operation at high speed and extreme temperatures**
- **Measure temperature of bearings and rotor and the motions of rotor for increasing rotor speeds, shaft temperatures, and cooling flow rates**
- **Quantify effect of gas flow on cooling bearings (max. 500 L/min)**
- **Compare the experimental results (rotor responses and bearing temperatures) to predictions from an in-house computational program**

TAMU Hot rotor-GFB test rig

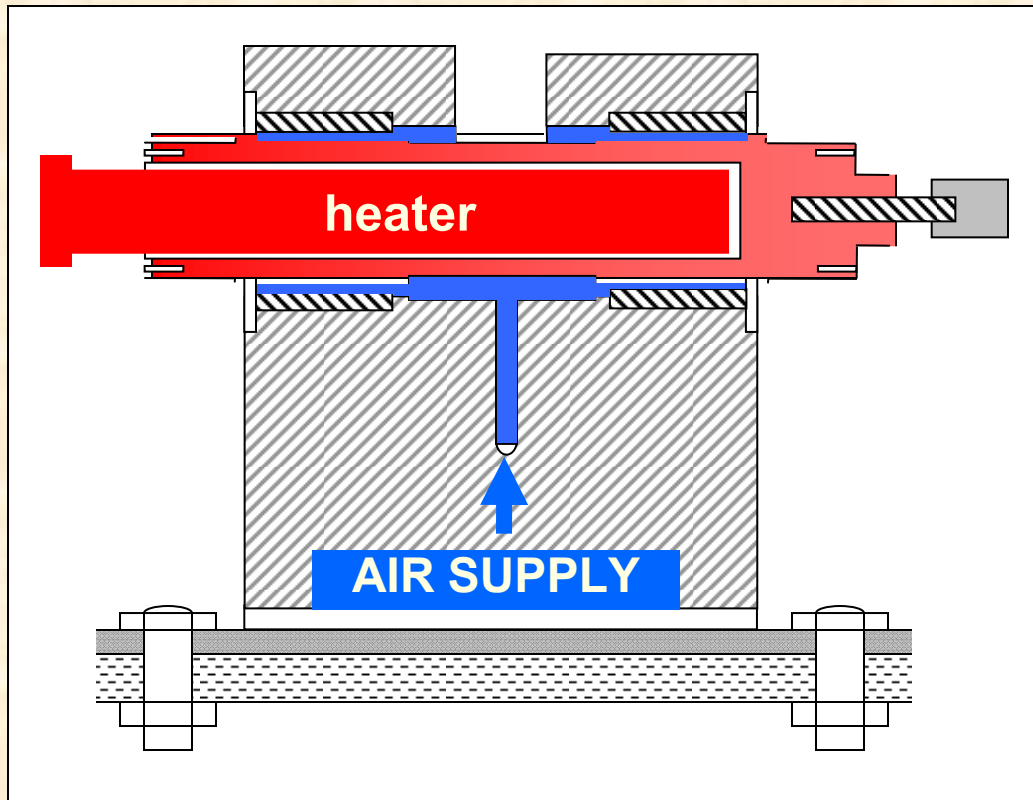
Instrumentation for high temperature

Gas flow meter (Max. 500 LPM). Drive motor (max. 50 krpm)



Cooling gas flow into GFBs

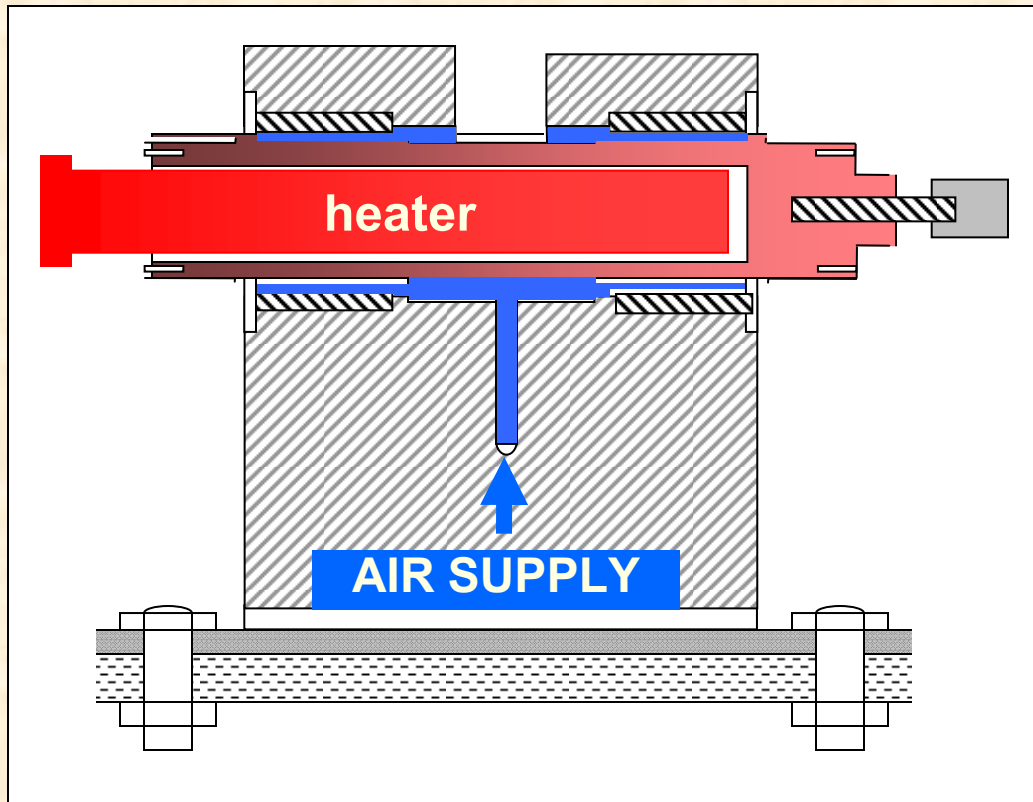
Gas pressure Max. 100 psi



Cooling flow needed
for **thermal**
management:
to remove heat from
shear drag or to
reduce thermal
gradients from **hot**
to **cold** engine
sections

Cooling gas flow into GFBs

Gas pressure Max. 100 psi



**Heater warms
unevenly test
rotor.**

**Side cooling
flows cool
unevenly the
rotor.**

Overview – Thermal management

Component-level tests

- **Ruscitto et al (1978)**: Perform load capacity tests on **1st gen. GFB** up to 45 krpm (1.7 MDN) and static load 111 N with **110 L/min cooling flow at 315C** bearing temperature.
- **DellaCorte (1998)**: **No cooling flow. 3rd gen. GFB** up to 70 krpm (2.4 MDN) at 700C. Bearing load capacity and torque decrease with temperature because of reduced bearing preload.
- **Dykas (2006)**: Investigates thermal management in **foil thrust bearings**. Cooling flow rates, to **450 L/min**, increase bearing load capacity at high rotor speeds. Inadequate thermal management can give thermo-elastic distortions affecting load capacity of test FB
- **Radil et al (2007)**: Evaluate effectiveness of **three cooling methods (axial cooling, direct and indirect shaft cooling)** for thermal management in a hot GFB environment

Overview – Thermal management

System-level tests

- **LaRue et al (2006)**: Oil-free Turbocharger. Thermal management achieved by **cooling the TC rotor and FBs**.
- **Lubell et al (2006)**: Commercial oil-free micro-turbines. Cooling air flows axially through **hollow rotor ID** remarkably decrease rotor temperature.
- **Heshmat et al (2005)**: Demonstrates hot (650C) GFB operation in a turbojet engine to 60 krpm. Cooling flow rates to 570 L/min still give **large axial thermal gradients (13°C/cm)**
- **San Andrés et al (2009)**: Forced cooling flow has limited effectiveness at low rotor temperatures. At high test temperatures, **large cooling flows (turbulent) remove heat more efficiently**.

Gases have limited thermal capacity,
hence (some) bearings demand large cooling flows to remove heat from hot rotor sections.

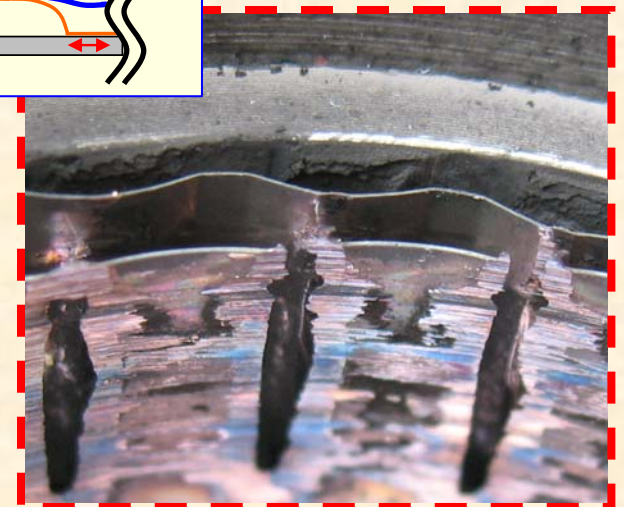
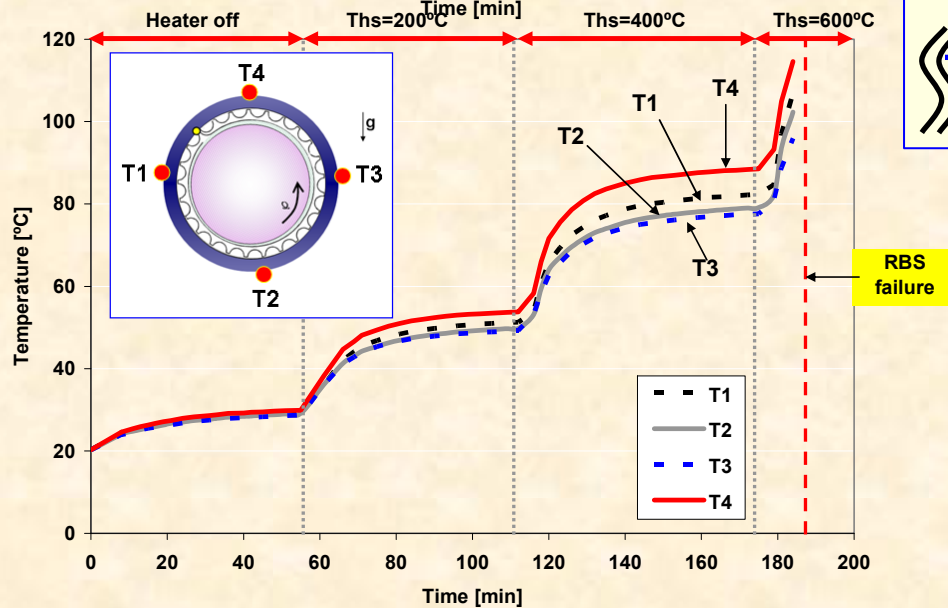
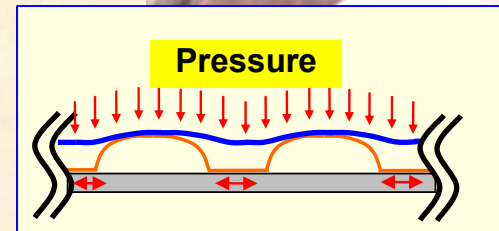
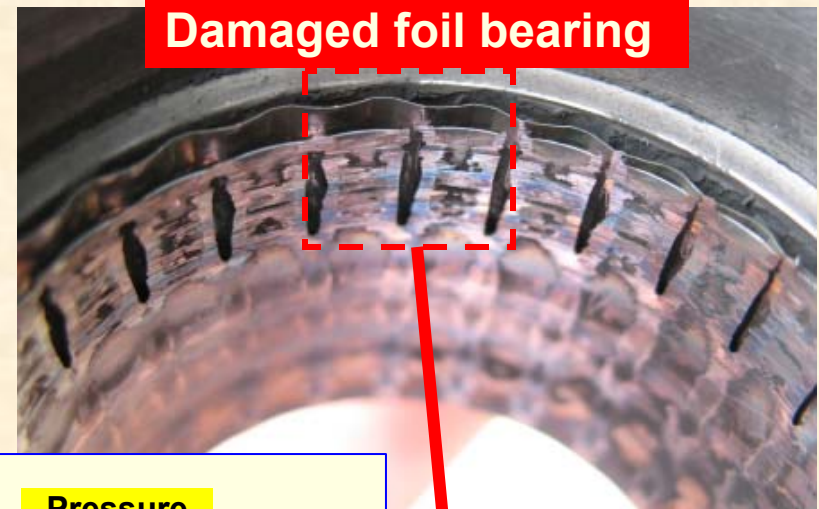
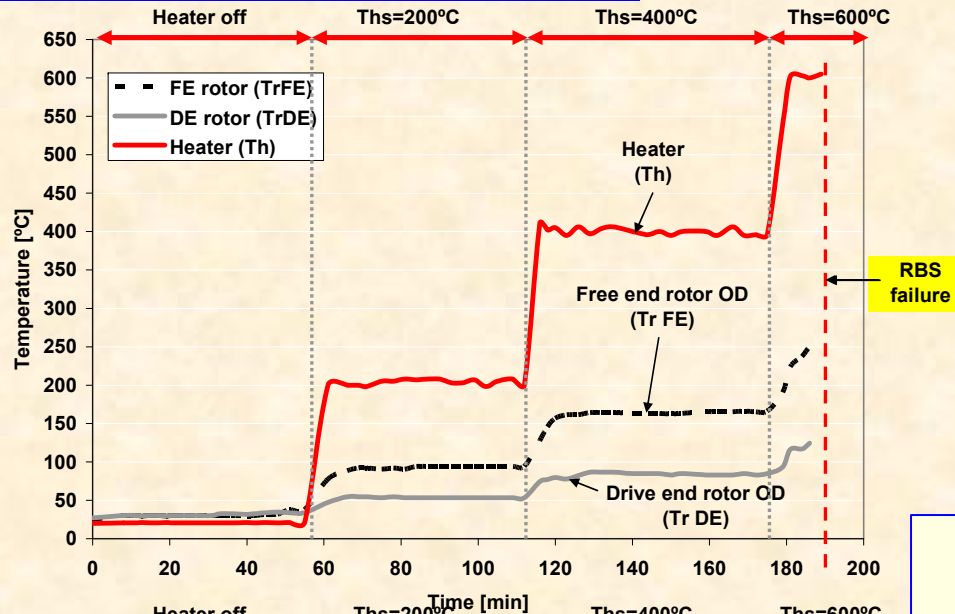
Why thermal effects are important?

Gas bearings (when airborne) are nearly friction free, hence they show small (drag) power loss and temperature rise. With **hot rotors** the “lubricant” in the bearings must also **cool** components. But gases have small thermal capacity and conductivity, and hence, get **hot!** Rises in temperature change material properties (solids and gas), and most importantly, **change bearing clearance!**

Lesson from previous demonstration

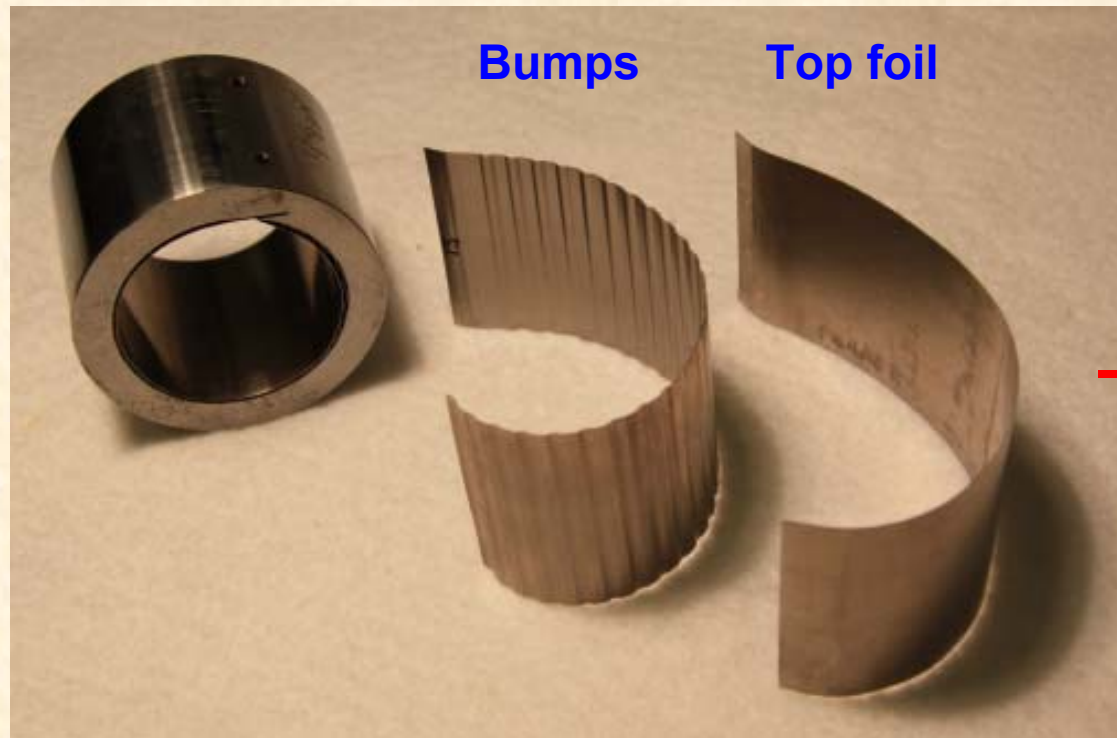
12/2009: HT GFB test

NO COOLING FLOW!!



Test Gas Foil Bearing

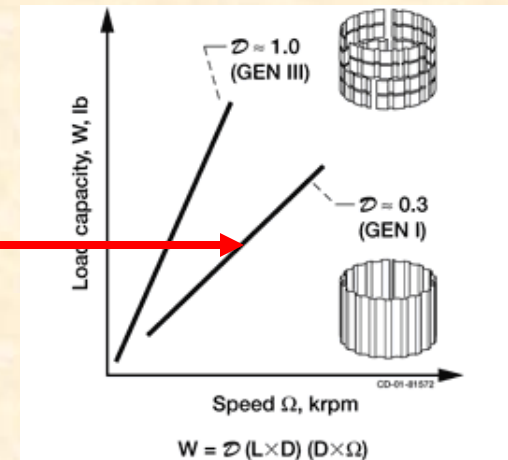
2010: GFBs donated by KIST



Test Gas Foil Bearing (Bump-Type)

1st Generation. Diameter: 36.63 mm

Foil material: Inconel X-750



Where

W is the maximum steady-state load that can be supported, N, lb

\mathcal{D} is the bearing load capacity coefficient,

**Reference: DellaCorte (2000)
Rule of Thumb**

UNCOATED TOP Foil !

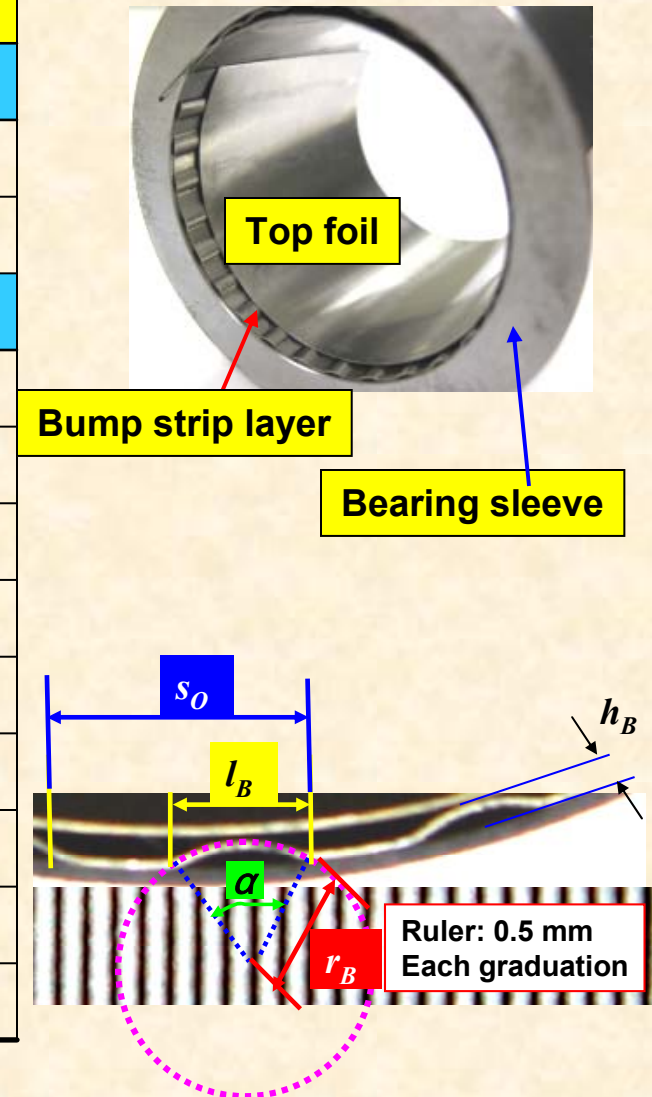
Hollow rotor (Inconel 718): 1.360 kg. Length: 200.66 mm. OD 36.51 mm and ID 17.9 mm. HT Coating up to 400C

Foil Bearing Dimension

KIST FB uncoated (Gen. I)

	Parameter [mm]
Bearing cartridge	
Outer diameter	50.8
Inner diameter	37.95
Top foil and bump strip layer	
Top foil axial length	38.1
Top foil thickness	0.12
Bump foil thickness	0.12
Number of Bumps	26 × 1 axial
Bump pitch, S_o	4.4
Bump length, l_B	2.5
Bump height, h_B	0.50
Bump arc radius, r_B	2.25
Bump arc angle [deg]	67

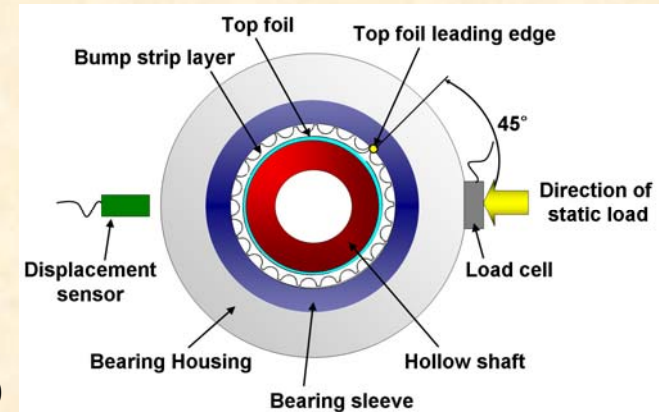
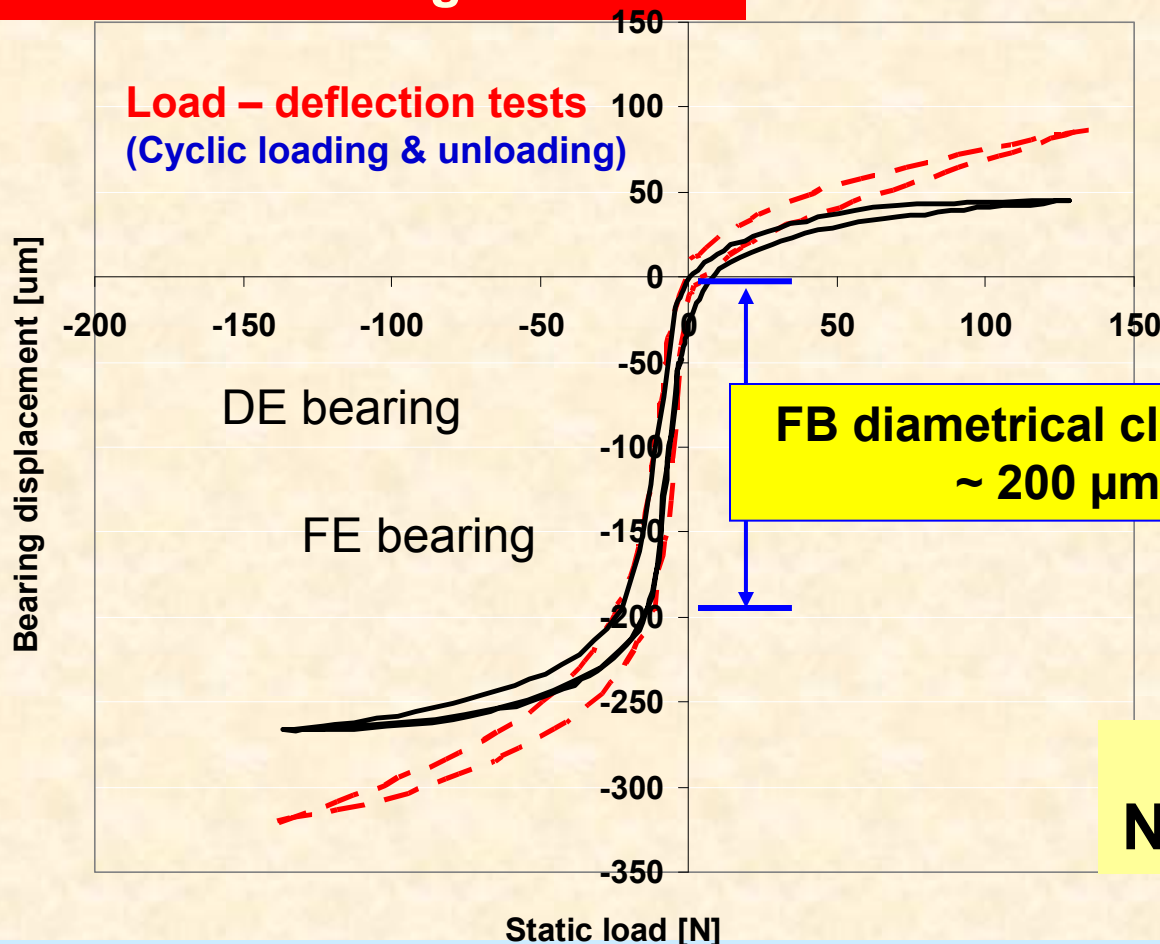
Foil material: Inconel X-750



FB deflection versus static load

Room temperature tests:
Estimation of bearing clearance

45° bearing orientation

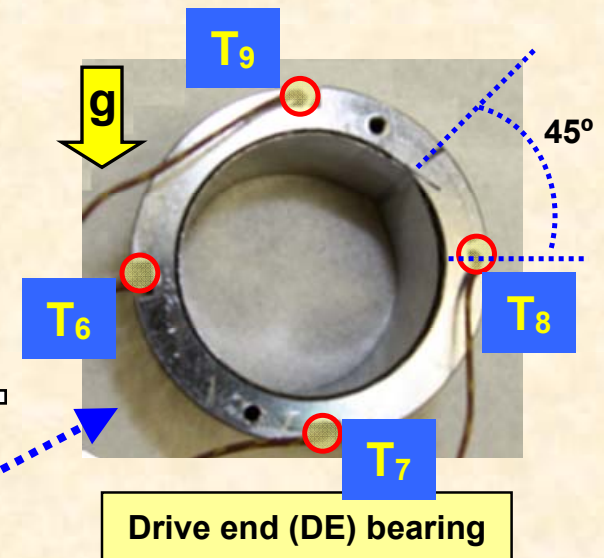
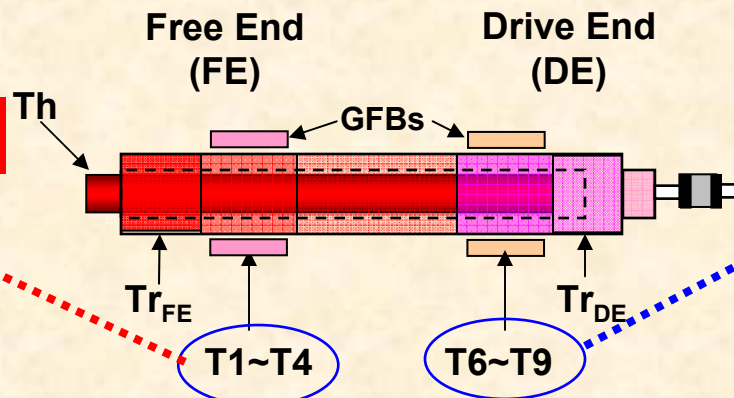
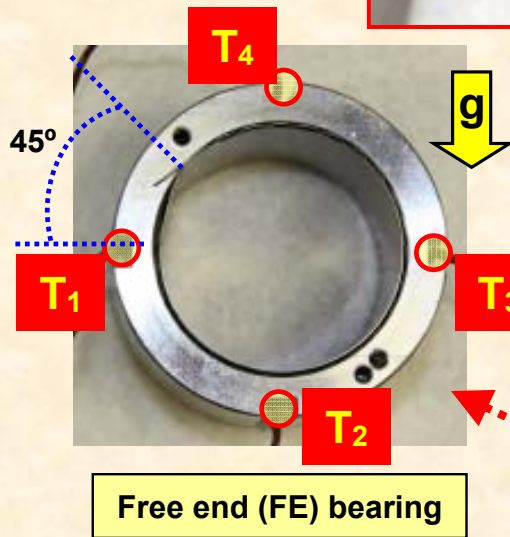
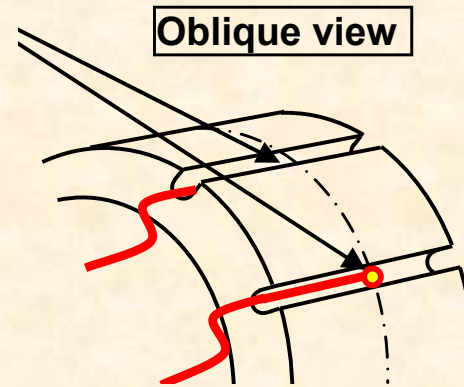
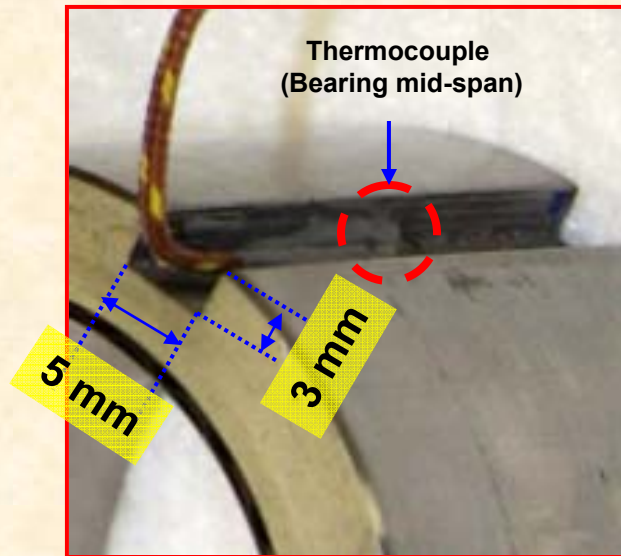


$F \neq KX$
Nonlinear $F(X)$

Hysteresis loop : Mechanical energy dissipation

due to dry-friction between top foil contacting bumps and bump strip layers contacting bearing cartridge

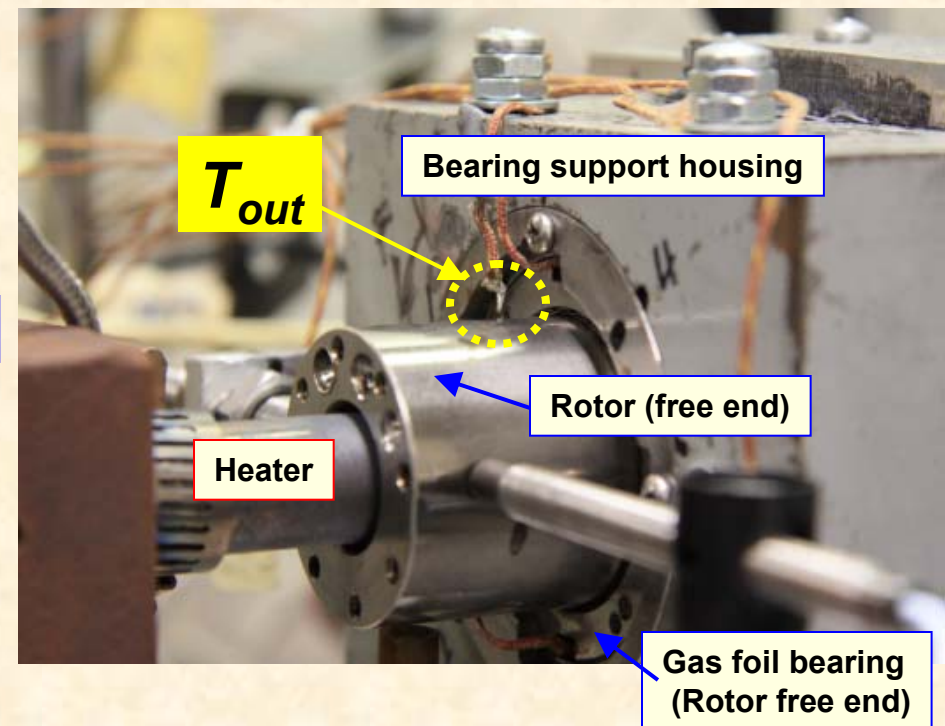
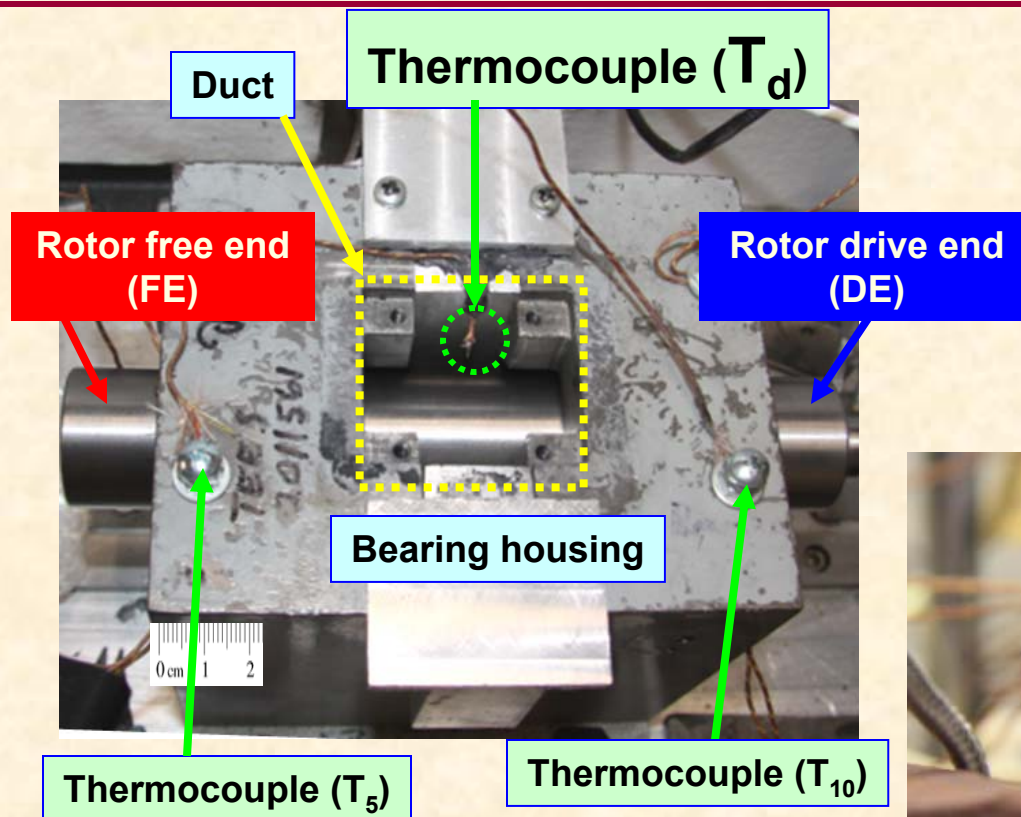
Thermocouples in test GFB



KIST FB uncoated (Generation I)

Four (4) thermocouples placed within machined axial slots.

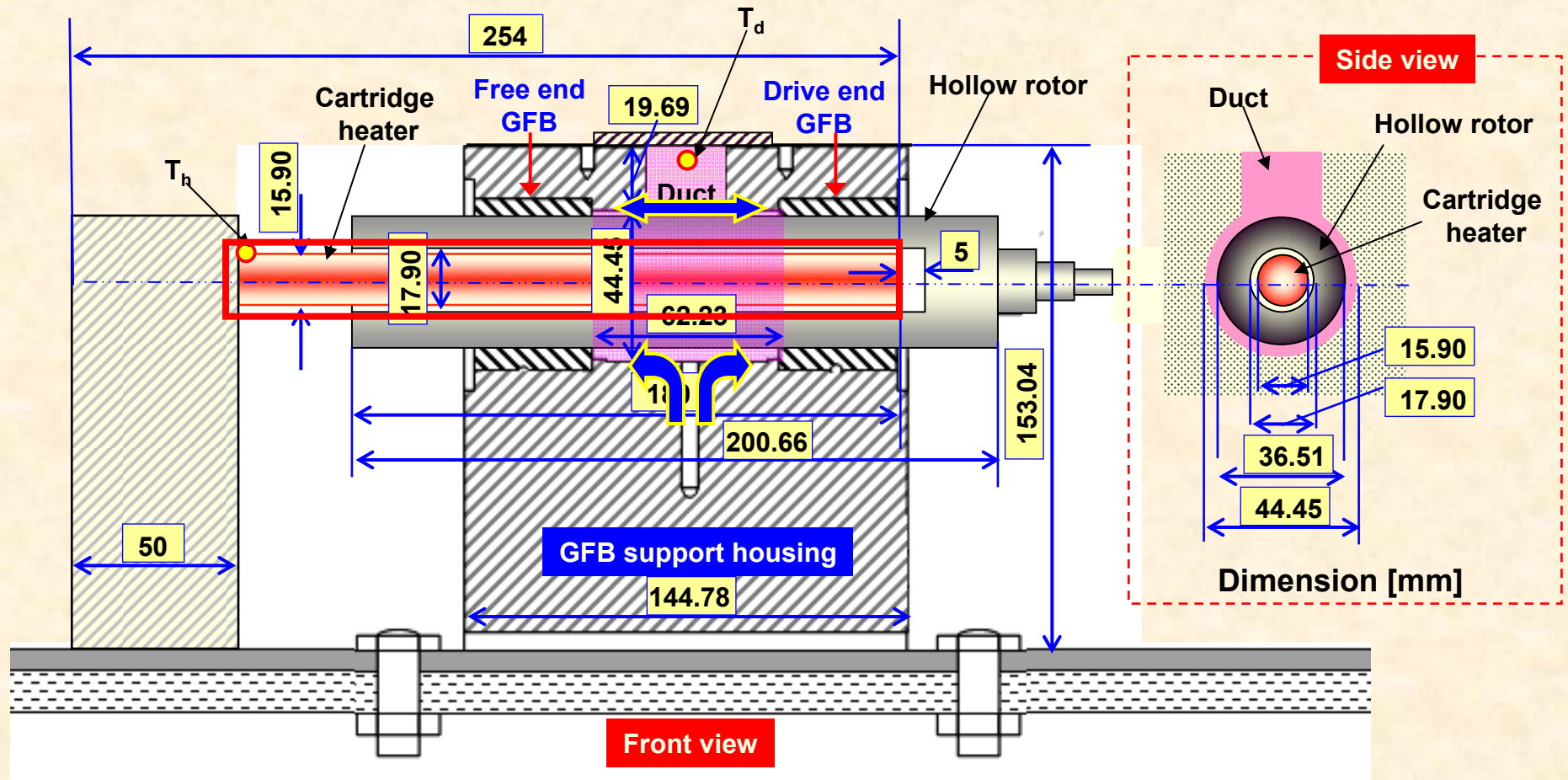
Thermocouples in bearing housing



Forced cooling stream temperature

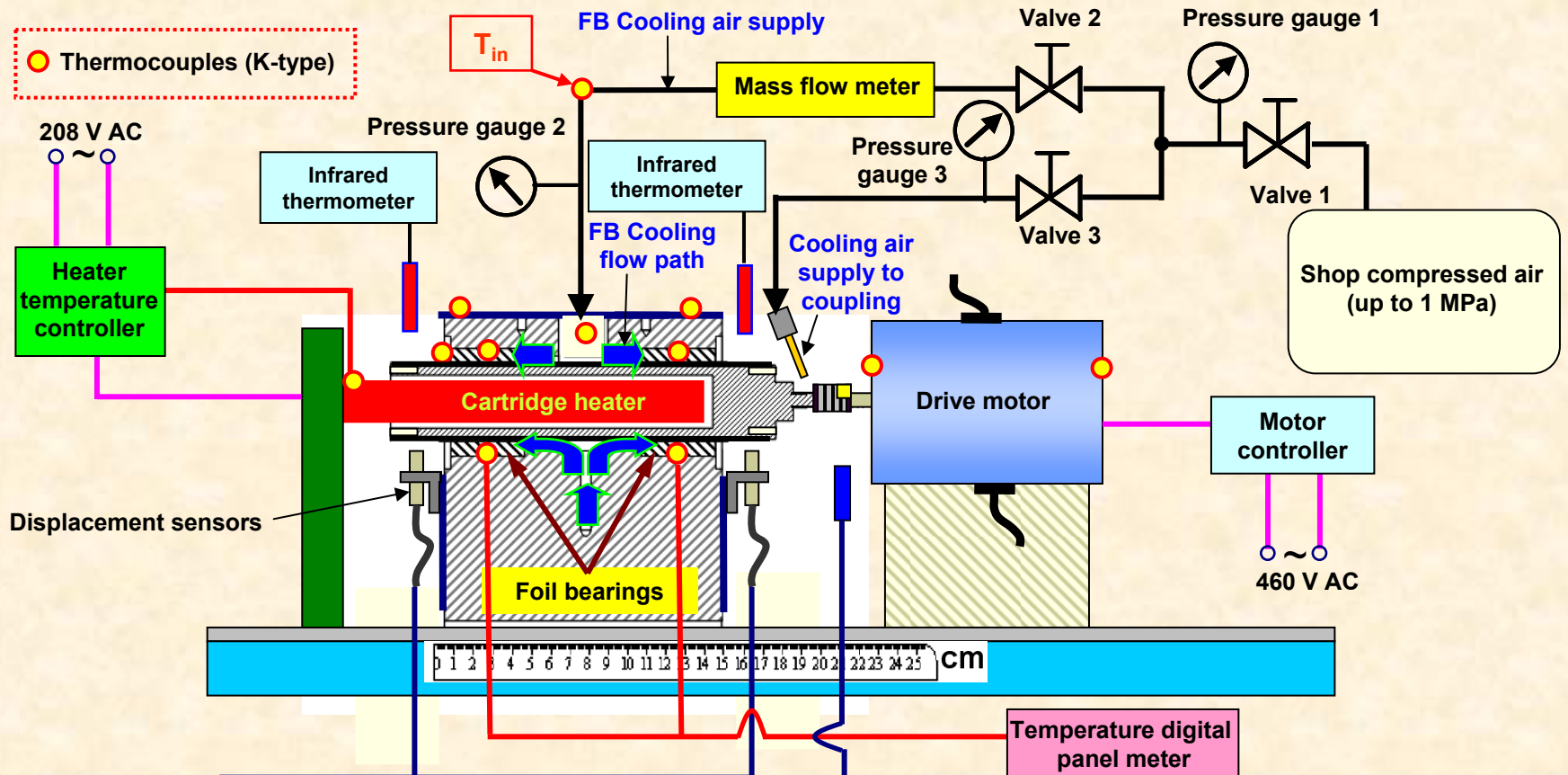
1 in housing duct + 1 at outboard plane of free end bearing

Hot rotor-GFB test rig



Dimensions

Hot rotor-GFB test rig



Thermocouples:
1 x heater, 3 x cooling air
2 x 4 FB outboard, 2 x Bearing housing
2x Drive motor, 1 x ambient
+ infrared thermometers 2 x rotor surface
(Total = 19)

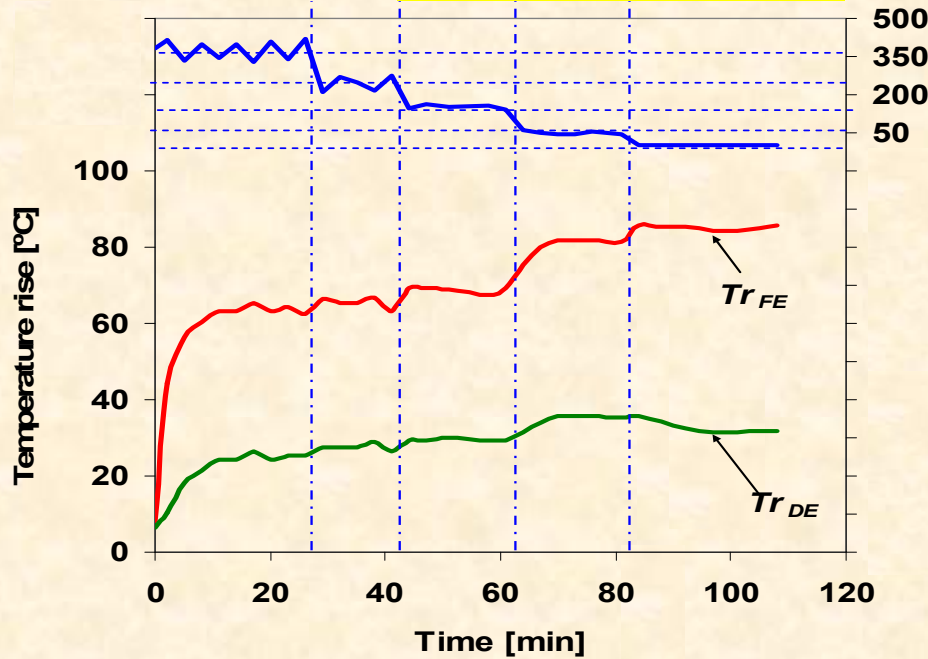
Instrumentation

Test Cases

Test case #	Heater set temperature [°C]	Rotor speed [krpm]	Set cooling flow rate (into two bearings) [L/min]	Time [min]
1	65	0	350 → 250 → 150 → 50 → 0	87
2	100	0	350 → 250 → 150 → 50 → 0	84
3	150	0	350 → 250 → 150 → 50 → 0	108
4	65	10 → 20 → 30	350 → 250 → 150 → 50	248
5	100	10 → 20 → 30	350 → 250 → 150 → 50	266
6	150	10	350 → 250 → 150 → 50	136
7	Off	30	350	30
8	65	30	350	30
9	100	30	350	30
10	100	30	50	30
				Overall 1049 min

Rotor OD Temps. vs Time

No rotor spinning

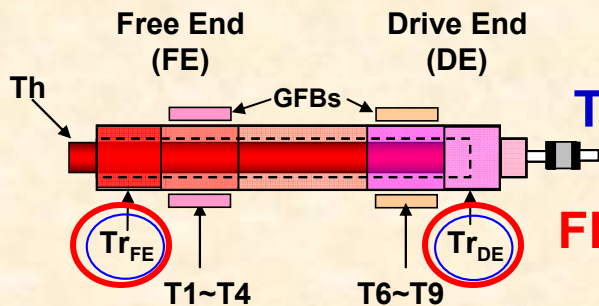


Test cases #1 and #4

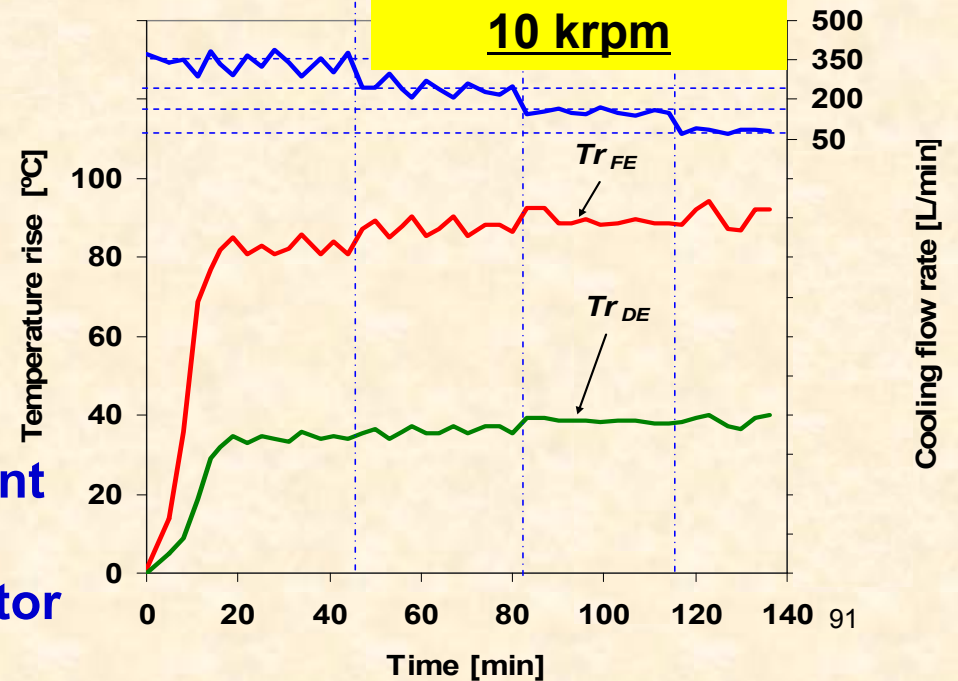
Heater set temperature = 150°C

Temperatures on shaft OD increase steadily with elapsed test time at each rotor speed and cooling flow rate condition

The rotor is a source of HEAT!



**Thermal gradient
Hot to cold
FE rotor > DE rotor**



Cooling flow rate [L/min]

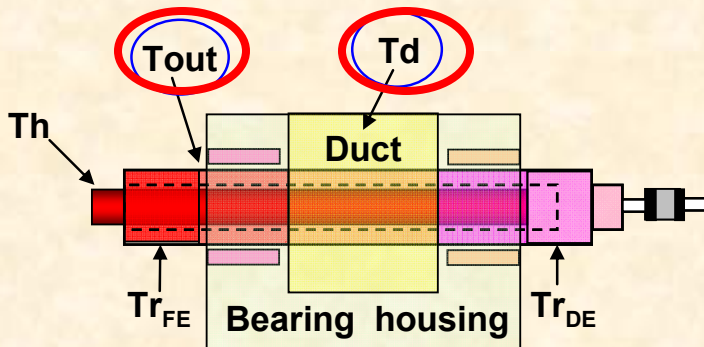
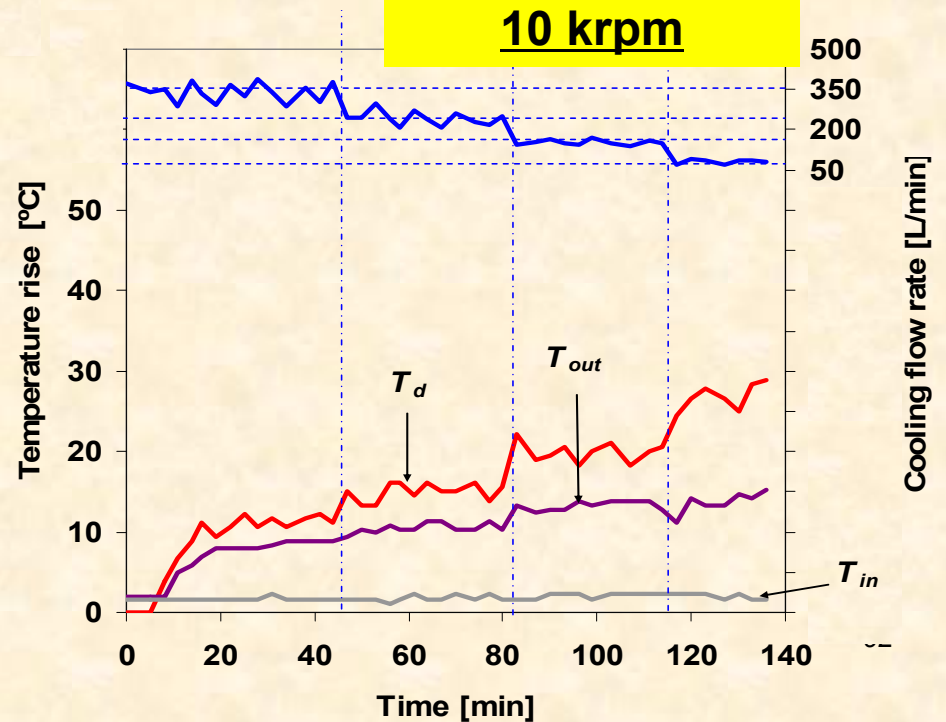
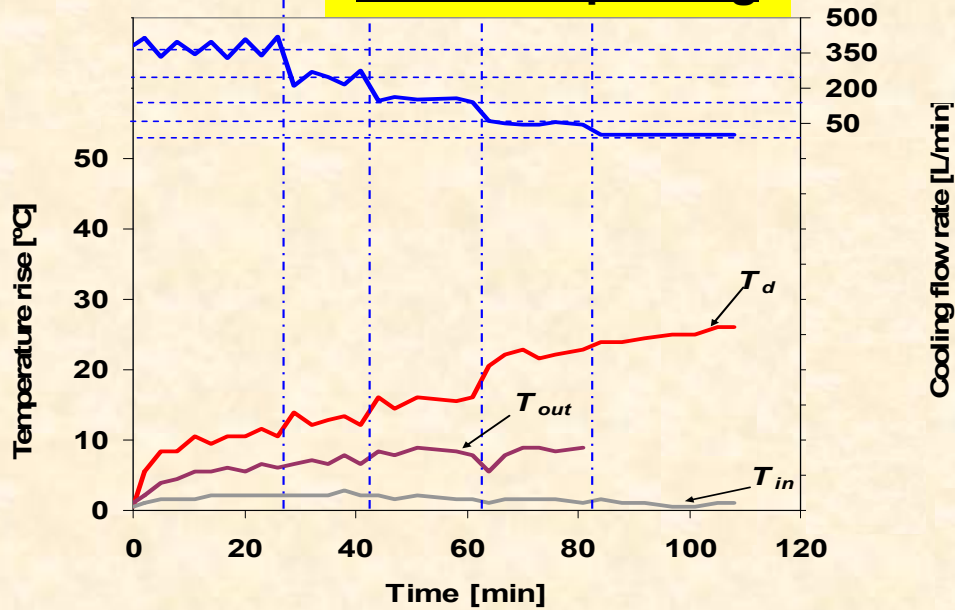
Duct & Outboard temperature rises vs time

No rotor spinning

Test cases #1 and #4

Heater set temperature = 150°C

**$T_{in} \sim T_{amb}$
 $T_d > T_{out} > T_{in}$**

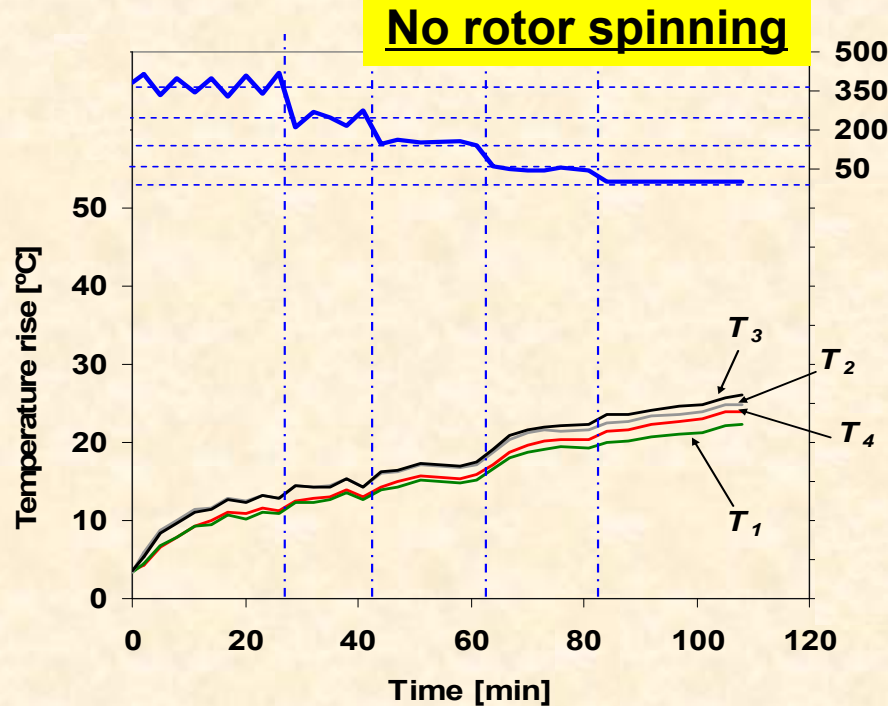
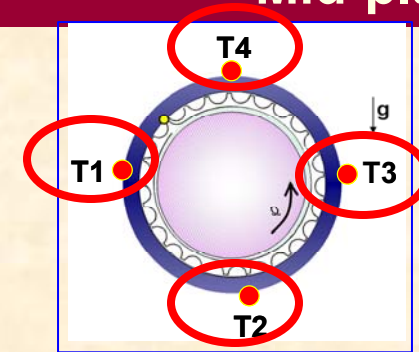


FE bearing temperature rise vs time

Test cases #1 and #4

Heater set temperature = 150°C

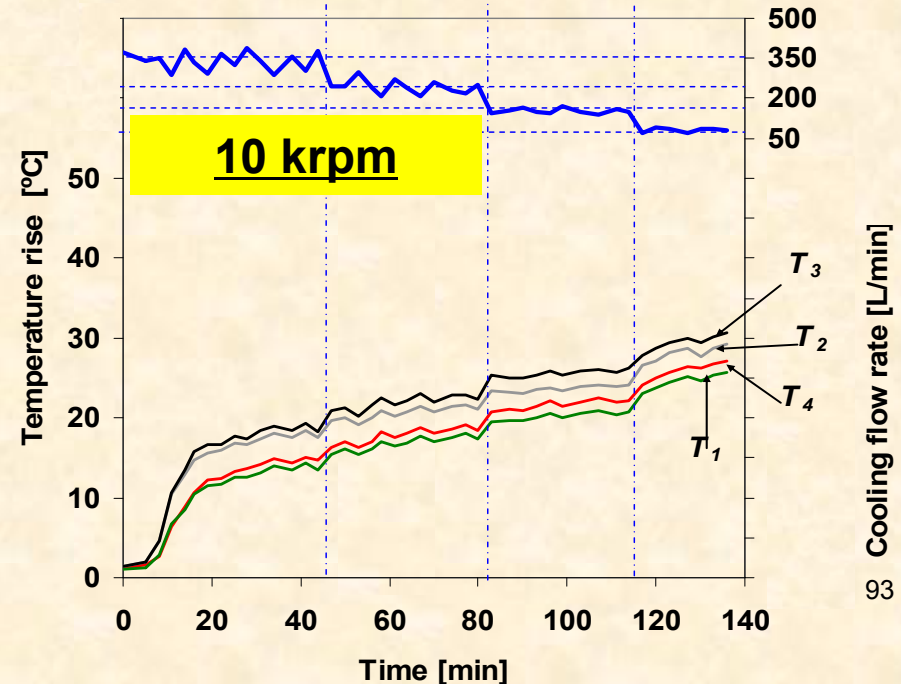
Free End Bearing
Mid-plane



Cooling flow rate [L/min]

Temperature rise [°C]

10 krpm



Cooling flow rate [L/min]

93

$T_3 > T_2 > T_4 > T_1$ due to differences in rotor OD temp. along its circumference

Rotor speed makes bearings slightly hotter (a few deg C)

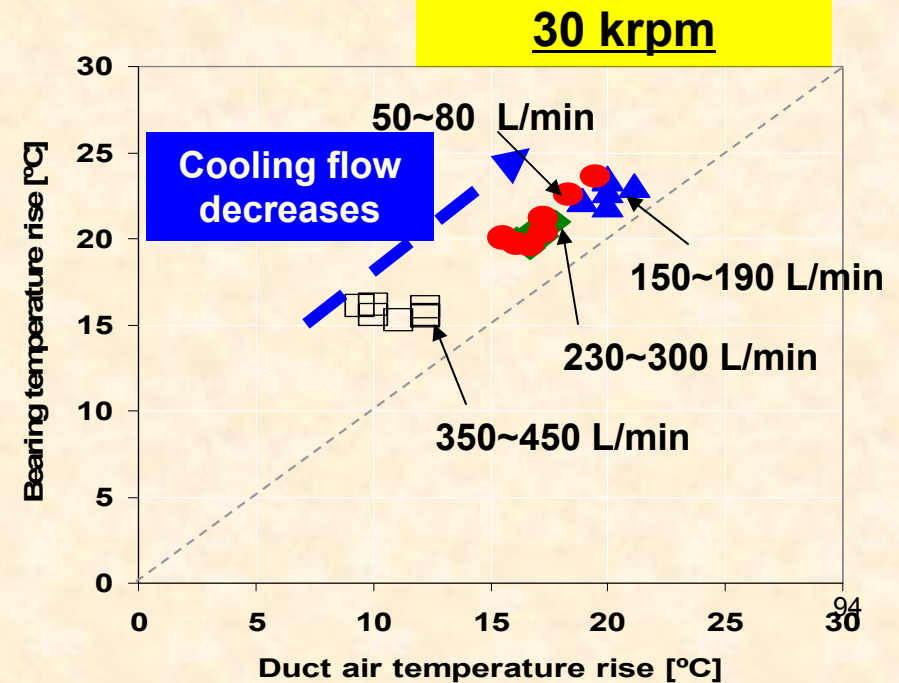
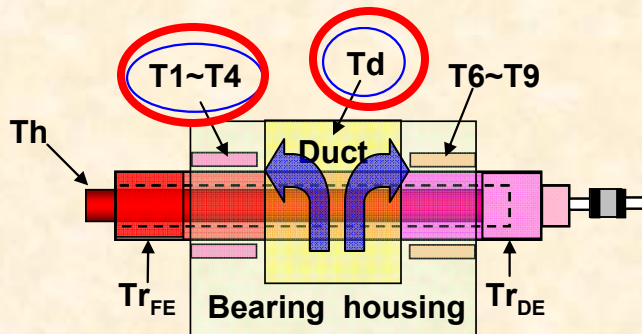
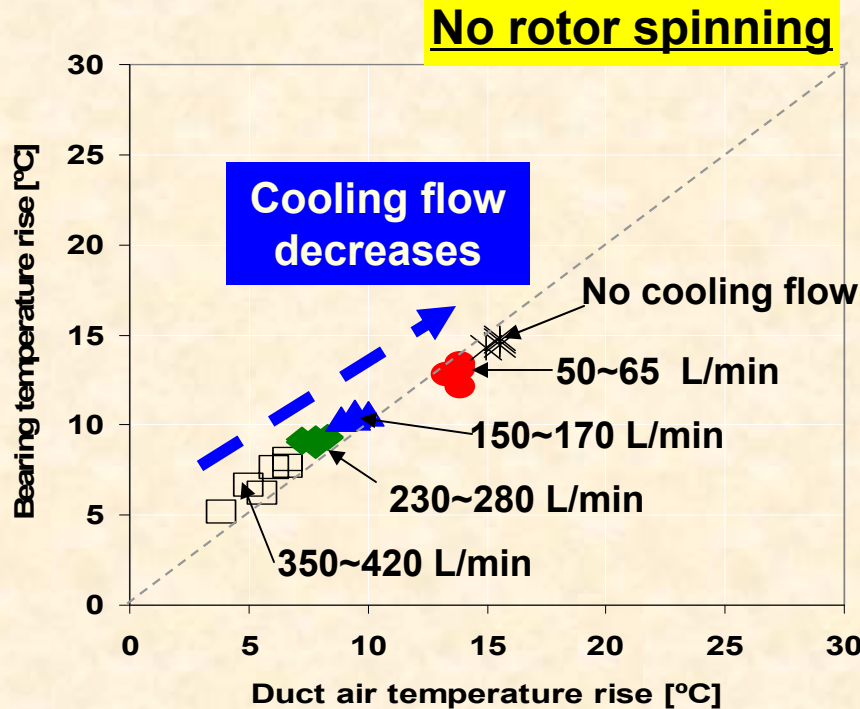
Bearing temperature rise vs duct temp.

Test cases #2 and #5

Heater set temperature = 100°C

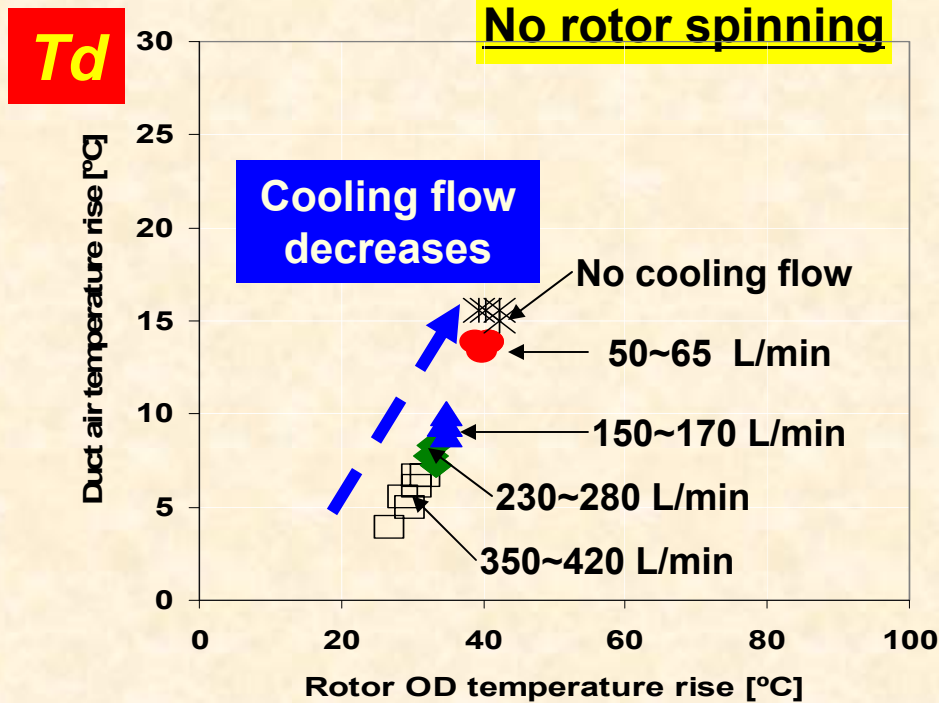
Free end Bearing

Temperatures on bearings ODs linearly increase with duct air temperature as the cooling flow rate into the bearings decreases



Rise in temperatures: Duct vs Rotor OD

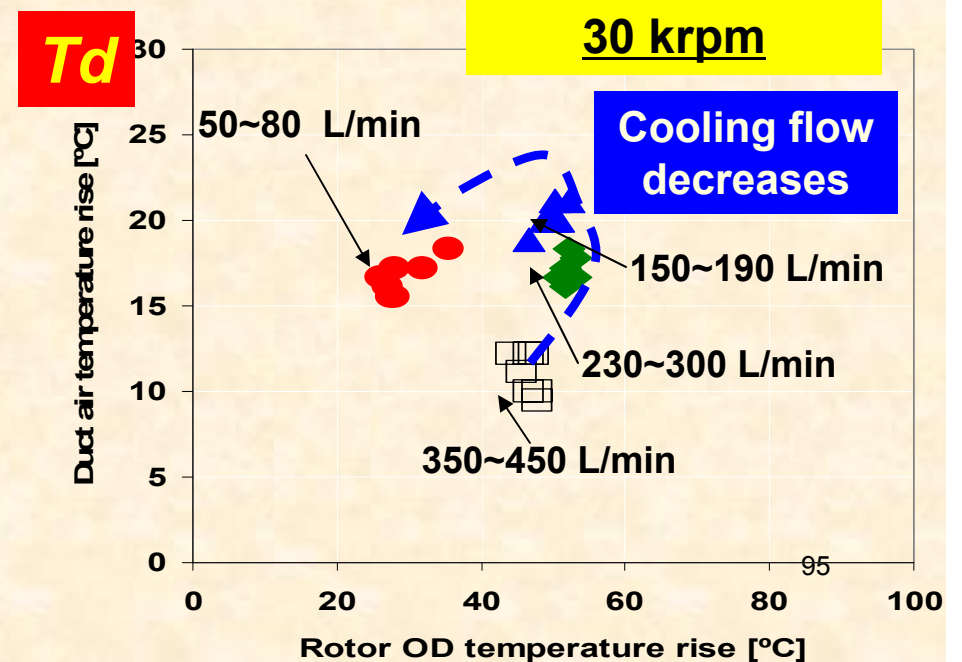
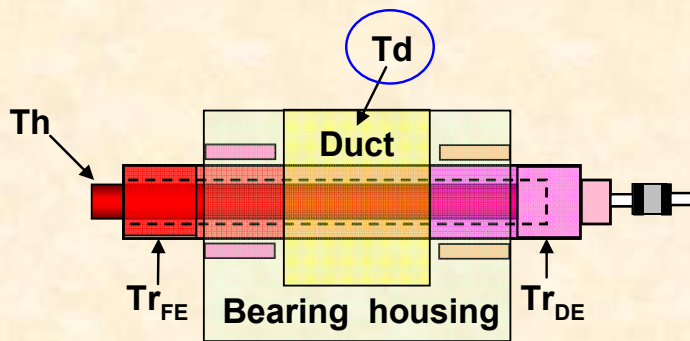
Test cases #2 and #5



Heater set temperature = 100°C

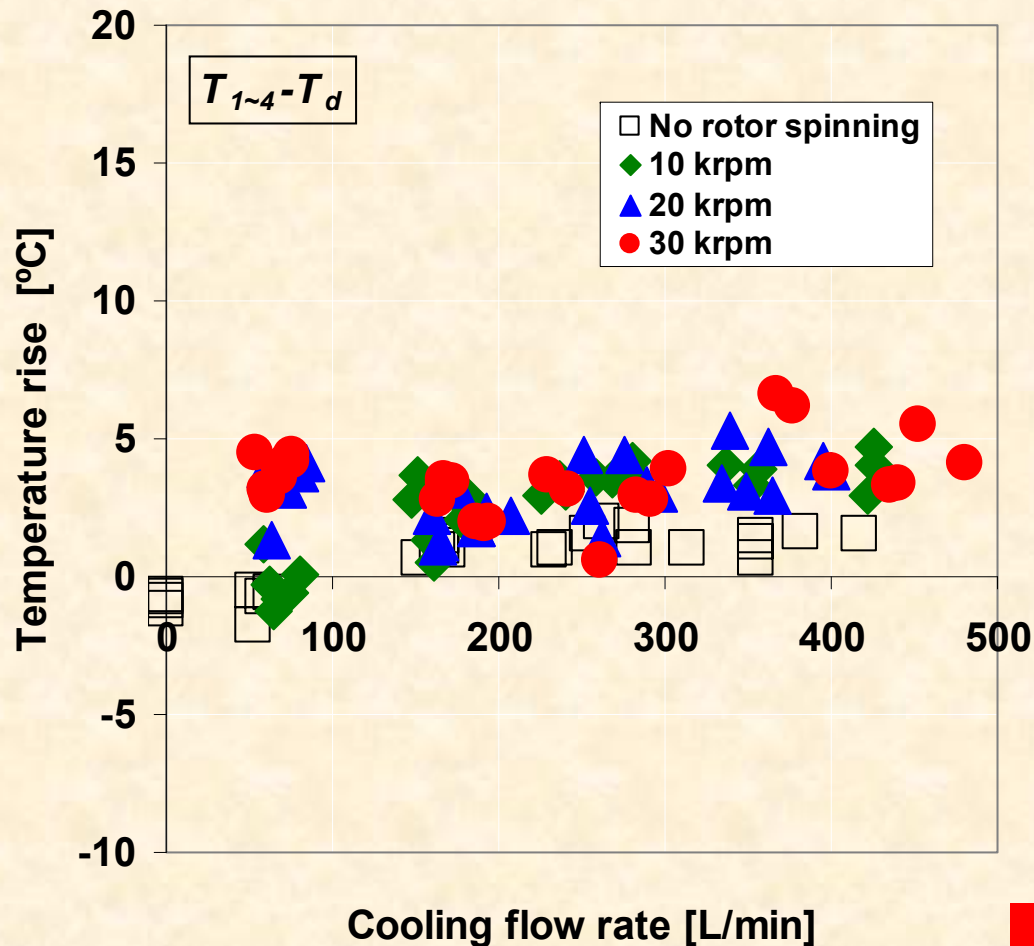
T_d decreases with cooling flow due to longer residence of air particles in the duct

T_d increases with rotor speed due to windage effect

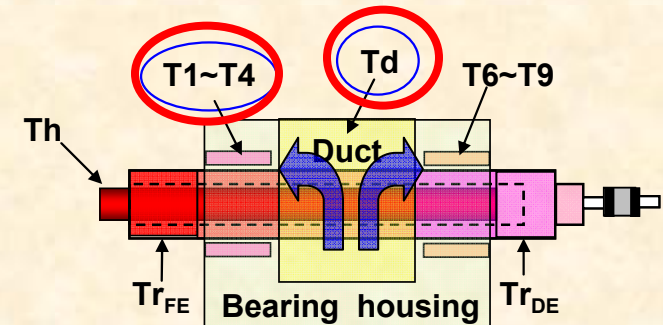


Bearing OD temperature rise vs. cooling flow

Test cases #2 and #5



Heater set temperature = 100°C



Free end Bearing

Temperature difference
($T - T_d$) is invariant
while increasing cooling
flow rate!

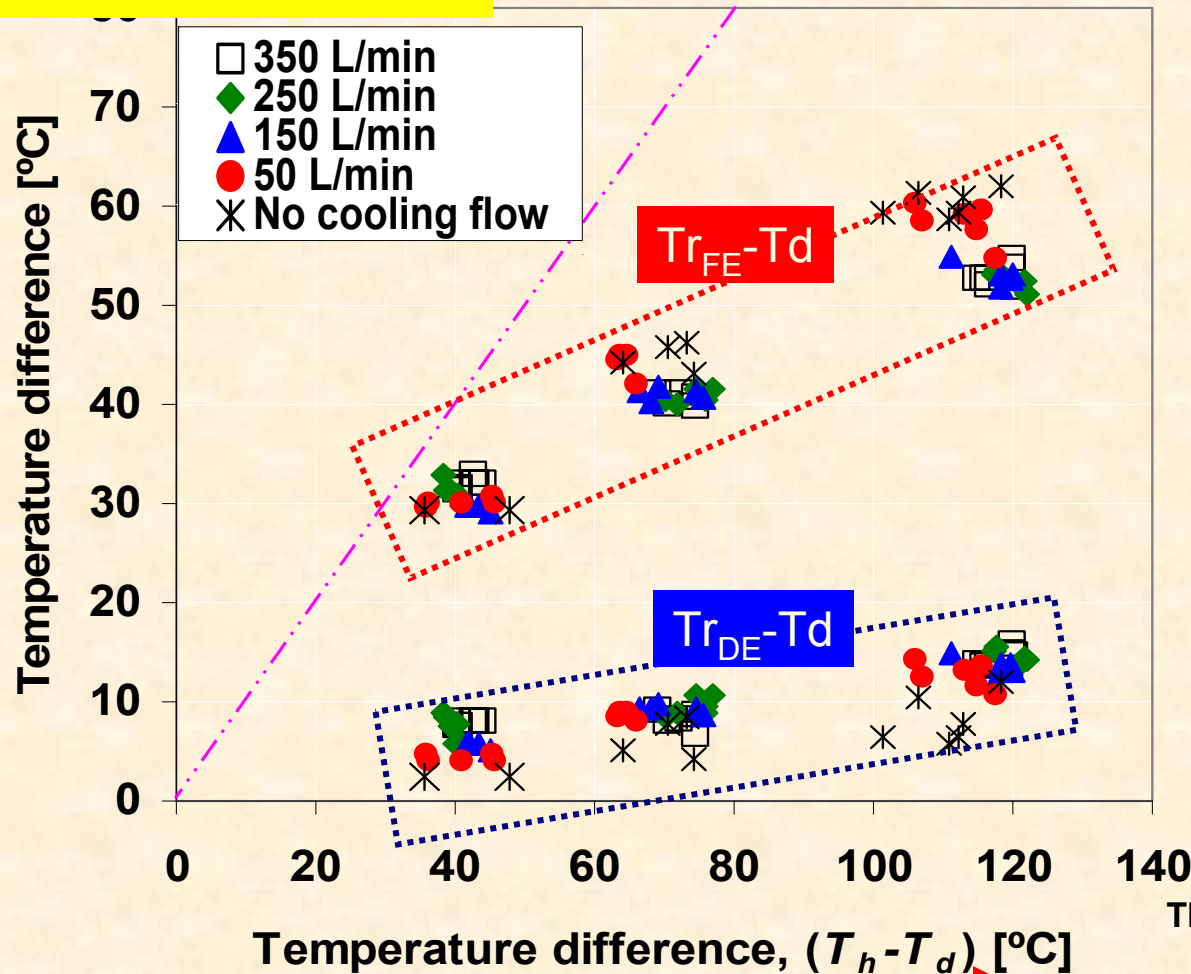


Bearing temperature is a
small fraction of the heat
source temperature
(heater and duct air).

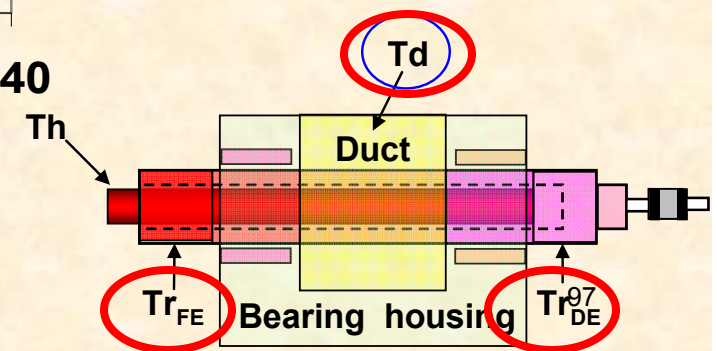
Rotor OD temp. vs heater temp. (- duct ???)

No rotor spinning

Test cases #1~#3



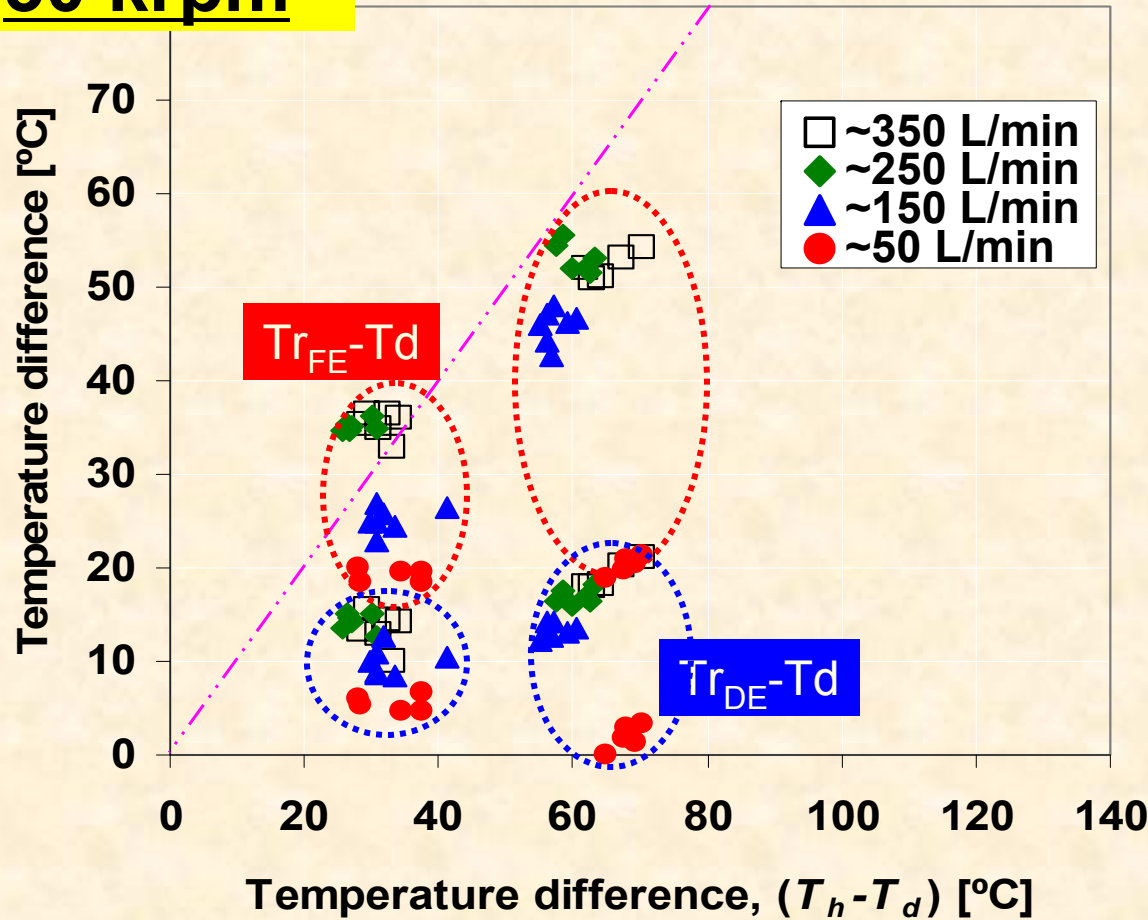
The cooling gas flow **removes heat from the top foil back surface**, thus **cooling the rotor OD**



Rotor OD temp. vs heater temp.

Test cases #4 and #5

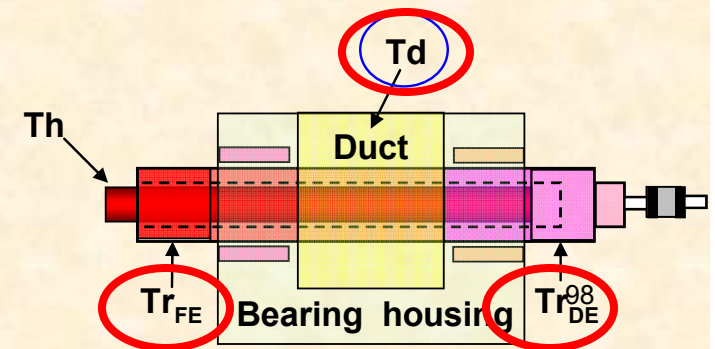
30 krpm



Rotor OD temp
(relative to duct
temp T_d)
decrease with
cooling flow

Temperature difference, ($T_h - T_d$) [°C]

Cartridge temperature (T_{hs})
increases



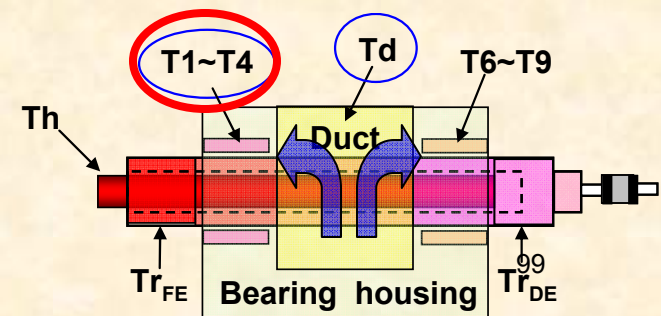
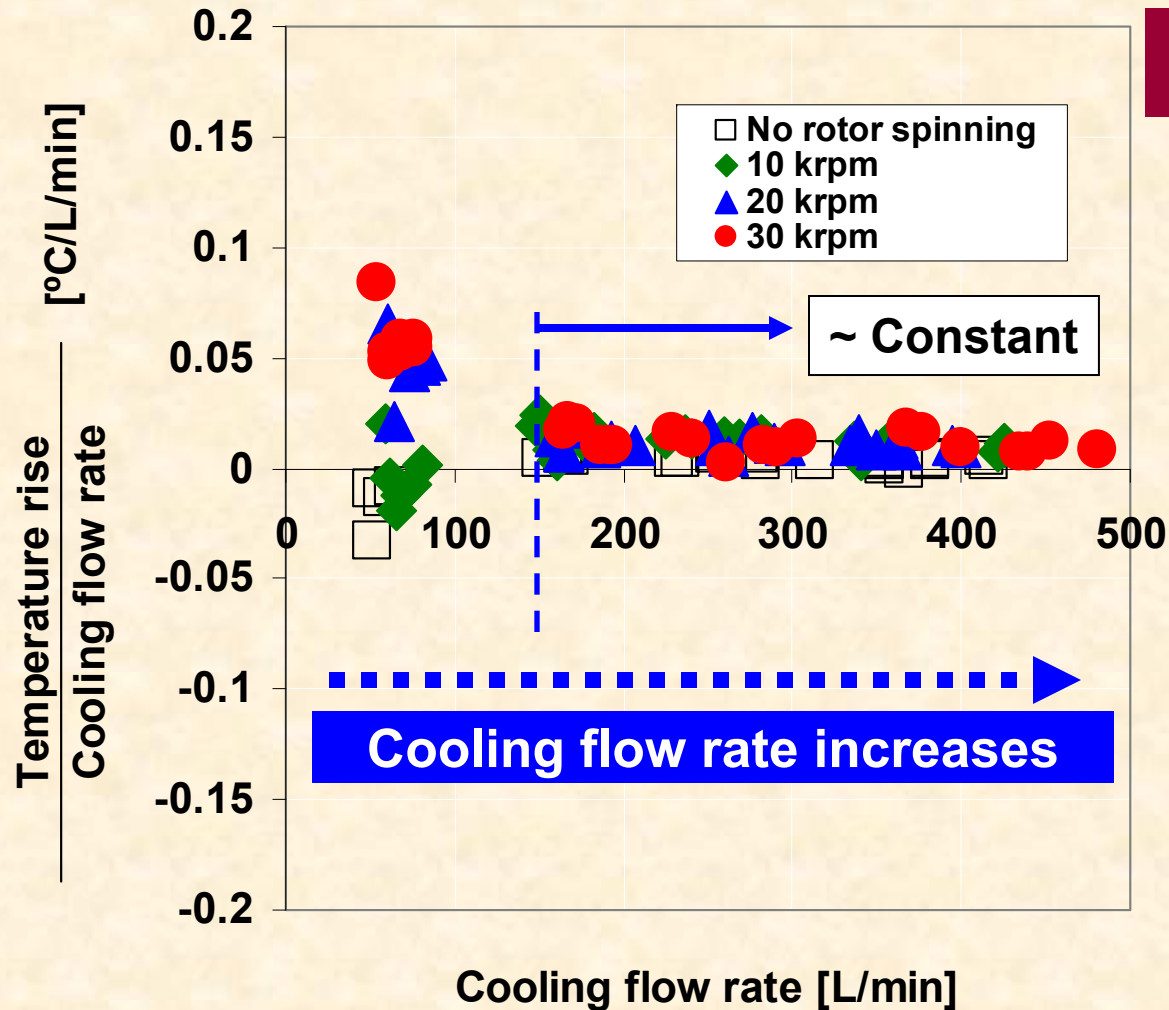
Cooling Capability: Bearing OD temp.

Test cases #2 and #5

Heater set temperature = 100°C

Free end Bearing

The cooling capability of the forced axial flow on the bearing temperatures changes little with flow rate



Cooling Capability: Rotor OD temp.

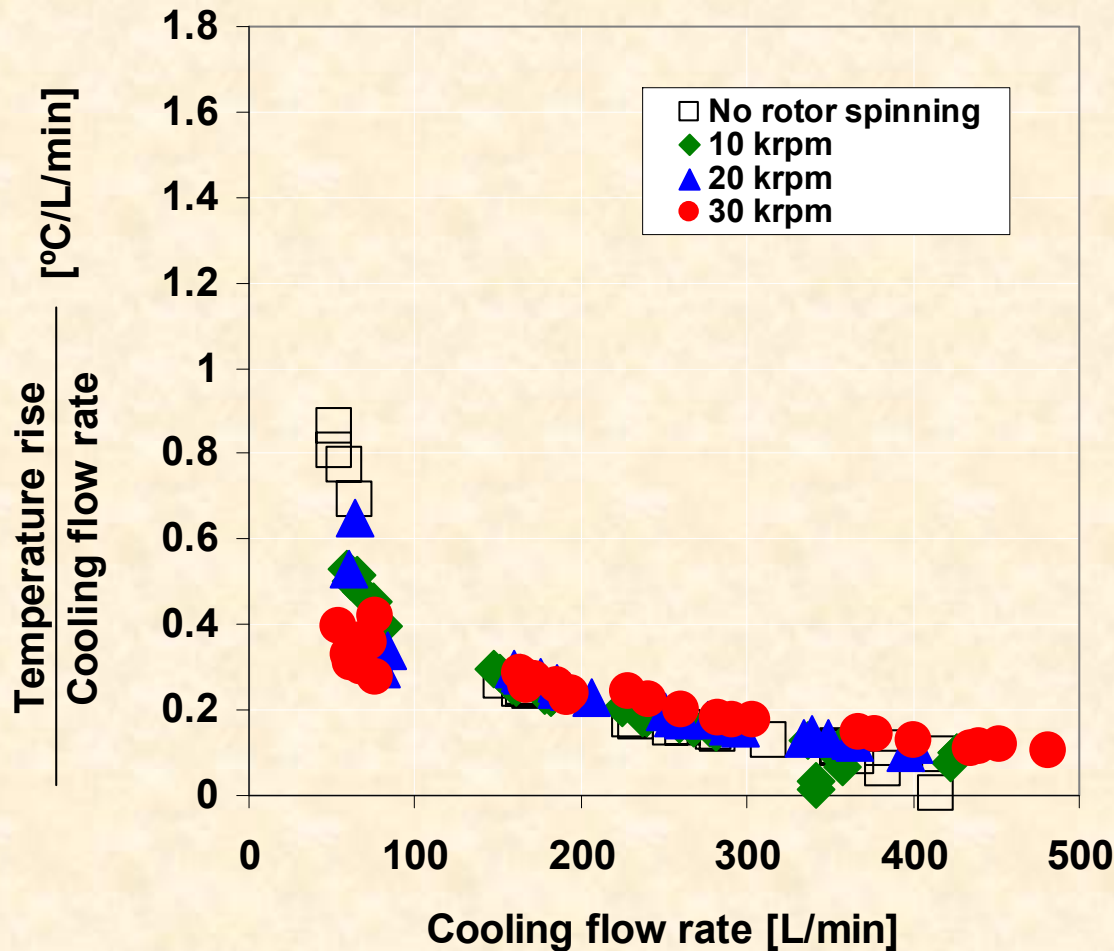
Test cases #2 and #5

Heater set temperature = 100°C

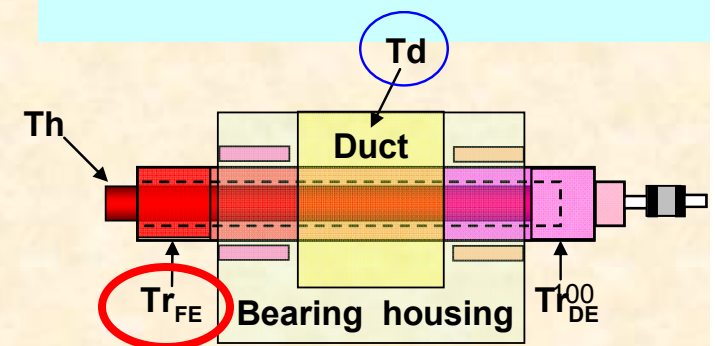
Free end rotor

The cooling capability of the forced axial flow on the rotor temperatures appears to have an exponential decay character.

The cooling effectiveness of the forced cooling stream is **most distinct at the free end rotor OD.**

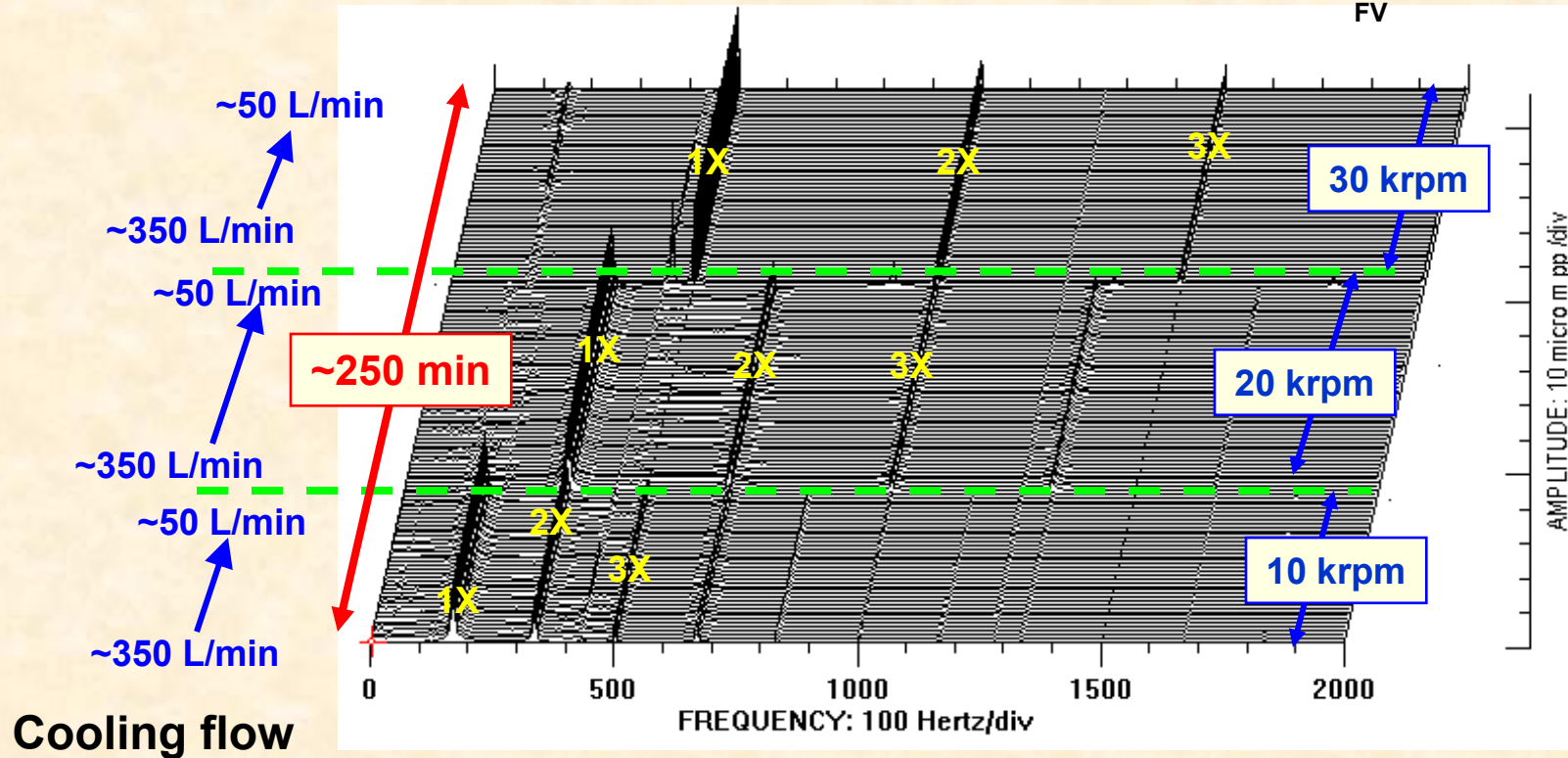
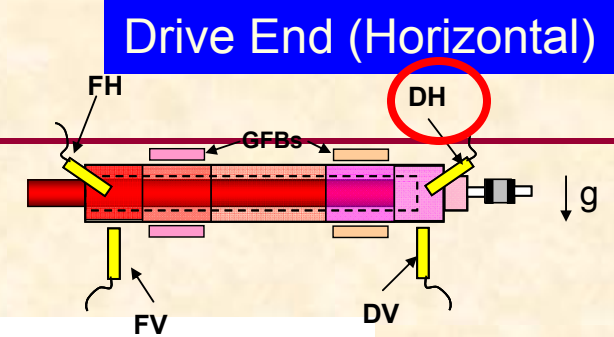


Cooling flow rate increases



Waterfalls of rotor motion

Baseline, $T_{hs}=65C$



Test case #4

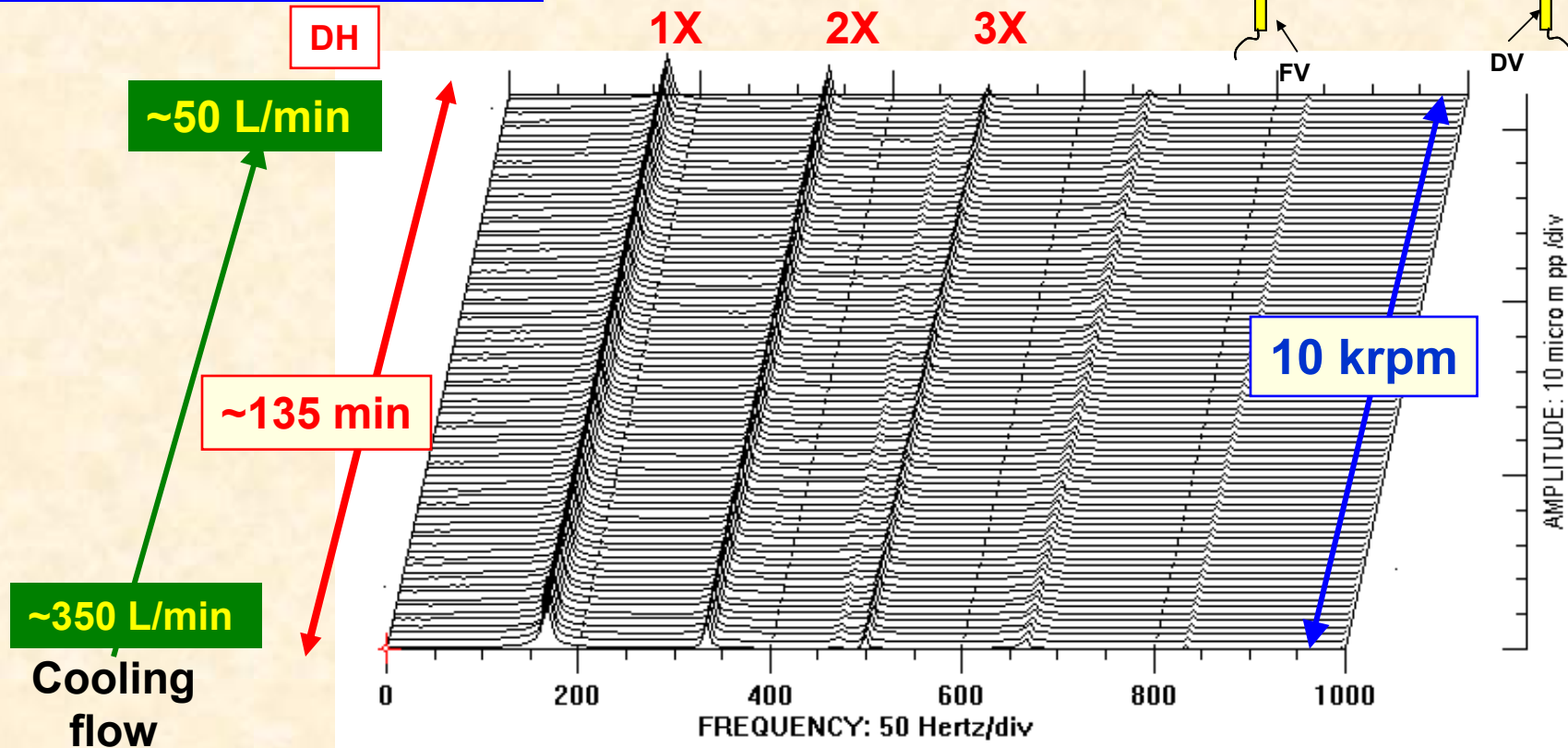
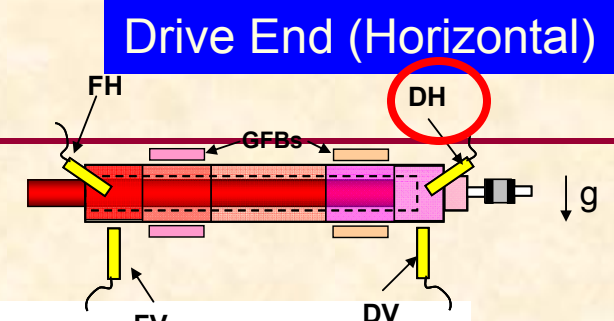
Free of sub synchronous whirl motions

Cooling flow rate does not affect amplitude and frequency contents of rotordynamic displacement

Rotor motion measurements

Waterfalls of rotor motion

Baseline, $T_{hs}=150C$

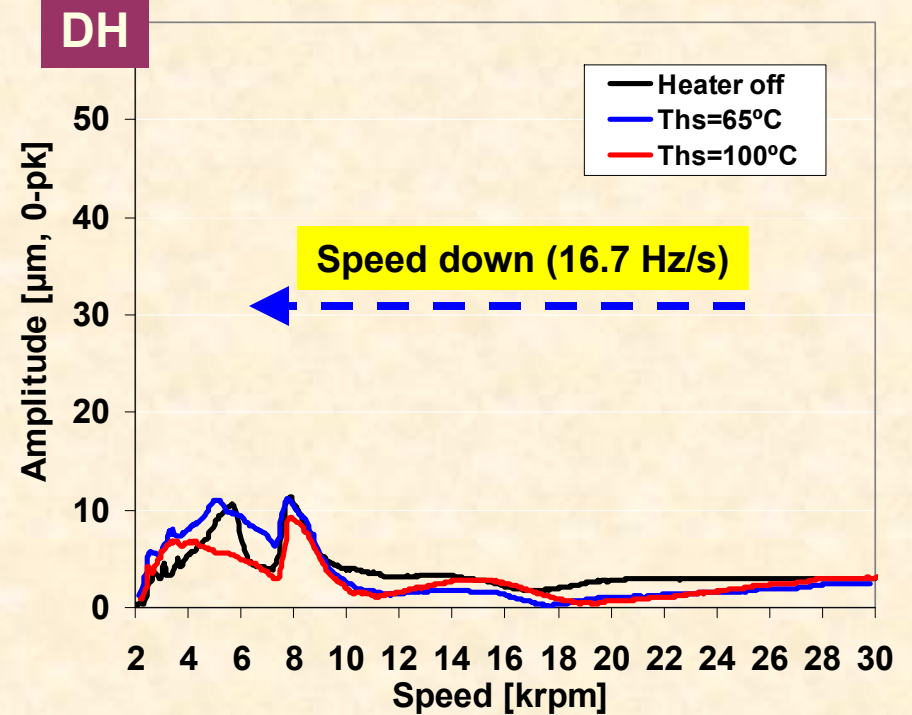
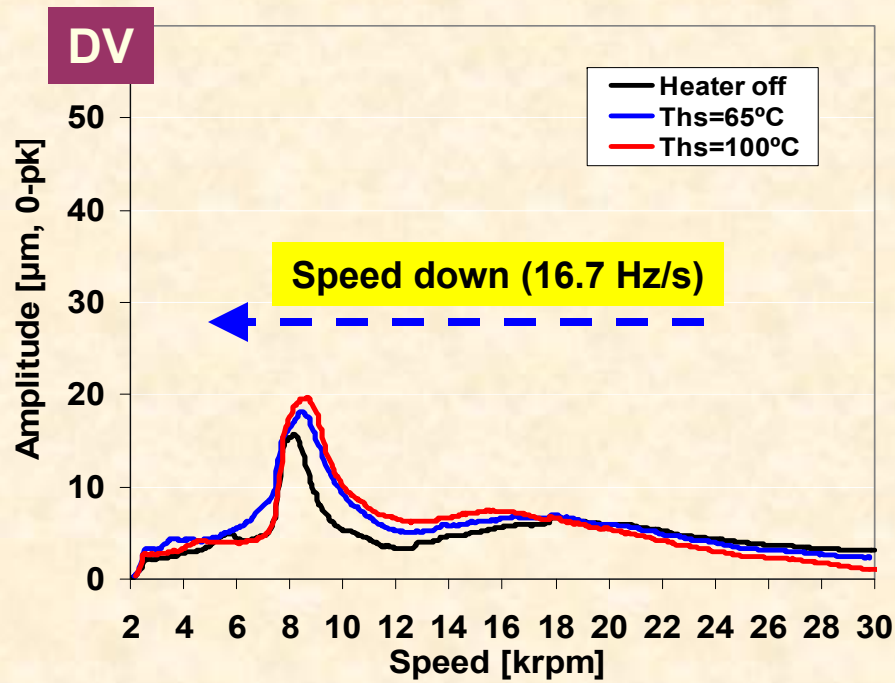
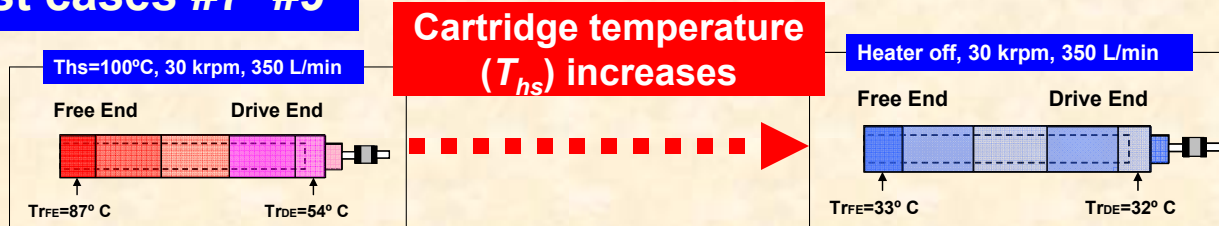


Test case #6

Rotor OD temperature does not affect rotor dynamic displacements!

Synchronous rotor response: effect of shaft temp.

Test cases #7~#9



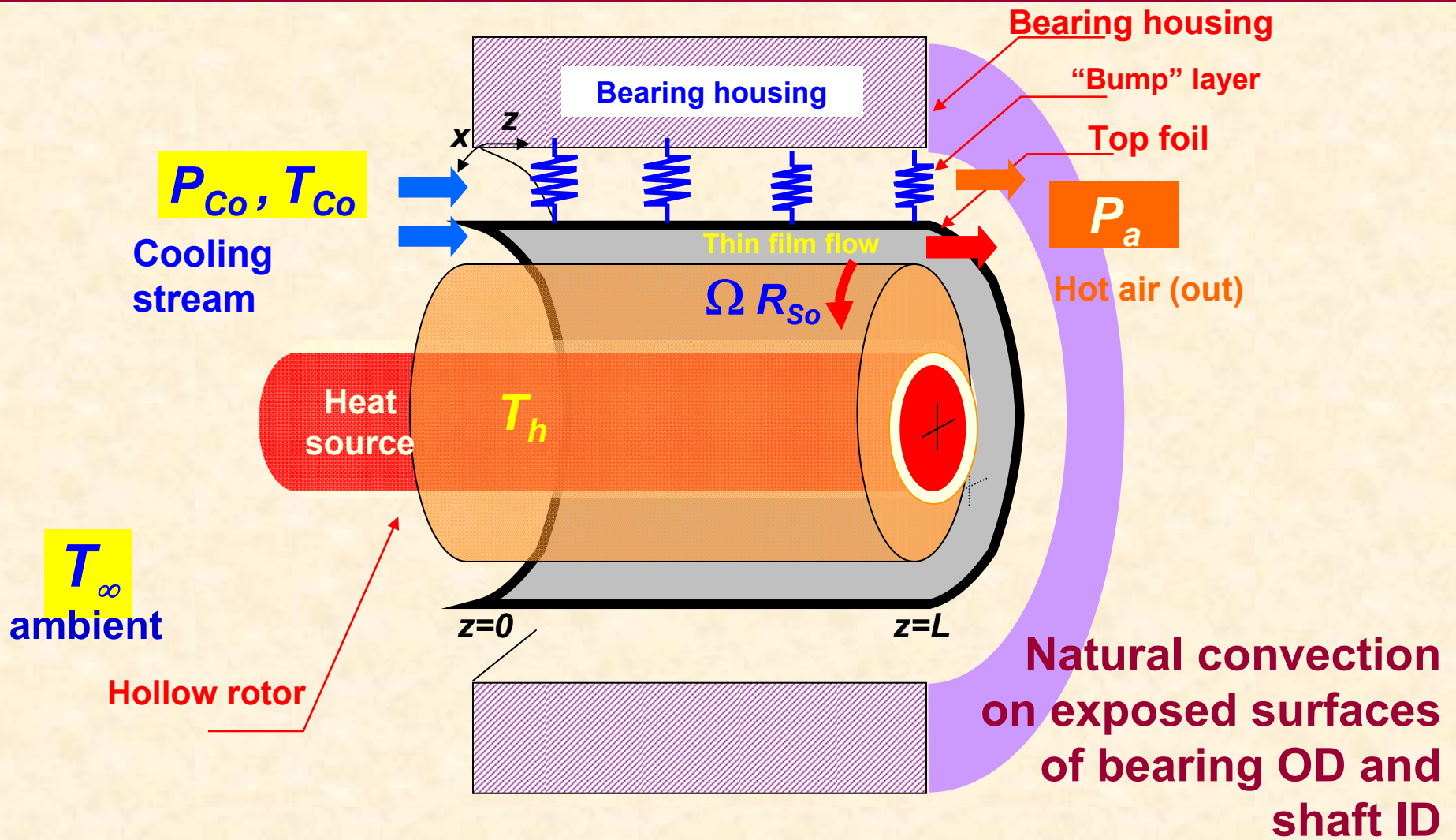
Test cases #7~#9

Flexible rotor mode at ~90 krpm (rap test)
Critical speed (Rigid body mode) ~ 5 and 8 krpm

No major differences in responses between cold and hot

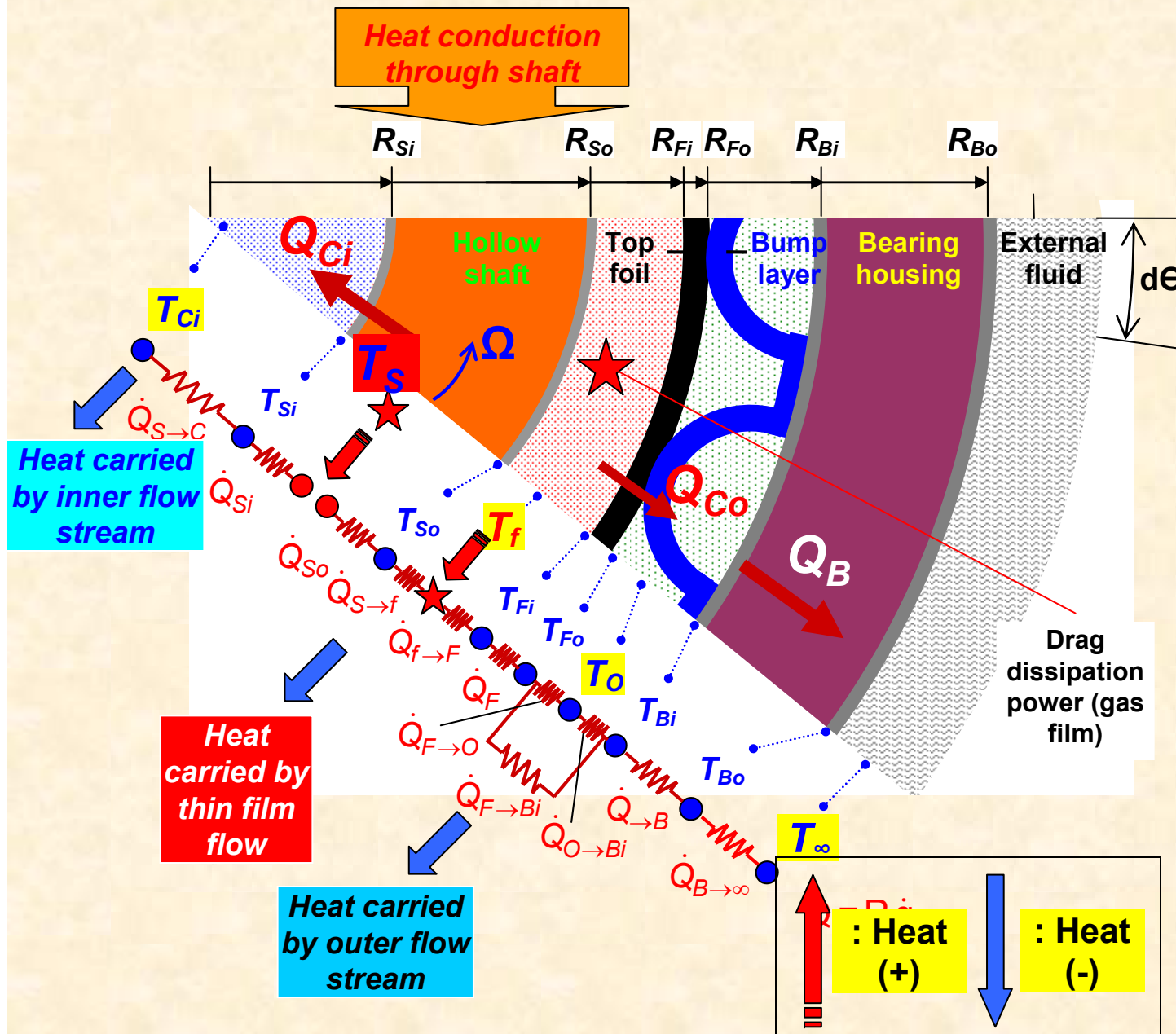
Gas film	Reynolds eqn. for hydrodynamic pressure generation Energy transport eqn. for mean flow temperature Various surface heat convection models Mixing of temperature at leading edge of top foil
Top foil & underspring	Thermo-elastic deformation eqns. Finite Elements and discrete parameter for bump strips. Thermal energy conduction paths to side cooling flow and bearing housing.
Bearing clearance	Material properties (gas & foils) = f (Temperature) Shaft thermal and centrifugal growth Bearing thermal growth

Recap: test rotor and FB



Schematic view of rotor and heater cartridge + side cooling stream

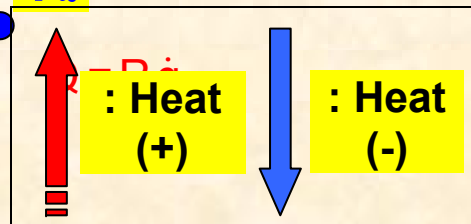
Heat flow paths in rotor - GFB system



Heat flows & thermal resistances in a GFB & hollow shaft

Heat conducted into bearing

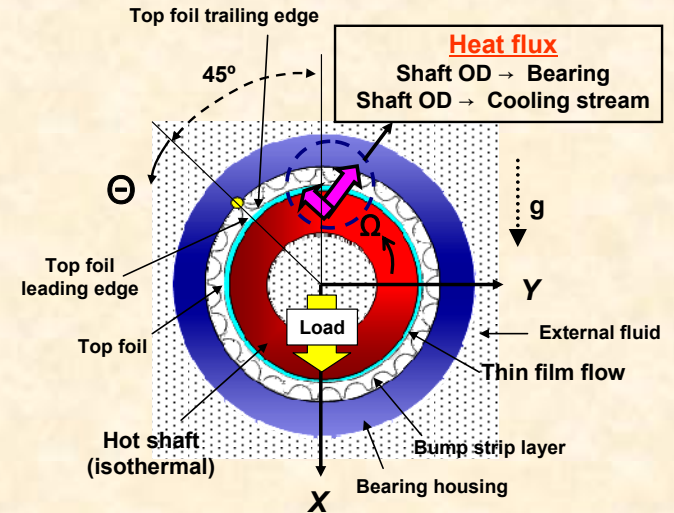
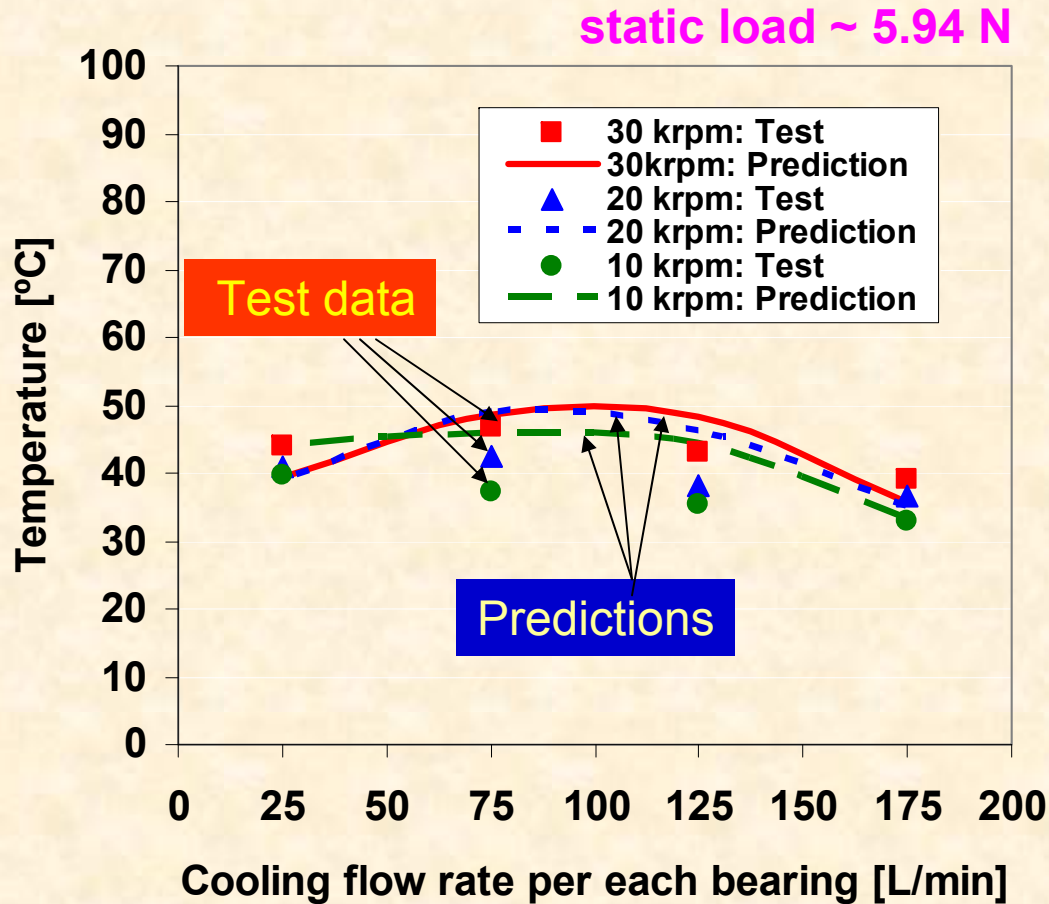
Cooling gas streams carry away heat



Bearing temperature

predictions & tests

Free end FB



Input:
Measured ambient,
rotor OD &
inlet cooling flow
temps.

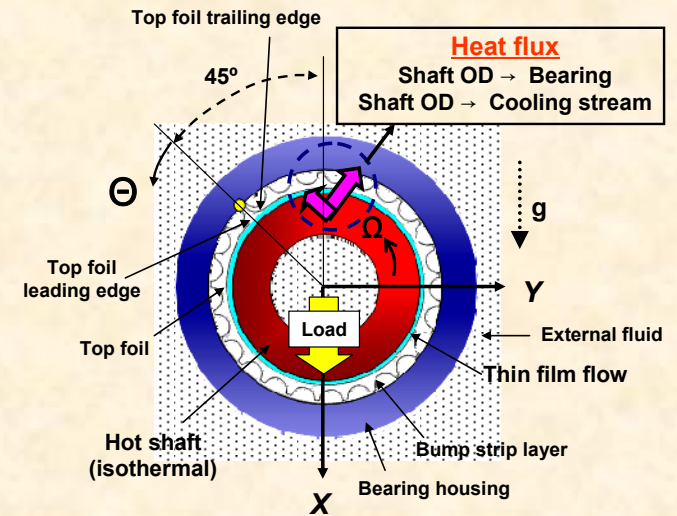
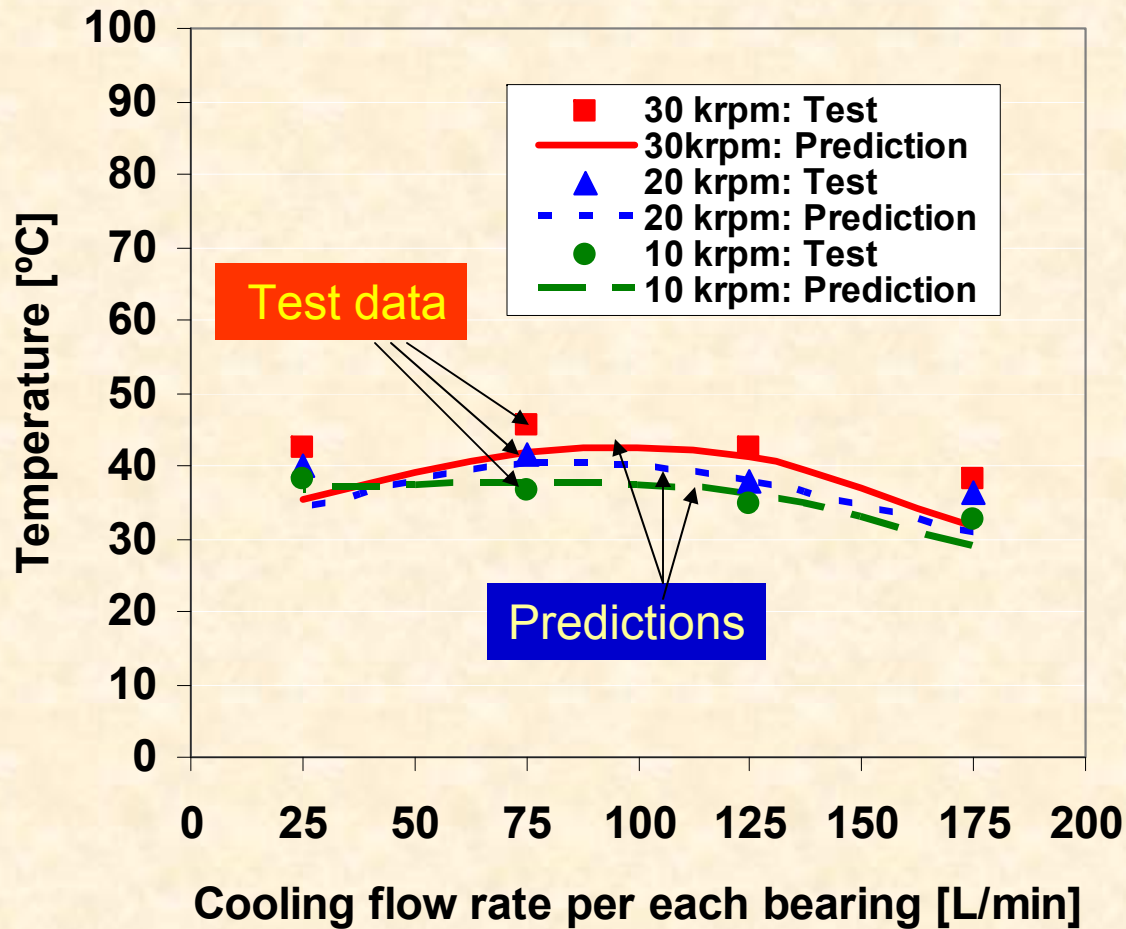
Predictions agree with test data!!

Bearing temperature

predictions & tests

Drive end FB

static load ~ 7.39 N



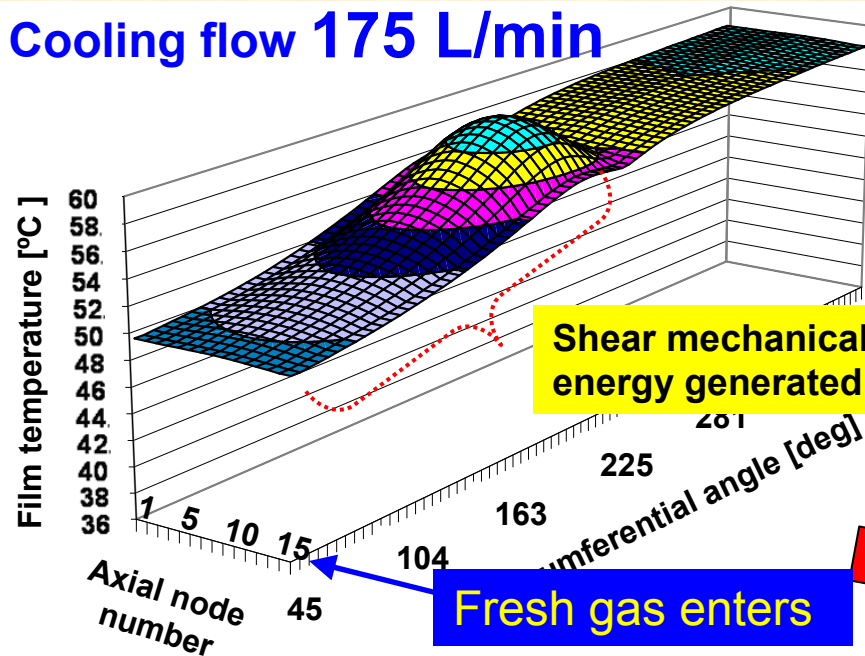
Predictions follow test data: better at DEB since smaller temperature gradient along heater axial length

Predictions: *Temperature* fields

Test case #5

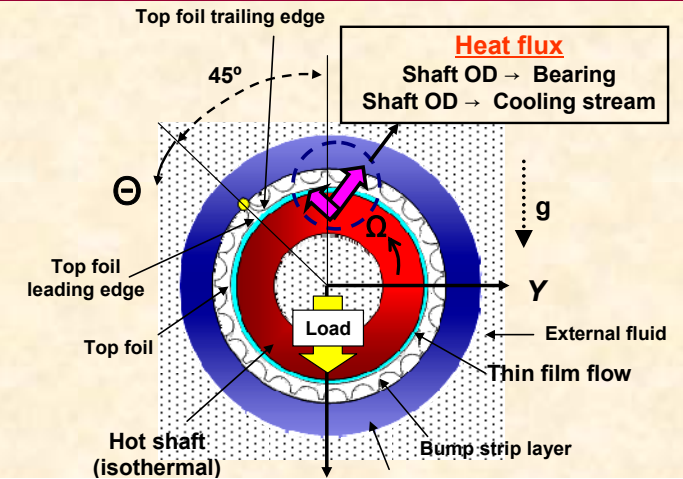
$T_{hs}=100C, 30$ krpm, Free end bearing

Cooling flow 175 L/min

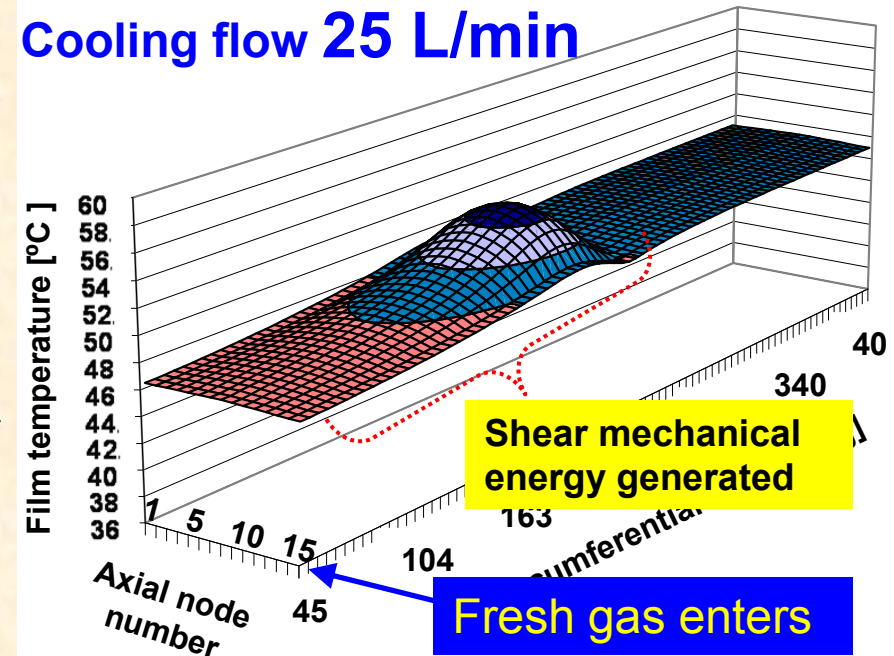


Shaft = 80C

Cooling stream inlet = 33C



Cooling flow 25 L/min



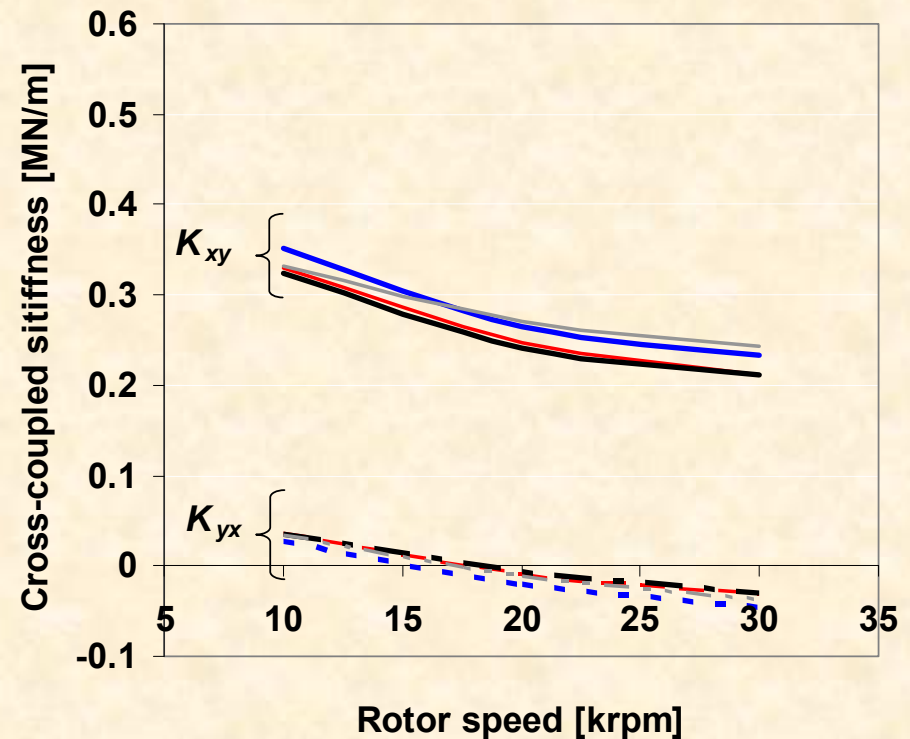
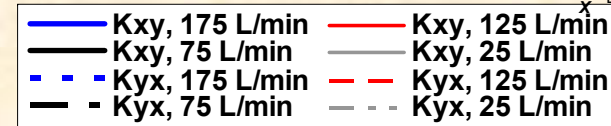
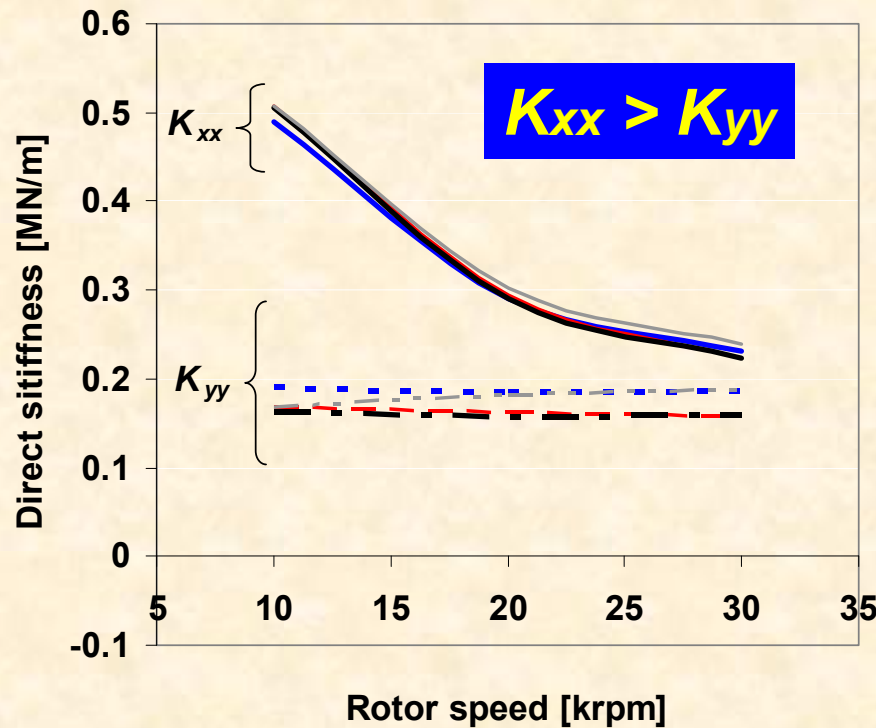
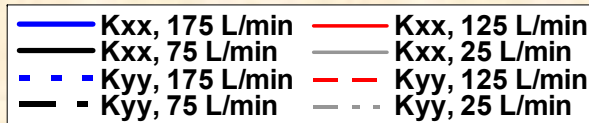
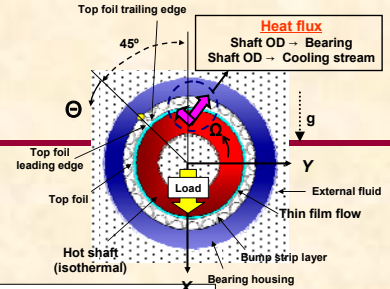
Shaft = 56C

Cooling stream inlet = 41C

Bearing stiffnesses predictions

Free End FB

static load 5.94 N

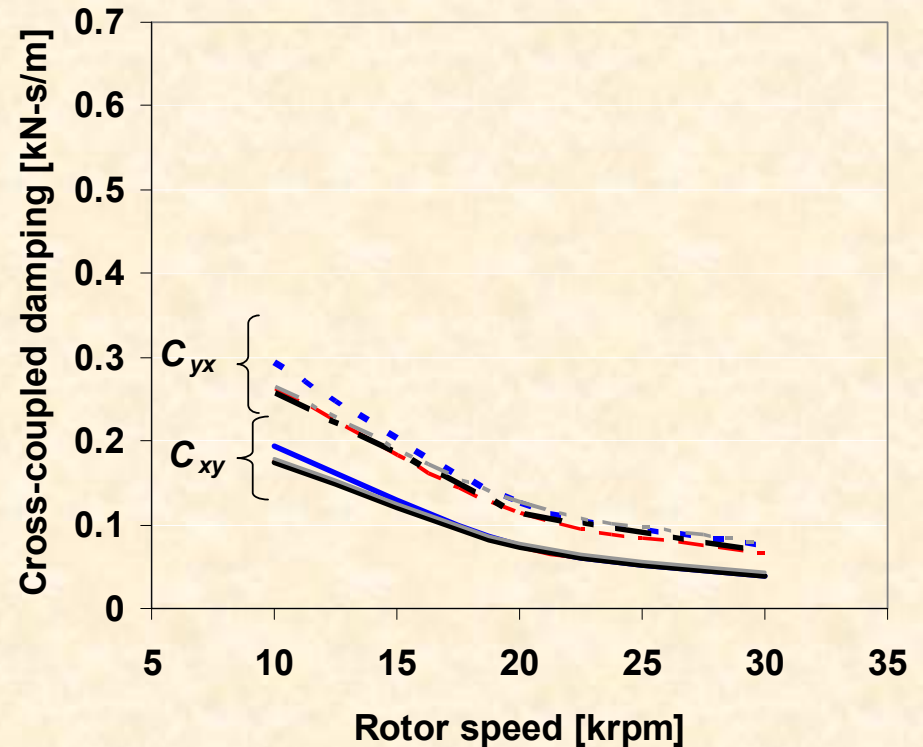
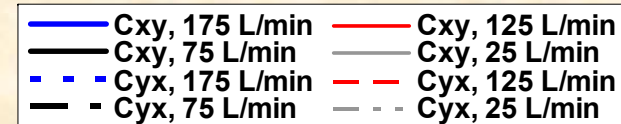
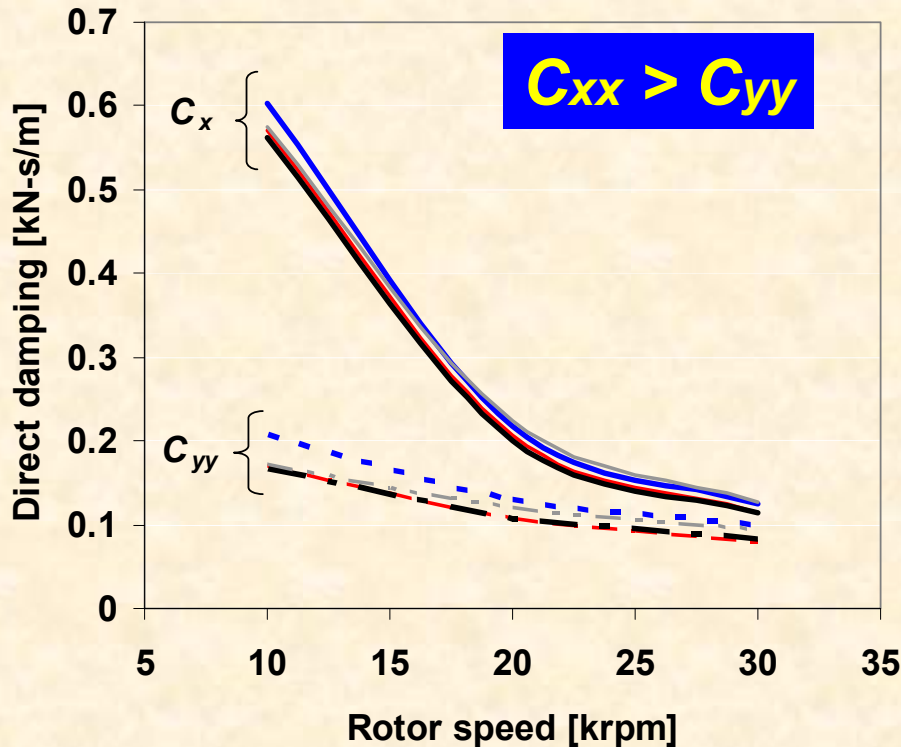
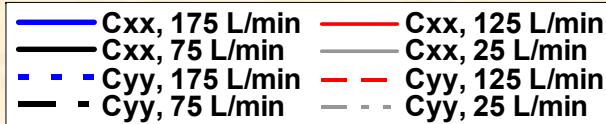
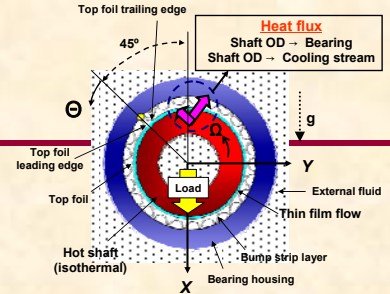


GFB rotordynamic force coefficients do not change with the strength of cooling flow rate

Bearing damping predictions

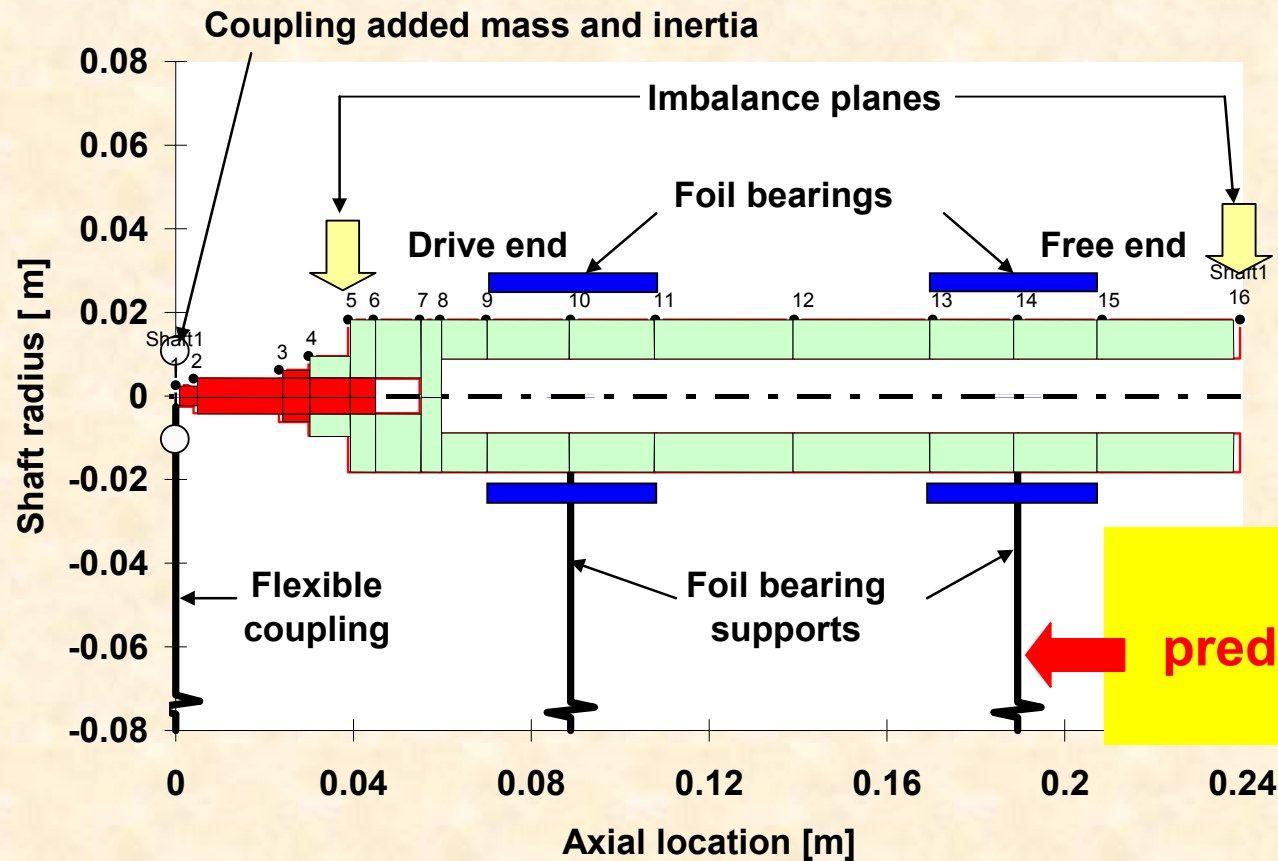
Free End FB

static load 5.94 N



GFB rotordynamic force coefficients do not change with the strength of cooling flow rate.

FE Model of Test Rotor-Bearing System

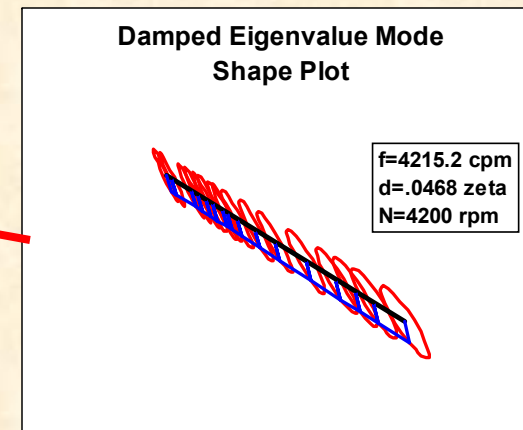
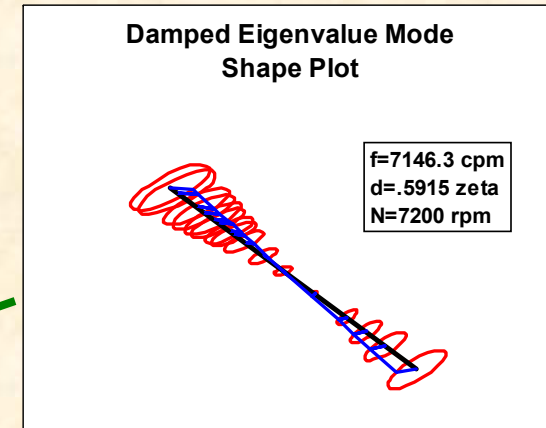
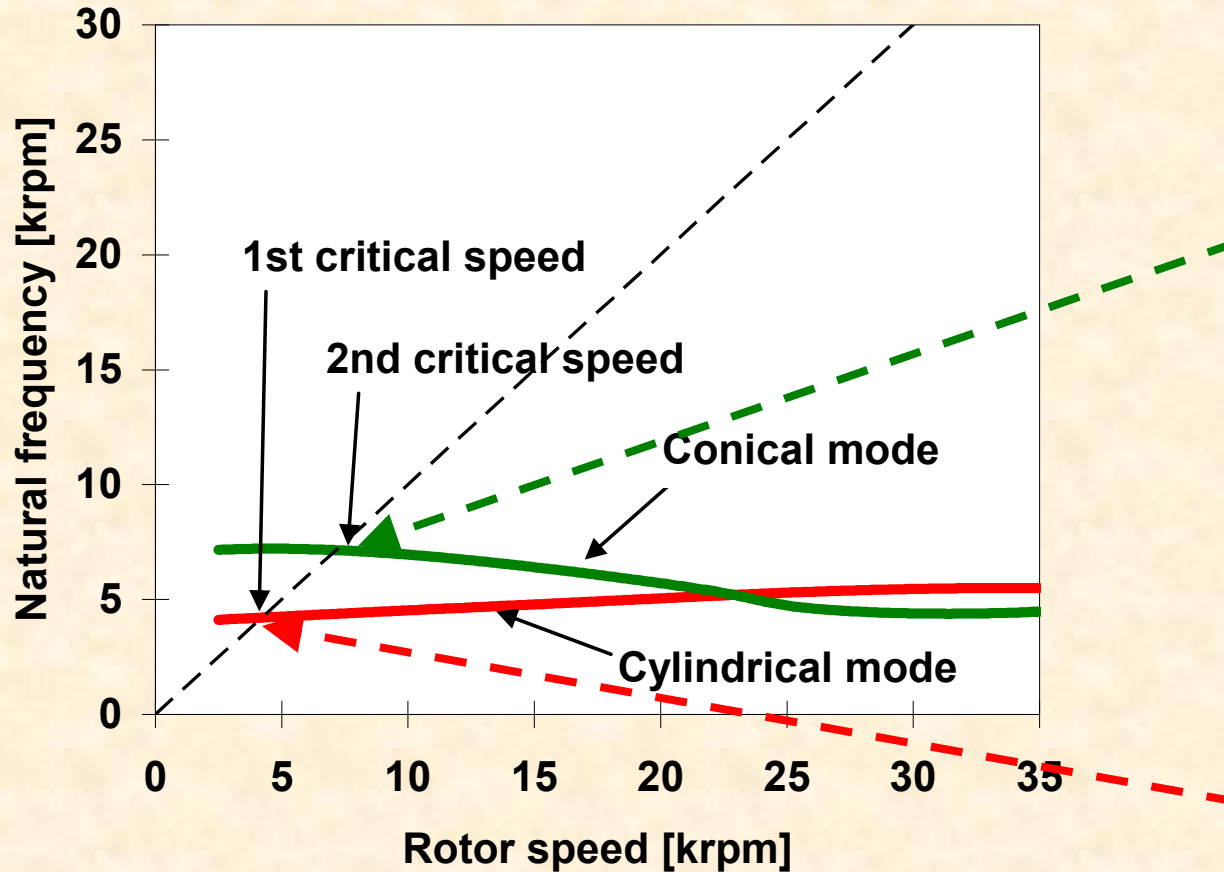


XLGFBTH
predicts synchronous bearing
force coefficients

A linear rotordynamics software (XLTRC2®) models test rotor – GFBs system and predicts the rotor synchronous responses

Damped Natural Frequency Map

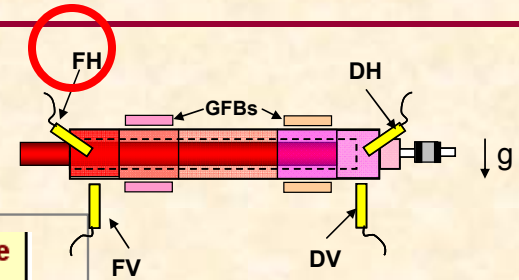
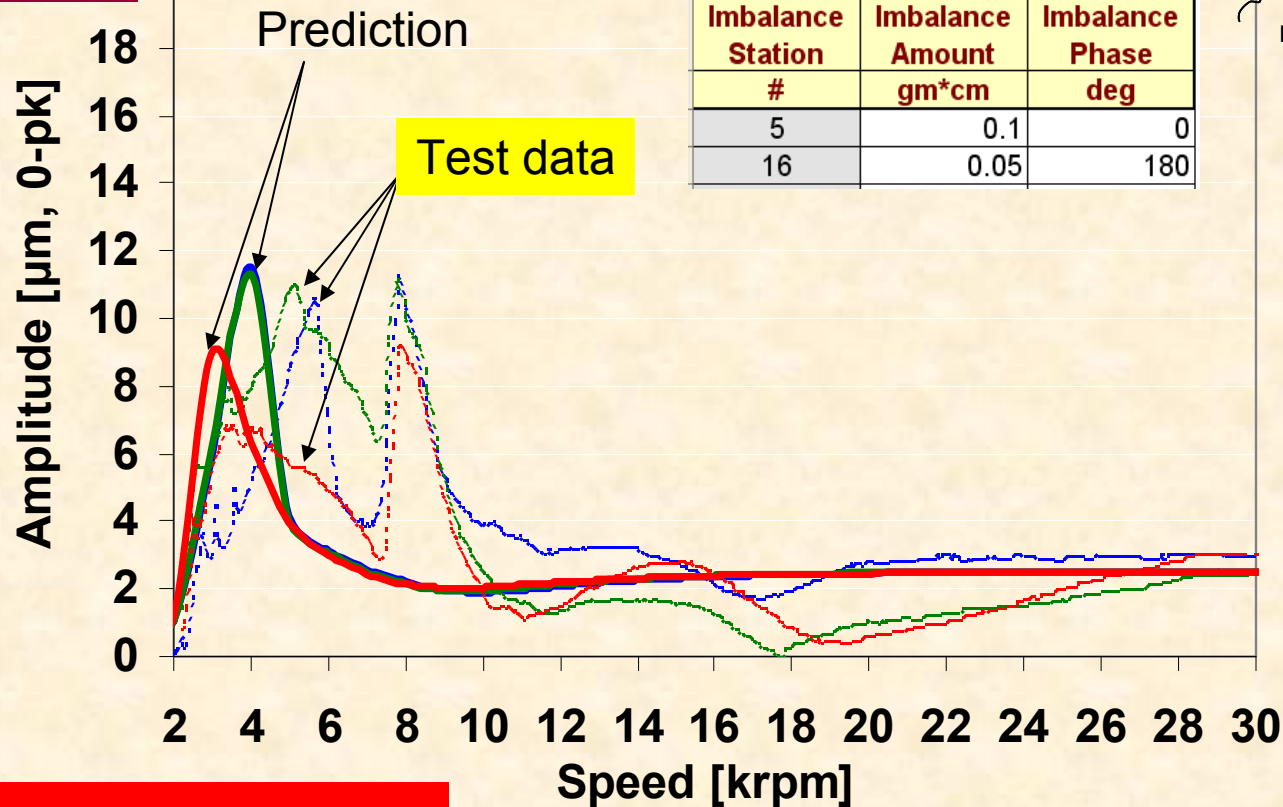
Test case #7, Heater off



1X rotor response predictions & tests

Forced cooling 175 L/min per bearing

Free End (H)



Test cases #7~#9

The predicted rotor responses reasonably correlate with the measurements.

Conclusions

- **GFB temperatures** linearly increase with the **inlet cooling air temperature**.
- When the rotor spins, **the bearing sleeve temperatures do not change with the cooling flow rate**; albeit the **rotor OD temperature increases with the strength of the cooling stream**,
- The **cooling effect** of the forced external flows is **most distinct when the rotor is hottest and at the highest rotor speed**.
- **Forced cooling flows** do **not affect the amplitude and frequency** contents of the rotor motions. The test system (rigid-mode) critical speeds and modal damping ratio **remain nearly invariant** for increasing the rotor temperature and cooling flow strength.

Conclusions

- **A physics-based** computational THD model predicts accurately **measured FB OD temperatures** for **increasing shaft temperatures** with **cooling flow**
- **Rotordynamic analysis** integrating predicted FB force coefficients reproduces **recorded rotor dynamic responses** with **increasing cooling flow rate and shaft temperature.**

Predictive tool validated & benchmarked to reliable test data base !!!

Major contribution

The present work provides the most complete to date measurements of GFB temperatures and rotordynamic response thereby extending the GFB knowledge database. Comprehensive experiments and benchmarking of predictive tool serve to advance GFB applications for use into high temperature microturbomachinery.

Topic

- **Statement of Work & Sources for Presentation**
- **Objectives and accomplished work in 07-08**
 - Computational model. Validation with published data.
 - Rotordynamic measurements at TAMU
- **Objectives and accomplished work in 2008-09**
 - Description of test rig and foil bearings at TAMU
 - Effect of temperature on bearing temperatures, coastdown speed and rotor motions
 - Effect of cooling flow on bearing and shaft temperatures. Validation of computational model
- * **The computational code**
 - Graphical User Interface. Further predictions
- **Current work with MiTi Bearings**
- **Added value & closure**

NSF-Research Undergraduate Experience in Microturbomachinery & Manufacturing

To conduct hands-on training and research in mechanical, manufacturing, industrial, or materials engineering topics related to technological advances in microturbomachinery

To develop microturbines to enhance defense, homeland security, transportation, and aerospace applications.

(10 students /year) x 3 y

NSF (06-09) \$ 259 k

Added value to NASA Project

2009 REU MTM Program

Project #1

Experimental Identification of Structural Stiffness and Damping in a 1st Generation Gas Foil Bearing for Oil-free MTM

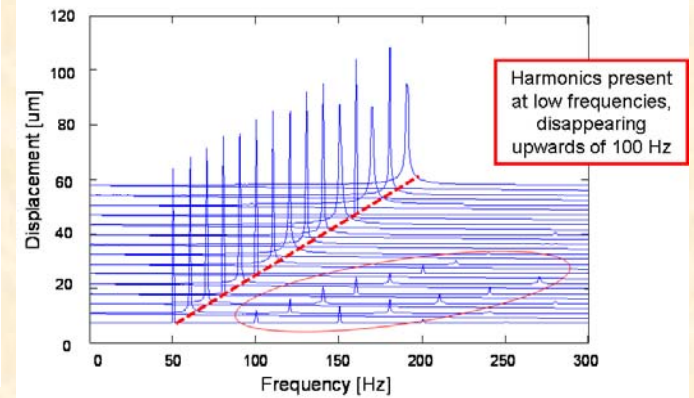
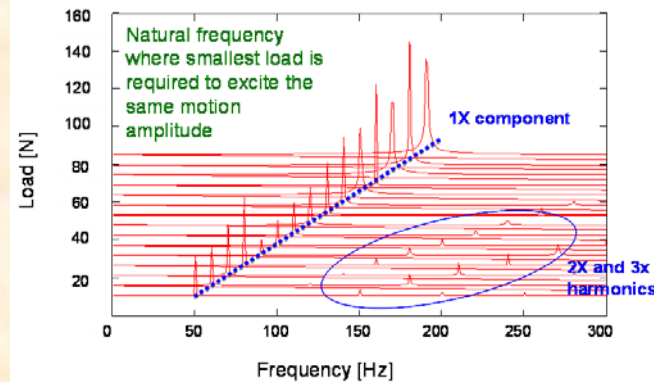
REU student

Shane Muller

Mechanical Engineering

Calvin College

KIST FB (1st generation)



Project #2

Measurement of Drag Torque, Power Loss, Friction Coefficient, Temperature, and Wear in a Foil Bearing & Coated Rotor System

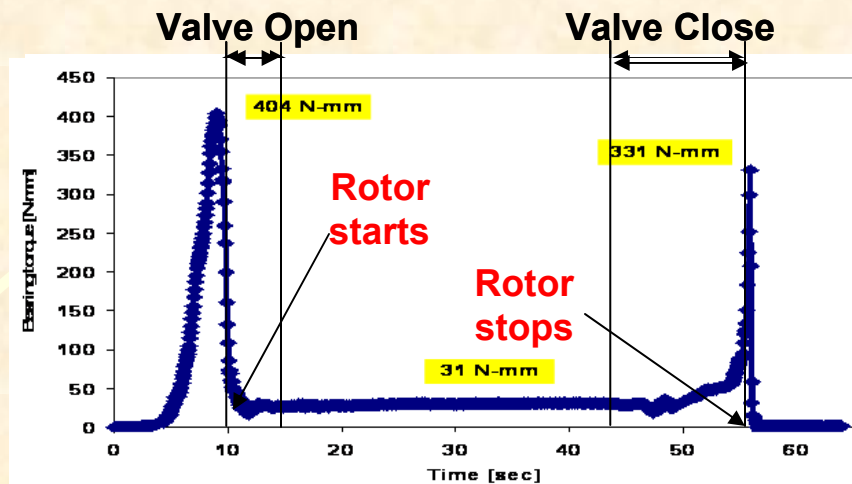
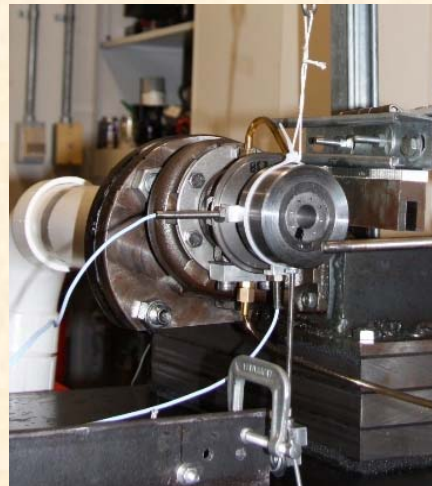
REU student

Jose Camero

Mechanical Engineering

U. of Texas, San Antonio

KIST FB



Closure: objectives accomplished

- To develop a physics-based computational model of GFB including thermal effects
- To develop a fully tested and experimentally verified design tool for predicting GFB performance
- To measure the rotordynamic performance of a HOT rotor supported on GFBs
- To quantify the effect of feed gas flow on cooling GFBs

Predictive tool validated & benchmarked to reliable test data base !!!

Acknowledgments

- **NASA GRC: Drs. S. Howard & Dr. C. DellaCorte**
- **Turbomachinery Research Consortium**
- **NSF REUP**
- **Capstone Turbine, Inc.**
- **MiTi©, Foster-Miller**
- **KIST: Korea Inst. Science & Technology**
- **Honeywell Turbocharging Technologies**

Learn more at: <http://rotorlab.tamu.edu>

Back up slides

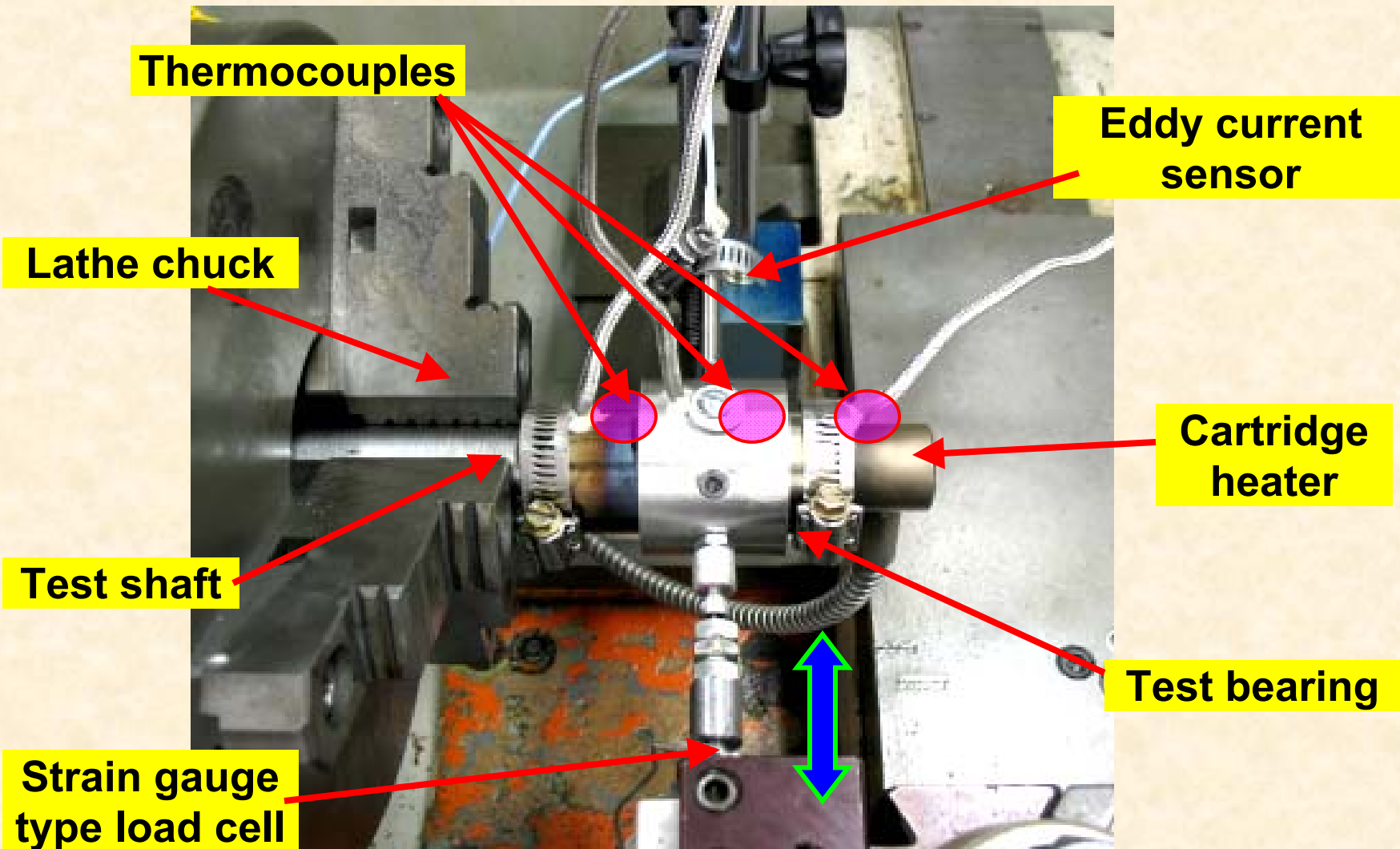
THD Model Validation

Bearings at TAMU

Parameter [mm]	Foster-Miller (2 nd gen.)	KIST (1st gen.)	MiT (2 nd gen.)
Bearing cartridge			
Outer diameter	50.85	50.80	44.575
Inner diameter	39.36	37.95	37.921
Top foil and bump strip layer			
Top foil axial length	38.2	38.1	25.4
Top foil thickness	0.100	0.120	0.127
Bump foil thickness	0.100	0.120	0.102
Number of Bumps	25 × 5 axial	26 × 1 axial	24 × 3 axial
Bump pitch	4.581	4.300	4.640
Bump length	3.742	2.100	3.950
Bump height	0.468	0.540	0.510
Bump arc radius	5.581	4.161	4.079
Bump arc angle [deg]	68	59	58

Elastic Modulus 214 GPa,
Poisson ratio=0.29

Static load test setup



Steady static load (or unload) proportional to linear movement of lathe tool holder

High temperature rotor

NO COST!

Under cut, depth 0.25 mm,
to be coated with KIST high temperature coating



Inconel 718 shaft

: photos taken by manufacturer (KIST)
prior to machining of threaded holes at
rotor ends and coating shaft at bearing
locations.

Locations of 8
threaded holes of
4-40 tap with
13mm depth

***KIST* proprietary solid
lubricant (400 °C)**

Closure Y2

➤ **Assess effects of temperature (to 160 C) on the structural properties of FB from static load (250 N) tests:**

Loading and unloading tests show hardening nonlinearity and mechanical hysteresis.

FB structural stiffness reduces with temperature due to increase in bearing radial clearance (atypical).

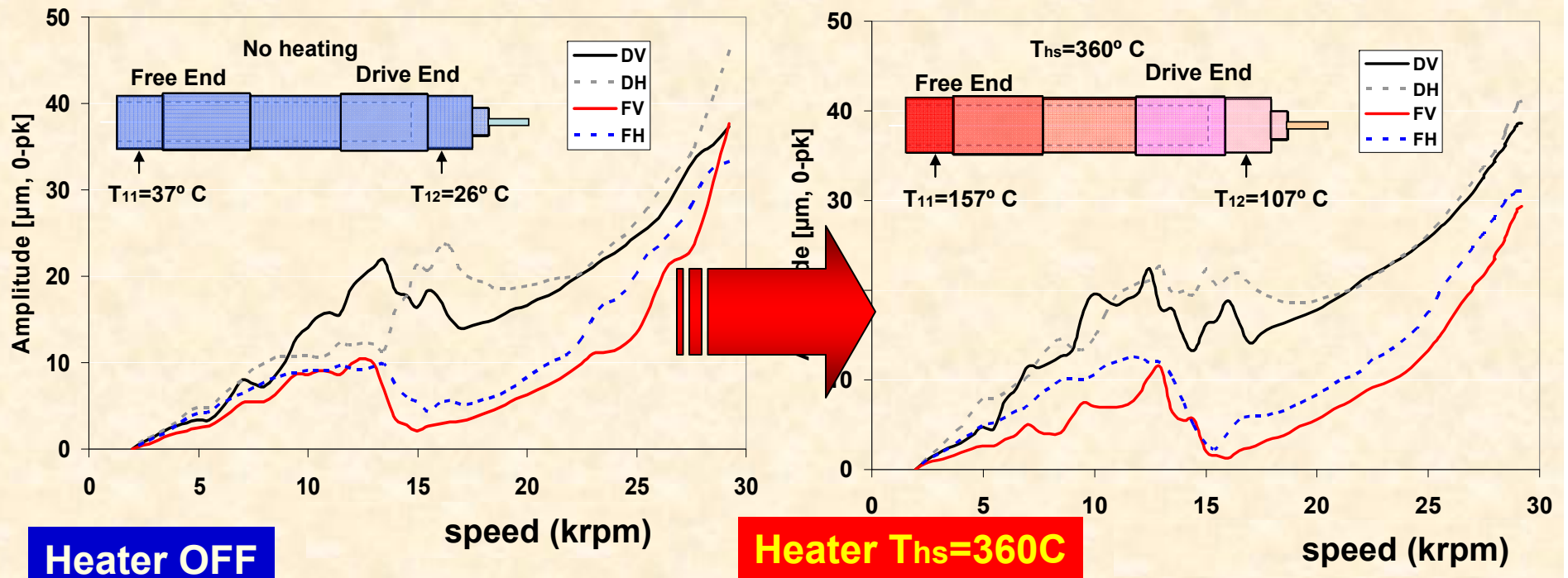
Model predictions reproduce test data, when accounting for thermal effects in materials properties and components' expansion.

➤ **ADDED VALUE:**

08 & 09 Summer NSF-REU in microturbomachinery educated six undergraduate students (US citizens).

1X response with cold and hot rotor

Baseline coastdown, **No forced cooling**



Elastic rotor mode at 29 krpm (480 Hz) : soft coupling and connecting rod
Critical speed (rigid body mode) ~ 13 krpm

Test Data

Similar rotor responses for cold and **hot** rotor operation